# Primary Photodetection Process in Humans & most members of *Chordata*

James T. Fulton –July 4, 2019

Current Version https://neuronresearch.net/vision/pdf/12primary.pdf
Memorialized as DOI: xxx on date TBD

**Abstract:** Like nearly, if not, all members of *Chordata*, humans exhibit four spectrally independent chromophores in their retina. These chromophores are defined explicitly in this Chapter 12. The four chromophores are members of the Rhodonine family of *resonant* conjugated retinoids, also known as members of the carboxylic acid system. They form a liquid-crystalline coating of the opsin proteins forming the discs of the outer segments of the photoreceptor neurons, but are not chemically combined with opsin. The photoreceptor neurons used by humans, and all members of *Chordata* are also described in detail, based on The Electrolytic Theory of the Neuron. The Pauli Exclusion Principle plays a crucial role in defining the spectra of the chromophores. The fact that both endothermic and exothermic members of *Chordata* employ a biological temperature range independent of that defined by Arrhenius is critically important. This biological temperature range is critically important in interpreting the performance of the eye in going from the photopic to scotopic illumination range. The fundamental photo-transduction process employs a quantum-mechanical mechanism that has not appeared previously in the vision literature. The Activa employed inside the photoreceptor neurons is a PNP semiconducting material based on a liquid-crystalline form of water. A single closed-form equation, the P/D Equation of Section 7.2, is relied upon here to describe the operation of the photoreceptor neurons under all illumination and temperature conditions. The equation, when reduced to a Poisson Equation form, includes the Hodgkin Condition. The details of the electrostenolytic power supply used by all neurons is cited in this chapter.

**Keywords:** Electrolytic, Biological temperature, quantum-mechanical, Rhodonine, retinoid, liquid-crystal, semiconductor, PNP, 2-exciton mechanism, adaptation, excitation/de-excitation equation, electrostenolytics, Pauli Exclusion Principle, Hodgkin Condition, P/D Equation

**Table of Contents, List of Figures**, and **Index** appear at end of this Chapter.

**REFERENCES TO SECTIONS** beginning with a numeric indicate a Chapter in "Processes in Biological Vision" available on line at https://neuronresearch.net/vision/ by clicking on *Download Chapters* on the left navigation panel and then selecting the Chapter, Appendix or ancillary material.

# Excerpts from

# PROCESSES IN BIOLOGICAL VISION:

## including,

# ELECTROCHEMISTRY OF THE NEURON

This material is excerpted from the full β-version of the text. The final printed version will be more concise due to further editing and economical constraints. A Table of Contents and an index are located at the end of this paper.

**James T. Fulton**
**Vision Concepts**

**jtfulton@neuronresearch.net**

**July 4, 2019**

**Copyright 2001 James T. Fulton**

# 12 Primary Signal Processing--Signal Detection [1]

## 12.1 Introduction

This chapter will focus on the performance characteristics of the Stage 1 visual process based on the overall block diagram (roadmap) of **Section 11.1.4.2.1**. This Stage encompasses the operation of the photoreceptor cells in both their signal detection and signal equilibration roles. Signaling is the primary function of the photoreceptor cells. This chapter presents the first detailed description of the signaling path of the photoreceptor cell to appear in print. The description relies upon the background developed in previous chapters and the appendices. It relies on a clear understanding of four separate areas:

+ the complexity of the photoreceptor/IPM/RPE interface, **Section 4.5.1.1**

+ the complete solution to the Photoexcitation/De-excitation Equation, P/D Equation of **Section 7.2**

+ the quantum-mechanical processes incorporated into the chromophores and the Outer Segments of vision, **Section 5.4.3**

+ the role of the metabolic system in the transient performance of the complete stage, developed in **Section 8.6** and section 3.2 of The Neuron and Neural System[2].

The output signals of the photoreceptor cells are essentially fixed in peak-to-peak amplitude regardless of the absolute amplitude of the input illumination. This is achieved through the use of an adaptation amplifier controlled by a low pass filter in its power supply. The subsequent signal manipulation processes rely on the essentially fixed amplitude of the signals from the photoreceptors of Stage 1.

As late as 1973, Rodieck[3] wrote that: “The nature of the coupling mechanism between light absorption on the lamellar membrane–the photocurrent generated by the outer-segment plasma membrane–is one of the most important unsolved problems of retinal physiology.” Little has changed since then with regard to the actual mechanism involved. Only additional concepts have appeared. Both the old and the new concepts have relied primarily upon kinetic analysis to support their feasibility. Kinetic analysis in the absence of an understanding of the underlying mechanism, is a very weak tool.

The situation in the literature has not changed significantly since that time. Although considerable analysis of possible conceptual mechanisms has appeared, these have not provided a viable hypothesis. This is illustrated by the question marks in figure 13.29 of the 1999 book by Oyster[4]. A key problem has been the adoption of a proposal by Young that the Outer Segment was enclosed by a plasma membrane of the parent photoreceptor cell. Only within the last few years have images of the Outer Segment appeared at sufficient magnification to show conclusively that there is no membrane surrounding the disk stack called the Outer Segment. The disk stack is formed by secretion from the wall of the cell. It is not formed by evagination. See **Sections 4.3.5** & **4.6.2**.

There has been a large amount of intellectual capital and laboratory time invested in concepts depending on the presence of a plasma membrane surrounding the disk stack of each Outer Segment. This is unfortunate. Lacking a plasma membrane, the concepts of gates in such a membrane is untenable. Lacking gates, the various cascade theories of how a potential is generated across the membrane are untenable.

### 12.1.1 Glossary

---

[1]Released: July 4, 2019
[2]Fulton, J. (2014) The Neuron and Neural System. *online* https://neuronresearch.net/neuron/
[3]Rodieck, R. (1973) The vertebrate retina. San Francisco, CA: W. H. Freeman pg. 328
[4]Oyster, C. (1999) The Human Eye: Structure and Function. Sunderland, MA: Sinauer Assoc. pg 582

Because of several differences in terminology between the conventional wisdom based on chemistry and the alternate hypotheses presented in this work, it is very important to present the following definitions here. The term transduction has a significantly different meaning when used in discussing communications via hormones and communications related to sensing the external environment. This separation has frequently been overlooked during attempts to use the hormonal concept to describe the sensory process.

**Signal transduction–**

1. (with respect to the hormonal system) An intracellular cascade of biochemical event that follow the interaction between extracellular growth factors and their membrane receptors, ending in the switch of nuclear mechanisms controlling the proper biological responses. (Battistini, et. al. 1993 in Papa & Tager)

2. (with respect to the sensory mechanisms of the neural system) The transfer of acoustic energy, electromagnetic energy or tactile motion by quantum-mechanical sensors into free electrons that can be further processed by the neural system.

## 12.1.2 Background

### 12.1.2.1 Relative Physics

As an example of the multi-disciplinary problem, the descriptions found in the vision literature regarding the photodetection process and mechanism are quite unlike the similar descriptions found in the realm of physics and engineering. Photodetection is usually defined in terms of one of three fundamental processes, photo-emission, photoconduction and thermally mediated conduction due to absorption of photons. Both photo-emission and photoconduction are features of solid state physics and involve well understood phenomena at the atomic level. Thermally mediated conduction is a much simpler process at the atomic level. It involves the heating of the bulk material. The change in the conductivity of the bulk material reflects this change in temperature. This process is seldom found in high performance photodetection systems, although, lacking any other uncooled technique, it has occasionally been used as a low performance detection scheme in infra-red sensors. The process exhibits an absorption spectrum that is independent of the energy, and hence the wavelength, of the incident photons.

Photoconduction is achieved by a photon impacting a crystalline lattice, of either a solid or liquid crystalline material, and creating a long life electron-hole pair. During the lifetime of this pair, multiple electron charges are able to pass through the lattice. The result is a charge current that may be significantly larger than the quantum flux of the photons. This process typically exhibits a broad absorption spectrum for photons above a specific energy level.

Photo-emission occurs in two distinct forms in physics, photo-emission from the valence band of a material into a vacuum (the historically more conventional process of external photo-emission) and photoemission from the valence band into a higher level conduction or excitation level (so-called internal photoemission). External photo-emission is characterized by a broad absorption spectrum that begins at a very precise photon energy level (described by Fermi-Dirac statistics) and extends to indefinitely higher energies. Internal photo-emission exhibits a similar, though less extended, absorption spectrum in most in-organic materials because the conduction band is quite wide. The long wavelength absorption edge is still defined by Fermi-Dirac statistics and can be described precisely by the Fermi-Dirac function. In the case of organic materials, there is normally no conduction band. The conduction band is replaced by an excitation band that is quite explicitly defined and usually narrow. In these materials, the absorption spectrum involves the difference in energy between two bounded energy levels, the valence or unexcited band and the excitation band. The absorption spectrum in this case is defined by the difference in energy between possible energy states between the two bands (while observing the Pauli Exclusion Principle. This spectrum is precisely defined by the product of two Fermi-Dirac functions. One describes the short wavelength edge of the absorption band. The second describes the long wavelength edge of the absorption band. This is the situation observed in the chromophores of vision.

It must be appreciated that the photochemistry of resonant organic molecules is basically different from that of inorganic semiconducting materials. In inorganic photodetecting materials, which typically involve the excitation of an electron from the valence band to the conduction band, the observed spectral band is a broad, generally flat, one. This is because the conduction band is generally wide and any photon with an energy greater than the valence-conduction band energy difference will cause excitation. This is not generally the case in organic photochemistry. The energy transition of interest does not usually involve a conduction band; alternately, it is a transition between one or more unexcited energy bands to an excited energy band. Both of these bands are described quantum

mechanically--and their energy difference is similarly described. Thus the spectral absorption coefficient due to any individual transition is generally peaked, with a shape much like in a resonant circuit of electrical engineering (where it is also possible to combine the features of both resonant and nonresonant elements to achieve unique spectral performance) In photography, the elements of an organic molecule and an inorganic molecule are nearly always combined to achieve the desired broad overall spectral response. Moreover, the most important organic molecules in photography involve multiple auxochromes, i. e. more than three, in each chromophore to achieve wide spectral response and long stable shelf life for the product (while always abiding by the rules of liquid crystal chemistry to insure an increase in sensitivity and not a decrease).

In developing the mechanism of the chromophoric excitation-neural de-excitation process, another embellishment will be added to the variety of excitation methodologies available. Most investigations of a neuron as a signal repeater (action potential regenerator operating in the phasic mode) do not focus on the minimal energy required for excitation of the neuron at a synapse. In the case of the photoreceptor cell (an analog, or electrotonic, amplifier creating generator waveforms), it appears that a minimum energy level is required and the neuron must be biased properly.

### 12.1.2.2 Common wisdom of the past

The primary signal detection process has been studied at a number of different times in the past but the needed tools were usually not available for adequate interpretation. In the 1930's, isomerization was one of the few chemical mechanisms known to the general scientific community that could be caused by photon effects.

The dominant hypothesis of photodetection in vision for the last half century has been that proposed by Hubbard, and extended by Kropf based on the work of Wald. The hypothesis being that photodetection involves the isomerization (by what they call internal photo-emission) of a retinene attached to a protein through a protonated Schiff base. The de-excitation of the molecule was via a physical re-isomerization. This method of photodetection has been carried forward as analogous to a switch that initiated the transfer of charge, between specific elements that are undefined at this time, and that a second action was necessary to terminate the transfer of charge in a timely manner. Based on this switching analogy, Baylor & Burns recently defined a set of "strong functional constraints" on any second mechanism[5].

At that time, the photography field was beginning to introduce color photography to an ever wider range of applications. However, the technical processes of how it worked were poorly understood. The photo-chemists had just discovered that it did work and commercial pressures caused a rush to market of a basically cook-book understanding of the physics (and chemistry). The process did not involve photo-isomerization. The quantum-mechanical process used in color photography is quite similar to the process actually used in animal vision.

Neither the isomerization or re-isomerization process, has ever been demonstrated to occur in the *in-vivo* animal as part of the vision process. It is a relatively high energy process and not well suited to achieving the near quantum limited performance of animal vision. By any standard, the previously proposed method of operation in the vision process is a convoluted and involved one. As the field of semiconductor physics has evolved and the field of liquid crystal chemistry has appeared, a variety of additional mechanisms have appeared that offer more satisfactory solutions to the *in-vivo* photo-detection process. Effective understanding and use of these mechanisms will once again require a multi-disciplinary approach if one is to understand the operation of the Outer Segment of the photoreceptor of animal vision.

The most recent redefinition of the above hypothesis in a theoretical context was that of Torre, et. al[6]. In that work, "a quantitative reconstruction of the *kinetics* of phototransduction was attempted." The resulting model was based primarily on proposed chemical kinetics instead of detailed descriptions of the processes involved. It included a large number of degrees of freedom as indicated by the number of arbitrary constants employed. No attempt was included to treat the quantum mechanical situation. The term phototransduction was employed, rather than photodetection, to describe the overall "process by which the absorption of a photon by a molecule of rhodopsin in a photoreceptor is transformed into an electrical signal." This description skirts the subject of how this is achieved. The next sentence says "the electrical signal is caused by the modulation of a current, usually called a photocurrent, flowing across the light-sensitive channels in the plasma membrane of the outer segments." What fundamental

---

[5]Baylor, D. & Burns M. (1998) Control of rhodopsin activity in vision. *Eye* vol 12, pp. 521-525

[6]Torre, V. Forti, S. Menini, A. & Campani, M. (1990) Model of phototransduction in retinal rods. Symposia on Quantitative Biology, vol. LV, Cold Spring Harbor, NY: The Cold Spring Harbor Laboratory Press pp.563-573

mechanism is used by the light-sensitive channels in the plasma membrane is not discussed. Kamiyama et. al.[7] have combined the transduction model suggested by Torre, et. al. with the excitable membrane model of Hodgkin, Huxley & Katz to create an ionic current model of the photoreceptor cell. This model is the first to delineate the outer segment from the inner segment in an electrical analog. It also recognizes the two separate polarity signals recordable from one photoreceptor cell (note the similarity of their figure 1 to Laughlin discussed below). Beyond those features, the model is a synthesis of a large group of individual variable resistors in series with arbitrary voltage and polarity batteries, all in parallel with a current source and a capacitor. The majority of the network is meant to represent the membrane of the inner segment of the photoreceptor cell. The model was implemented as a computer simulation program.

Leibovic has also addressed the transduction and adaptation processes[8]. However, the result does not satisfy. He notes "the processes which activate the responses to light are better understood than those which inactive them." He goes on "Whatever the details, we can imagine how thresholds and response amplitudes can be related to the biochemistry." This work suggests that "to imagine" is a scientifically weaker mechanism than that associated with intuition.

The mathematical solution to the equations of the proposed system reduce in a special case to a form explored by Fourtes & Hodgkin[9,10]. This special case involves a single processing stage as opposed to the general n-stage equation they presented. They used a circuit analog employing a pentode vacuum tube in the series arm of each of their n-stages. This analog is clearly not appropriate based on later investigations. Their n-stage solution was adopted by a variety of later investigators who defined multiple stages in order to obtain additional degrees of freedom in their mathematical manipulations. The goal was to account for the delay in output signal versus excitation that varied with stimulus level. However, Fourtes & Hodgkin were careful to note that "it must be said at once that the results do not provide real evidence for the existence of anything formally equivalent to a cascade of ten elements". Their analysis employed a variable number of elements, or stages, to accommodate a wider range of excitation levels.

The primary reason for the n-stages in their analysis was to provide sufficient delay between the onset of excitation and the response of the observed biological cells. Their equations did not include an independent delay term because they did not use complex notation in the solution of their differential equation. Additionally, their model was written in terms of voltages. For a quantum mechanical process, it is more appropriate to use a charge analog and quantify the maximum number of excitable but initially bound charges available in the photoreceptor. The limitation on the total number of charges available in the system transforms the analog into a state variable system. This is the methodology employed in this work.

### 12.1.2.3 Framework of this theory

This work does not support the conventional wisdom concerning the process of photosensing in vision. **It does not support:**

+ the photoconduction of rhodopsin as the excitation mechanism,

+ the isomerization of a retinene as the excitation and de-excitation mechanisms within the photodetection process,

+ the switching analogy required to explain the separate excitation and de-excitation of the putative CGMP cascade,

+ the putative cGMP cascade as an explanation of the gain mechanism, nor the use of variable resistors without a means of controlling them in vision.

Neither does this work rely upon chemical kinetics as a foundation.

---

[7]Kamiyama, Y. Ogura, T. & Usui, S. (1996) Ionic current model of the vertebrate rod photoreceptor. Vision Res. vol. 36, pp. 4059-4068

[8]Leibovic, K. (1990) Science of Vision NY: Springer-Verlag pg 44

[9]Fuortes, M. & Hodgkin, A. (1964) Changes in time scale and sensitivity in the ommatidia of *Limulus*. *J. Physiol.* vol. 172, pp. 239-263

[10]Borsellino, A. Fuortes, M. & Smith, T. (1965) Visual responses in Limulus. Cold Spring Harbor Symposia on Quantitative Biology. vol XXX, pp 429-443 This paper provides additional background re: Fuortes & Hodgkin

An alternate continuous flow process is proposed that does not require a separate and distinct terminating mechanism or any constraints on such a mechanism. It is based on an entirely electrolytic hypothesis using quantum-mechanical (internal photoemissive) detection techniques. The hypothesis relies heavily on the presence of the chromophores, membranes and specific minute volumes of water to be present in the liquid crystalline state of matter. **The success of this schism with the past is illustrated by the results; the first comprehensive, consistent and rigorous explanation of the photosensing process of vision process**.

> **From this point on, the term transduction will be used only in the electronic sense defined in Section 12.1.1.**

The proposed photodetection process is based on a simple first order physical system defined by a single first order differential equation (and a very specific set of boundary conditions). The physical model is quantum mechanical and appropriate for organic photodetectors. The photodetection process is redefined into two mechanisms, transduction of photons (TD) into excitons (constrained electrons) mechanism and the translation of excitons into free electrons within a microtubule (TL) . The transduction mechanism is *passive*. The translation process is based on an *active* electrolytic semiconductor device (actually one of two) within the photoreceptor cell. The resulting model is much simpler and does not involve a computer simulation. It provides simple closed form mathematical equations describing all of the waveforms associated with the photoreceptor cell under all conditions of continuous and impulse illumination as well as dark adaptation in the absence of illumination. This equation is defined as the Photoexcitation/De-excitation Equation (P/D Equation). It is derived in a complete form in Appendix A as well as in a variety of simplified forms useful under certain simplifying certain conditions. One of these forms was originally postulated by Hodgkin (See previous paragraph), but without a model to explain its limited applicability.

### 12.1.2.3.1 Architecture & integration of the visual system

As indicated in **Section 4.5**, the photoreceptor cells of stage 1 do not stand alone. They are highly integrated into a photoreceptor/IPM/RPE complex. This complex in turn shares a highly integrated role in the overall operation of the eyes and the complete visual system. From an architectural (or system design) perspective, this integration is important to the many dynamic aspects of the system. Each system has been optimized with respect to a variety of design goals related to the environment of the animal. The resulting optimization has an impact on the performance of the photoreceptor cells of that animal.

For humans, the optimization has resulted in an adaptation function that is tailored to the diurnal illumination level defined by the earths rotation. Leibrock, et. al. have reviewed the debate in the vision literature concerning the inadequacy of the adaptation function in humans[11]. Such a discussion is parochial to the overall design tradeoff process. To achieve a significantly faster adaptation rate would compromise the rotational capabilities of the eye and seriously degrade the ability of the human to read.

The level of circuit integration found in the photoreceptor cell appears to be the highest of any neuron. This is due to the large number of discrete functions performed within the individual cell. From a system design perspective, the photoreceptor cell is a work of art. To achieve this level of integration, the signaling function of the photoreceptor cell is extremely nonlinear. The individual nonlinearities range from the simplest to the most complex, from the static to the dynamic. Analyses in the literature that have not recognized these nonlinearities have led to many unsupportable hypotheses. The concept of "dark light" is one of these.

## 12.1.3 Definition of the cytological situation

As was developed earlier, the photoreceptor cell found in the vision process is a complex, multi-functional one. The Outer Segment is not an integral part of the cell; the Inner Segment of the cell has both a exocrine glandular function and a neural function. It appears that the neural function is not actually involved with the photodetection process; therefore, it is generally categorized as a secondary receptor in Torrey[12] and similar texts. That is to say, the dendrites of the neuron receive irritation from something other than photons; in this case, the irritation is caused by interaction with the chromophoric liquid crystal when that element is in an excited state. This situation, involving the expression, “encapsulated nerve endings”, is well illustrated by the photoreceptor case, where the outer ends of the dendrites (actually a unique feature labeled a microtubule in the vision modality) are either enclosed in the deep fissures around the periphery of the disks or at least in intimate contact with the disks in these regions as illustrated in **Section 4.3.5.1**.

---

[11]Leibrock, C. Reuter, T. & Lamb, T. (1998) Molecular basis of dark adaptation in rod photoreceptors. Eye, vol. 12, pp 511-520

[12] Torrey, T. (1971) Morphogenesis of the Vertebrates. New York: Wiley & Sons. pg 466.

The complexity of the photoreceptor cell continues to present a problem for biological researchers. Because of the sizes involved and the tools available, we are still faced with a situation similar to that of sticking two probes through the outside case of a radio receiver and trying to define the type of music being received based on the signals detected. This is a particular problem with "intracellular probing" which is similar to contacting the face of a microcircuit chip with a probe large enough to contact 10-100 signal traces at one time; in this case the waveform on the probe may be a complex sum of signals and the internal circuits may be significantly damaged.

As indicated earlier, the techniques developed by the Baylor school are quite sophisticated and provide very interesting data. However, even these techniques leave several questions open. For instance, the replacement of the fluid of the IPM with a ringers solution may change the situation surrounding the OS significantly and create leakage paths to the polar ringers solution that may not exist in the real situation. It is well documented that the IPM *is* isolated from other interstitial fluids but the *reasons* for this are not documented. Secondly, although not discussed in detail by those authors, the technique used measures the net charge or current crossing an interface; it does not mean that only one conductor was involved. This is similar to placing a non-contacting current meter around a cable containing all of the wires going to a motor. The meter will read either zero or a leakage current but will not give any indication of how much current is actually passing through the motor windings; If you place the meter around only one conductor in the cable, you will get a correct reading for that individual conductor. In the Baylor case, it may be that the measured inward current is actually a leakage current to the ringer's solution Secondly, the net current measured may be due to a relatively constant inward current on one conductor subtracted from a second outward conductor on an adjacent conductor(s).

## 12.1.4 Derivation of the Circuit Analog

The circuit analog defined below may appear arbitrary on first viewing; however, it is able to accurately account for the performance of the visual system in considerable detail--the key criteria for a good model to meet. The equations of circuit synthesis do not lead to singular forms of a model but allow for models with different focus, i. e., in electronic modeling, it is frequently desirable to use either a voltage source model or a current source model but not both for the same source. **Chapter 9** addresses additional points relative to creating circuit analogs. This model has allowed many details of the mechanisms involved to be illuminated in a very useful way, specifically with regard to the mechanism of brightness adaptation. This process involves much more than the "bleaching" of a molecule. A model can never be complete, this one will surely be modified and expanded in the future, that is its basic reason for existing here.

As a starting point, no data could be found representing the measured signal output of the chromophoric material alone following excitation. Therefore, the problem was addressed as a typical 4-port black-box consisting of two internal stages, transduction of photons to excitons and then translation of the excitons into free electrons on (in) a conductor. The boundary conditions were available, particularly the output conditions as illustrated in Figure 3 of baylor & Hodgkin[13]. The challenge is to define a simple (or the simplest) circuit that can provide these characteristic in a biological context. In 2016, a paper was found describing, indirectly, the transfer function of the chromophoric material of the outer segment (Baylor, Lamb & Yau, 1979, **Section 12.8.1.3**).

In the literature, transduction has generally been used to describe an overall conceptual process of converting a photon into some kind of signal useful neurologically. In this work, a much more specific description of this overall process will be given and the terminology will necessarily be further definitized. Specifically, transduction will be taken as, and limited to, the process of absorbing an incident photon and creating an excited electron in the $\pi^*$ band of a chromophoric layer of the OS associated with a photoreceptor cell. Translation will be taken as, and limited to, the process whereby an excited $\pi^*$ electron of the chromophoric layer is de-excited and a free electron is produced within the dendritic structure of the neuron associated with the IS of the same photoreceptor cell. These are intrinsically different kinds of processes. **Figure 12.1.4-1** describes the operation of the Outer Segment in block diagram form, except where it introduces the active device, the Activa. An Activa of type AS is used in the microtubules of the photoreceptor cell.

One of the most important boundary conditions illustrated in this figure is the complete electrical and quantum mechanical isolation of the chromophoric material of the disk assembly in its two critical roles represented by the two functional blocks. These blocks are labeled the liquid crystal chromophore and the "piezo-electric convertor. The later name may be poorly chosen. The function involved is the de-excitation of an exciton in the chromophore

[13]Baylor, D. & Hodgkin, A. (1973) Detection and resolution of visual stimuli by turtle photoreceptors. J. Physiol. vol. 234, pp. 163-198

back to the ground state simultaneously with the creation of an electron-hole pair in the base region of the Activa. The only interactions with the chromophoric material are via quantum processes, either due to a photon exciting the material on the left or an exciton interacting with an electron-hole on the right. The excitation process is constrained by the limited energy acceptance range of the chromophoric material. Only photons with energy within this band can excite the bound electrons of the auxochromes of the chromophore. The material is essentially transparent to photons of other energy. A similar constraint exists at the interface between the piezo-electric convertor and the base region of the Activa on the right. The material forming the base of the Activa, believed to be a crystal of hydronium, has a minimum activation energy also. It is believed to be not more than 2.34 electron-volts at 37 degrees C based on analysis of the work of Sliney. It is probably closer to 2.0 electron-volts. Upon creation of an electron-hole pair in the base region of the active electrolytic semiconductor device, the Activa, a current is caused to flow in the collector and emitter circuits of the device. This current is no longer a quantum mechanical process. However, the amplitude of the current is very closely related to the number of quantum mechanical events occurring between the chromophore and the base region of the Activa and the lifetime of the electrons and holes formed in that region.

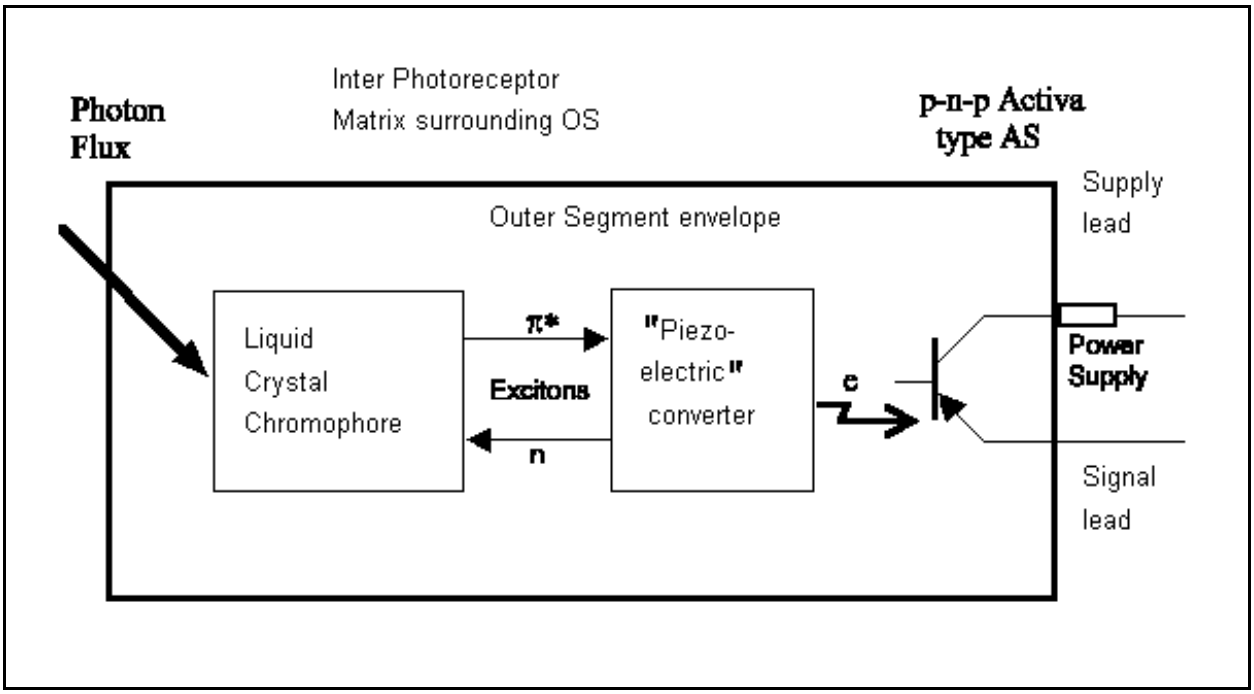


**Figure 12.1.4-1** Block Diagram of Outer Segment and the translation function. The piezo-electric convertor is the interface between the liquid crystalline chromophore layer surrounding the opsin discs and the dendrites of the stage 1 adaptation amplifier (p-n-p Activa) shown. The exciton is returned to the ground state, n, as an electron is inserted into the base region of the Activa. The outer segment envelope is not the lemma of the inner segment. It is merely an agglomeration of chemicals from the matrix.

**Figure 12.1.4-2** illustrates the electrolytic circuitry of the photoreceptor cell. There are no metallic conductors in such a circuit. On the other hand little if any current flows by common electrolysis. The liquid-crystalline nature of the neuron suggests most of the "current" flows within a liquid-crystalline semiconductor context.

The left side of the schematic is descriptive of one microtubule (cilia). The current from all of the microtubules pass through the ciliary collar and are joined to the output amplifier as described above. For simplicity in further description, all of the "first amplifiers" and individual microtubule leads will be replaced by a single equivalent amplifier that will be called the adaptation amplifier. Thus a single adaptation amplifier is connected to a single output amplifier. More will be said later about the multiple impedances and power sources shown.

The overall photoreceptor circuit is arranged as a differential pair, a common circuit in man-made analog circuits. In this case, the circuit is asymetric: the two axonal power supplies exhibit different impedances, and the two Activa may be of different net size. One of the principal features of such a circuit is the constant current through the dendritic impedance, $R_e$. Note also the fact that the base lead to the Activa on the left is not connected electrically to

any other potential. The junction associated with this Activa receives all of its excitation quantum mechanically from the transducer. This feature is common in man-made photo-transistors.

### 12.1.5 Falsification of "rods & cones" concept

A major discovery of the 1980's when placed in a system context, and a major take-away from a reader of this work is that the ancient and *archaic* concept of "rods and cones" is found in the laboratory to be unsustainable and in fact *falsifiable.*

***Individual photoreceptors exhibit a dynamic range of over 6 orders of magnitude***. as shown in **Section 12.5.1**. This dynamic range is exclusively a feature of the photochemistry of the chromophores (except for the function of the pupil over a range of less than a decade). It is not associated with the inner segment of the photoreceptors at all. The amplifiers within the inner segment will be shown to operate in a constant-amplitude environment.

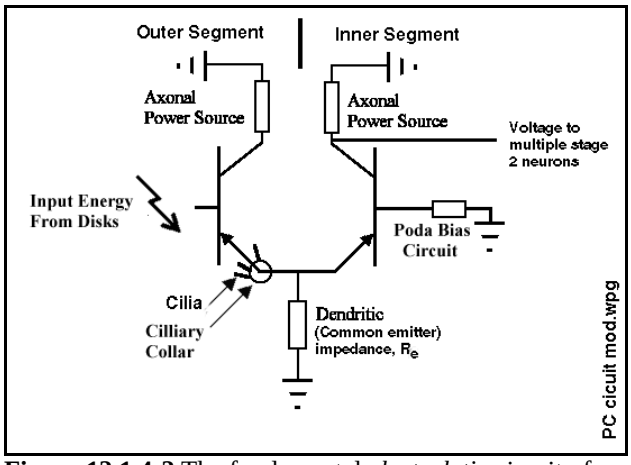


**Figure 12.1.4-2** The fundamental *electrolytic* circuit of the photoreceptor cell showing the adaptation amplifier within the outer segment and the distribution (output) amplifier within the inner segment. See text for details.

As a result of this dynamic range capability in all photoreceptors, there is no need for multiple types of photoreceptors serving different intensity ranges of stimulation!

Equally important, ***no investigator has ever reported a photoreceptor with a broad band spectral response attributed to a rod***. The scotopic spectral response of an eye is always subject to differential spectral adaptation demonstrating the scotopic spectral response is a perception formed from signals from two spectrally distinct photoreceptors.

***The concept of "rods and cones" must be immediately abandoned at the research level*** *in order for the truism of* ***no broad spectral band receptors of exceptionally high sensitivity are present in the retina****, to eventually trickle down in the introductory texts related to vision.*

## 12.2 The physiological character of the stage 1 photoreceptors

It is important to review the actual cytology and morphology of a stage 1 photoreceptor neuronbefore delving into the operational features of such a complex structure.

### 12.2.1 The cytological character of a generic neuron

The literature has occasionally associated the nucleus of the photoreceptor neurons with some undefined amplifier mechanism. This assertion has never been detailed or confirmed. In fact, the nucleus of any cell plays no role in the neural functions of that cell. This is specifically true with regard to the photoreceptor neurons (**Section 2.2.2.6.1 of the text, "The Neuron and Neural System**[14]**."**

Cantarow & Shephartz provided a detailed schematic of a prototype "cell" in 1967[15]. **Figure 12.2.1-1** from the above citation, extends their schematic to include the additional functions associated with a neuron (a neuro-sensory neuron). The central portion of the figure is similar to the Cantarow & Shephartz cell, with some of their detail omitted. The left-most portion adds the unique neural functions found in all neurons. The right-most portion adds the unique secretory functions. Both the neural and secretory portions are found in nearly all sensory neurons and

[14]Fulton, J. (2008) The Neuron and Neural System. Available Online; https://neuronresearch.net/neuron

[15]Cantarow, A. & Schepartz, B. (1967) Biochemistry, 4th Ed. London: W. B. Saunders. pg 2

are critical to the operation of the digestive system. However, the sensory neurons are more complex and are discussed initially in **Chapter 8** the Neuron and Neural System.

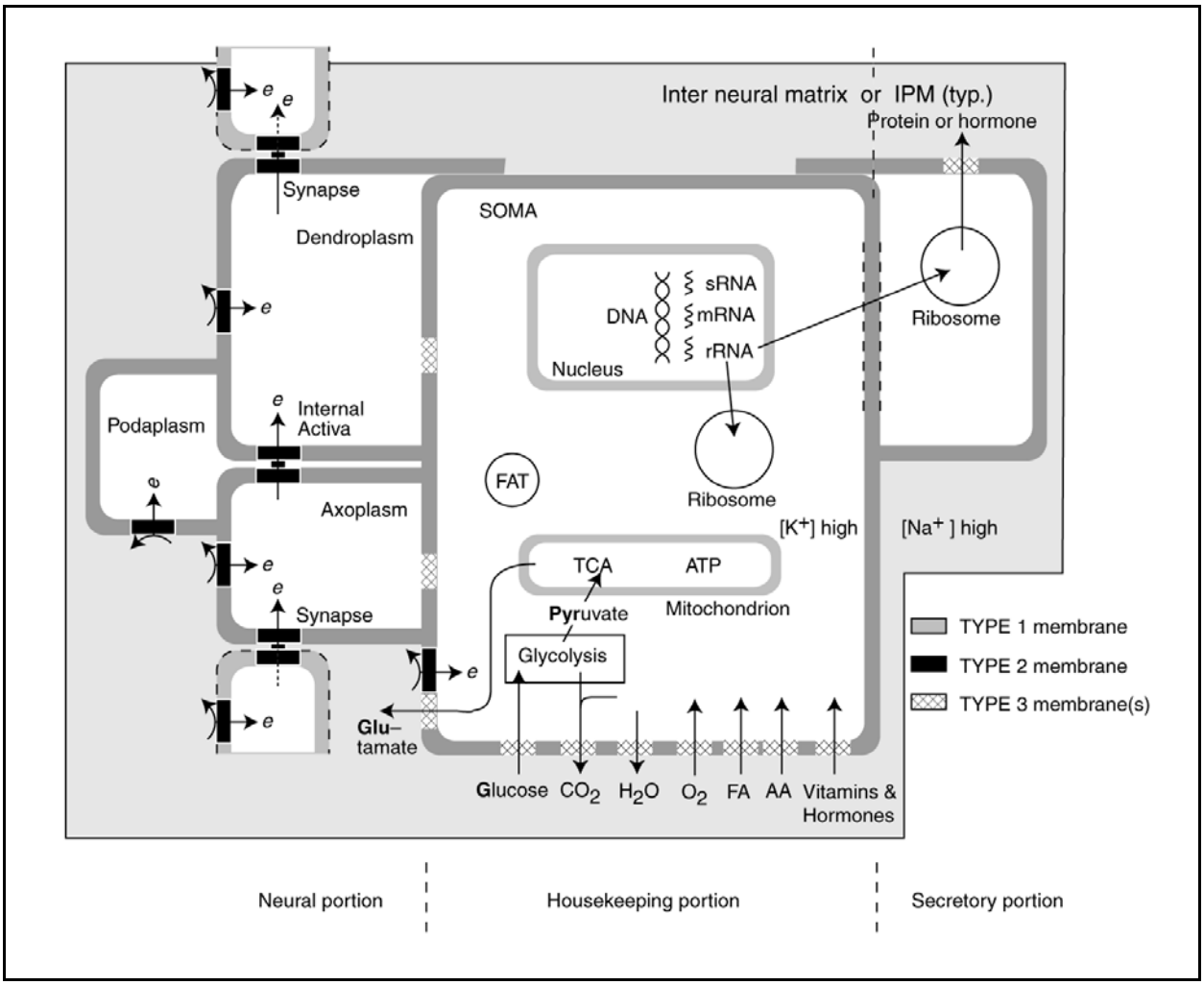


**Figure 12.2.1-1** A more fully elaborated *cytological* schematic of a fundamental neuron. All membrane junctions are lap joints (as shown only along the top edge). The housekeeping functions shared with the prototype cell are shown in the center. The label "Vitamins & Hormones" includes other complex molecular entities. FA; fatty acids. AA; amino acids. The additional secretory functions are shown on the right. The additional neural functions are shown on the left. Dotted shapes on the left are portions of adjacent neurons. Note the three separate conduits associated with the neural portion, including the podaplasm filled podite. See Text.

The neural portion consists of three distinguishable chambers (conduits) that are described in detail in the Section 2.2.2 of the cited text. Note the narrow region of the podite conduit containing podaplasm and separating the dendrite and axon conduits. This is the site of the Activa of the neuron. The secretory portion may or may not be a separate chamber, independent of the soma.

## 12.2.2 The morphological character of a photoreceptor neuron

**Figure 12.2.1-2** reproduces Figure 4.3.2-1 of **Section 4.3.2** in order to describe the morphology of a photoreceptor neuron in detail.

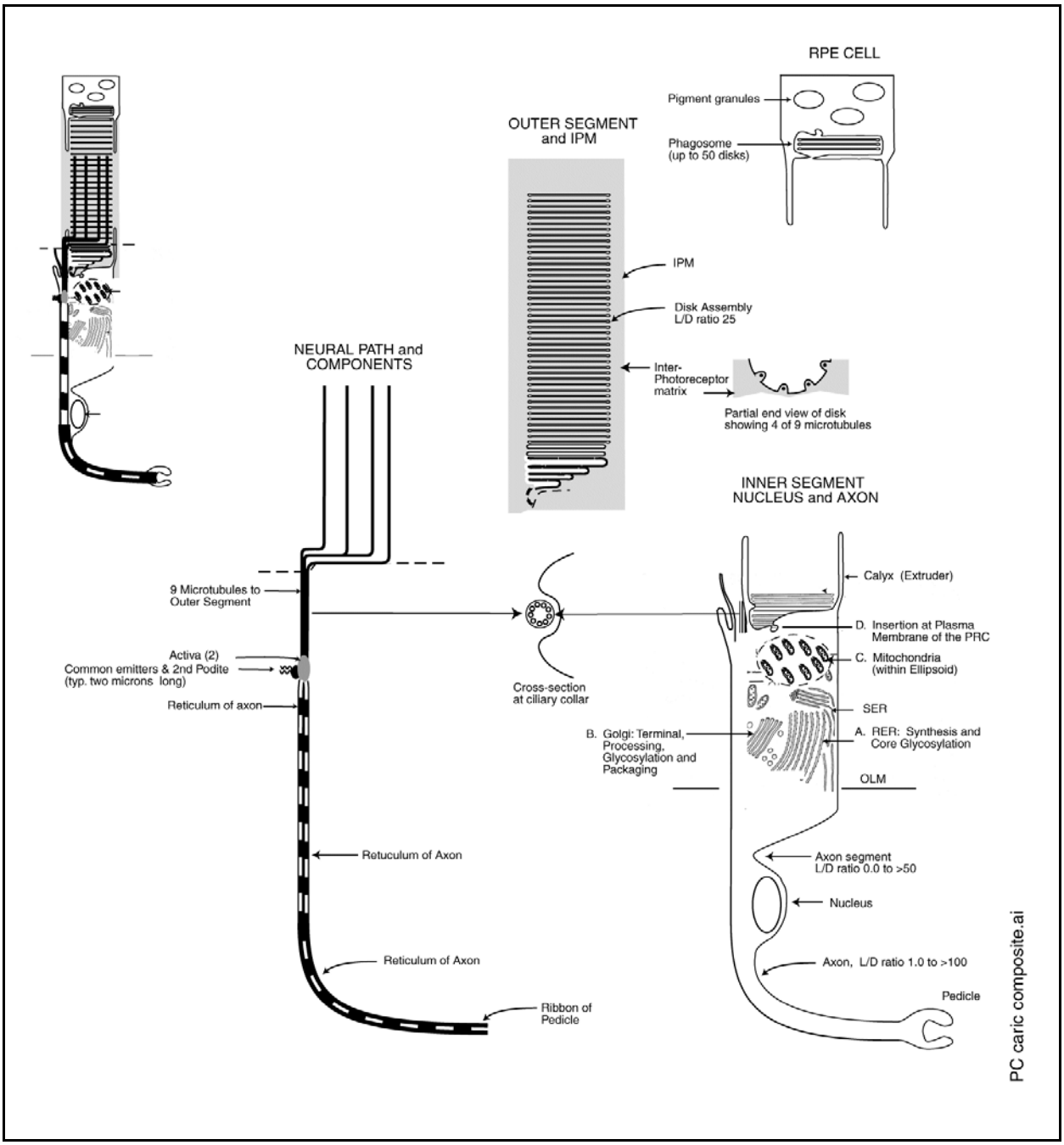


**Figure 12.2.1-2** An exploded *histological* view of the baseline photoreceptor cell configuration. An RPE cell is shown at upper right. The central image is the extracellular Outer Segment, i.e., the disk stack immersed in the IPM (foreshortened for convenience). The typical disk stack consists of 2000 disks, formed into a "spaceframe" structure and immersed in the IPM. The lower left shows all of the neural elements of the photoreceptor cell as a group (including both the distal and proximal axon segments). The distribution Activa is shown explicitly. The microtubules represent both the "quasi-dendrites" of the distribution Activa as well as the Activa associated with the adaptation amplifiers. The adaptation amplifier Activa cannot be shown at this scale. The lower right image shows all of the glandular portion of the photoreceptor cell (exemplified by the inner segment) as well as the other housekeeping functions (exemplified by the nucleus).

This figure was created before the presence of two Activa within every photoreceptor neuron was recognized. The label along the left side of the complete photoreceptor have been changed from earlier renditions of this figure. The labe Acitva has been changed to Activa (2) and the word below the word Activa has been changed to common emitter terminal and 2nd Activa podite terminal. In the exploded view two different names are given for a number of elements to ease correlation with the literature and language of various disciplines. A discussion concerning the most appropriate names to be used in further (and future) investigations will also be found in **Section 4.3**. The nine-microtubules emanating from the cilliary collar are in fact podites of the first Activa of the photoreceptor. They form a chalice that surrounds and interfaces with the discs of the outer segment of each photoreceptor.

## 12.3 Mechanism of the photodetection process

### 12.3.1 Electronic Characteristics of the Chromophores

The chromophore defined in Chapter 6 as the Rhodonine family are not easily defined in their entirety because of the nearly unlimited variety of characteristics available to a molecule that contains 19-20 carbon atoms and can be defined as a member of at least 10 organic molecule families. Although the initial construction of its chromogen was undoubtedly via the isoprene chaining process. The resultant chromogen can be defined as a Vitamin, as a derivative of a lipid, as having a hydrophobic characteristic due to its hexene ring, as being hydrophilic due to its carboxyl group, or as being an alcohol due to its -OH group, etc. When converted into an actual molecule of the chromophore, the situation becomes even more complex. The molecule now exhibits both a carboxyl group and an alcohol group at the same time. A test for only one of these groups is not definitive as to what chemical class the molecule belongs. A test for the simultaneous presence of both groups would be more analytical but could be more difficult if the chromophore is in fact in an ionic state as usually proposed in the literature. In this work, it is proposed that the chromophore is not usually in the ionic state and is in fact associated to any substrate by hydrogen bonding or Van der Waal forces, a common situation found between many of the types mentioned above and various proteins. In conclusion, it should be emphasized that the Rhodonines are derivatives of the Retinene family and will generally test positive for Retinene; in fact it will test positive for both the carboxyl and alcohol members of that family simultaneously. They may also exhibit some activity similar to that of Vitamin A.

At the individual molecule level, the Rhodonines are not spectacular pigments; they are small molecules with relatively low absorption cross sections. Each molecule does exhibit a completely conjugated carbon chain connecting the two auxochromes and it is able to absorb several photons but the minimum energy requirements may rise rapidly if enough empty excited states are not available. This is particularly true for the minimum energy situation involving the excitation of a non-bonded *n*-electron into a $\pi^*$ energy level. When the molecule is joined by other molecules in the spontaneous formation of a liquid crystal that is not associated with any other structure, the situation improves immensely. Under this condition the $\pi^*$ bands overlap and merge, forming in effect a form of continuous conduction band, and a band which has no preferential electric field vector. The individual *n*-electrons of each molecule can now be excited into the $\pi^*$ energy band without saturating that band locally and without exhibiting any polarization preference. Through this effect, the absorption cross section of the liquid crystal is expanded immensely.

While in the un-associated liquid crystalline state, the orientation of the liquid crystal is not controlled with respect to any incident photons and its absorption cross-section may vary considerably with the angle between the axis of the conjugated carbon chain and the Poynting vector of the incident light. If however, the liquid crystal is allowed to precipitate out onto a substrate, which it is very inclined to do, then the orientation of the molecules can be controlled easily and the light can be applied in the proper direction to achieve a maximum absorption cross-section.

This last situation is the culmination of the optimization process and is the same configuration used in the color photographic process, although this author is not aware that the art allows concentrating the liquid crystal on only the surfaces of the silver halide facing the incoming illumination.

#### 12.3.1.1 The Photo-Electron Excitation Process

Based on the material in Chapter 5.1.4, the Outer Segment is seen to consist of a space frame consisting of a series of disks stacked like poker chips, each of the chips near the Inner Segment end having a crenelated edge. The notches in these disks appear to be aligned and occupied by what histologists have called microtubules but which a neurologist would call dendrites. Each disk of the space frame consists of a core disk believed to consist of a heterogeneous structure of protein and lipid material which is coated with a mono-molecular layer of Rhodonine in a liquid crystalline structure. This structure surrounds both the surface and end pieces of the core disk. The disks are pressed together, but interestingly, the protein-lipid parts probably do not touch each other; the contact between the layers being between adjacent layers of the liquid crystals. Thus, if there is electrical, exciton or phonon (piezo-mechanical) transfer of energy between these layers, the result is a relatively large, monolithic structure of the

chromophores held in parallel planes; all (except those involved in turning the corner) with their conjugate chain axes aligned with the Poynting vector of the incident light. This provides a very large area for the absorption of the photons with a number of important features:

+ the photo-electrical properties of the structure do not exhibit any polarization preference for light traveling along the length of the space frame (although illumination from the side will show a polarization preference exactly as shown by Baylor, Lamb & Yau[16]).

+ the slow wave structure of the conjugated chain of the chromophore makes the effective distance between the auxochrome layers approximately 230 times their actual spacing according to Dewar[17] resulting in an almost perfect length for causing the peak absorption band to appear in the visual spectrum at one of three locations depending on which of the Rhodonine chromophore is present in that photoreceptor.

+ the spacing between liquid crystalline layers is such that the effective index of refraction of the entire column of material is not greatly different from that of the immensely more massive protein-lipid layer and/or the interstitial fluid which is water based with an index near 1.33. This prevents the incident photons from encountering a major change in index which would cause the photons to be reflected and expelled from the entrance end of the Outer Segment.

+ the large number of chromophores present in the shared structure of the space frame provide an immense number of photo-excitable *n*-electrons and a shared $\pi^*$ energy band structure which can accept them.

---

[16]Baylor, D. Lamb, T. & Yau, K-W (1979) The membrane current of single rod outer segments. J. Physiol. Vol. 288, pp. 589-611

[17] Dewar, M.(1952) Color and Constitution. III. Polyphenyls, polyenes, and phenylpolyenes; the significance of cross-conjugation *J Chem Soc* pp 3544-3550

The absorption cross-section of this structure is dependent on the number of unexcited n-electrons remaining in the unexcited state to the total number of n-electrons present prior to any excitation. Depending on this ratio, the effective absorption characteristic can vary over a very large magnitude, more than 10 to the eighth power. If the light continues to excite n-electrons faster than they are de-excited, the material will "bleach", thus reducing its absorption coefficient and resulting in the storage of a large number of electrons in the $\pi^*$ energy state of the liquid crystalline structure.

> It is important to note that an Outer Segment that is separated from its Inner Segment will continue to be light sensitive initially. However, the number of available unexcited n-electrons will continually decrease with photon excitation. The unique dipolar mechanical arrangement of the auxochromes of the chromophores prevent these materials from relaxing by thermal or flourescent mechanisms. As a result the material will become transparent. Its only mechanism of relaxation is by secondary means with time constants measured in hours. Researchers usually report that any excited material, derived from separated Outer Segments and stored in the dark, has relaxed when they return to work the next day.

### 12.3.1.2 The Electron-Neural De-excitation Process

Building on the foundation of the previous Section; one further assumption will be made. It is known that the de-excitation of photo-electrons of the OS alone in-vitro is a very slow or non-existent process. Generally, de-excitation will occur overnight which implies a second order thermal relaxation. This fact indicates two things. The protein/lipid layer at the core of a disk does not provide an effective medium for energy transfer from the liquid crystalline structure. Further, the no longer vital dendrites of the nervous tissue remaining within the Outer Segment structure do not provide an effective de-excitation avenue either.

It is quite reasonable to assume the disk substrate materials alone do not support de-excitation of the liquid crystal. Neither the protein or the lipid classes of organic material typically exhibit any energy band differences in the range below 3 electron volts.

It is also quite reasonable to assume the no longer living nervous tissue cannot continue to interface with the liquid crystal in its normal manner. As will be seen below, a biologist would say it is only able to interact with the liquid crystal when it is in the irritable state when alive, not while it is in its refractive state or when no longer "live". The physicist would suggest an alternate explanation. Unless the Activa is properly biased, the electron-hole pairs created within the base region of the Activa will not be removed from that region. The resultant unsustainable charge distribution within the region will no longer allow acceptance of energy from the pizo-electric convertor. Therefore, the chromophore becomes increasingly excited and it is said to bleach.

It is also well established that the chromophores, at least the chromogens of the Retinene family do not fluoresce when excited, indicating that they do not spontaneously de-excite by re-radiation, at least in the anticipated and observed spectral regions

Therefore, the proposition will be made that it is a function of the living neural component of the photoreceptor cell which is responsible for de-exciting the electrons occupying the $\pi^*$ energy state of the liquid crystal in the Outer Segment of that same cell.

This proposition introduces an interesting avenue of investigation. A neuron is normally a rate limited signaling device, with a maximum propagation velocity limited by the impedance of the axon sheath and a specific refractory interval before it can be caused to fire a subsequent time. A neuron exhibits a minimum input signal below which it will not fire. This level is generally in the neighborhood of 2.0 electron volts or more. For comparison, the energy threshold of silver bromide is approximately 2.6 eV. Since the energy of thermally excited electrons at the temperature of the body is approximately 25 milli-electron-volts, this provides a satisfactory margin against self induced firing. 2.6 eV is also equal to the energy of an absorbed photon with a wavelength of 0.48 microns, a very "blue" photon. 2.0 eV. corresponds to a photon at 0.61 micron, an "orange" photon.

## 12.4 Earlier conception of the amplification process in neurons

Rodieck[18] has provided a summary of the theories of amplification in vision *circa*. 1973. He found these to fall into

[18]Rodieck, R. (1973) Op. Cit. pg. 332-337

three categories; the proenzyme hypothesis, the photoconduction hypothesis, and the saccule hypothesis. These theories were primarily concepts at that time and they have not matured substantially. The saccule hypothesis has been advanced into the glutamate cascade hypothesis. However, this concept is also supported primarily on its ability to meet the perceived requirements based on kinetics and the use of certain chemicals found ubiquitously near neurons. As Rodieck said, "A general difficulty with all saccule hypotheses is that they fail to account for the behavior of cones whose outer-segment lamellar structure results from infolding of the outer-segment plasma membrane. . ." Concurring with another Rodieck statement, the photoconduction hypothesis, involving a change in conductivity, is not promising. Unfortunately, he also discounts the entire field of photoconduction and photovoltaic effects without further definition of the terms. The proenzyme hypothesis has not been pursued since the 1960's.

> **The primary problem with the saccule and subsequent cascade theories is the absence of any evidence of a membrane surrounding the outer segments of the photoreceptors**. To the contrary, recent electron microscopy has shown the total absence of such a membrane in a wide range of chordates. See the website, www.4colorvisioncom, for a substantial reward for any conclusive evidence for the presence of such a membrane in humans or other chordates.

MacLeod, et. al. have argued that the adaptation process is different in cold-blooded than in warm-blooded animals on purely psychophysical grounds[19]. They did not provide any rigorous model of the proposed mechanism or even quantify the gain mechanism involved. They built on a paper by Rushton in 1965 that claimed that the sensitivity of the rods (the putative achromatic detection mechanisms in vision) never changes and that the adaptation mechanism was found in a "pool" subsequent to the photoreceptor cells. These concepts are not supported here.

Based on this work, the mechanism of amplification can be clearly defined based on conventional semi-conductor electronics applied to the electrolytic environment of biology. The mechanism provides a recognized method and and achievable amount of amplification. It also explains the variation in the amplification based on the state of the applicable variables and circuits . The circuit details and results presented below contribute directly to the comprehensive understanding of the adaptation characteristics of vision presented in **Chapters 16 & 17.**

## 12.5 The Complete Stage 1 Photo Detection Process

The block diagram of a suitable network representing the photodetection function of the photoreceptor cell must contain the following elements:

1. The chromophoric transducer for which the transfer function is known and known to be nonlinear at high signal levels.
2. The exciton to electron transducer which is known to preserve the quantum nature of the signal at least at low light levels.
3. An amplifier with a passband of at least 100 hertz which is able to output approximately $3 \times 10^4$ electrons per input photon in the linear region but which exhibits a significant degree of saturation at output currents near 20 pA.
4. A power source able to provide the above number of electrons as a minimum to the amplifier when the incident flux level is measured in 100-1000's of photons per second per photoreceptor.

It must exhibit a variable time delay as a function of the input illumination. It is also necessary that some element in the network provide a level control such that the output signal excursions remain within the dynamic range of the output device, typically 0- 20 pA in the turtle but ranging up to 29 pA in both the turtle and salamander, while the input intensity varies slowly over a factor of $10^5$ or more. Although this may consist of an amplifier with a logarithmic transfer characteristic, this is unlikely. The signal saturation exhibited by the data indicates that a different approach is more likely.

The automatic gain control of vision is quite different. It is associated with the bleaching of the chromophores of the retina. It involves an internal feedback mechanism (**Section 12.5.3**). That is there is no identifiable external feedback path.

With these requirements and mechanisms in mind, the circuit of **Figure 12.5.1-1** is suggested. **(A)** shows the

---

[19]MacLeod, D. Chen, B. & Crognale, M. (1989) Spatial organization of sensitivity regulation in rod vision. *Vision Res*. vol. 29, no. 8, pp 965-978

functional block diagram. **(B)** shows individual portions of the proposed circuit for illustrative purposes and **(C)** shows the overall circuit as proposed after assembly.

The top level functional block diagram is shown as Stage 1 in **(A).** It is accompanied by several rows of labels to orient the reader and provide a consistent relationship between the labels found in the literature. A critical point to note in the top row of labels is that the dendritic structure associated with the IS is physically located within the OS. This places the functions of transduction, translation, and adaptive amplification all within the structure of the OS. The IS is the home of the output, or distribution amplifier, of the photoreceptor cell. This amplifier uses an Activa with a different performance characteristics and therefore a different type designation. The dashed vertical line indicates the probable location of the Outer Limiting Membrane, OLM. The primary purpose of this membrane appears to be the chemical separation of the specialized metabolic processing of the IPM from the more normal metabolic processing of the INM. This membrane is, however, an electrical insulator. It plays a significant role in the signaling function of the visual system. The two arcs crossing the OLM external to the complete photoreceptor cell represent the ground bridges that play an important role in creating the conventional ERG waveform.

**(B)** presents the individual circuits of the photoreceptor cell for ease of discussion. The two sections on the left are laid out according to the earlier discussion. The left most diode, labeled TD for TransDuction, is the symbol used for the electronic analog of the quantum mechanical process supported by the chromophoric material during excitation. This diode is shunted by a capacitor, $C_T$, representing the quantum mechanical equivalent of the excited state of the chromophoric material. The diode is also shown shunted by an impedance $Z_1$. As discussed above, the unique character of the chromophoric molecules makes the decay time constant of the equivalent circuit, $Z_1 \times C_T$, hours long. The second diode, labeled TL for TransLation, and impedance, $Z_2$, constitute the de-excitation process of the chromophoric material when in contact with the properly biased Activa labeled AS. The Activa is shown in its bulk form to emphasize the energy is transferred from the chromophore material to the n-type region of the p-n-p device forming the current amplifier. The impedance, $Z_2$, is a pure delay circuit representing the travel time related to the travel distance between the point of creation of an excited electron, an exciton, in the chromophoric material and its point of de-excitation along the fissures of the disk stack. This delay element is a variable related to the intrinsic repulsion between likely charged particles within the conducting region of the $\pi^*$ band of the liquid crystalline structure.

The impedance in the collector lead of the Type AS device is located within furrows of the disk stack and is in contact with the electrolytes of the IPM. There is no membrane separating the disk stack from the IPM. There are only the materials associated with the electrostenolytic supply. They are stored as coatings on the outside of the disk stack, including the volume within the furrows. These materials react on the outer surface of the dendrites in order to power the type AS Activas. That is why, the real impedances associated with the Activas are shown straddling the membrane wall of the photoreceptor cell. These are real impedances represented by standard electronic components. The part outside of the cell wall constitutes the battery element of the supply and the part inside the cell constitutes the diode representing the cell wall. Where appropriate, these impedances are shown shunted by a real capacitance. In the case of the type AS device employed in the variable gain adaptation amplifier circuit, this capacitance is an integral part of a low pass filter along with the electrostenolytic supply and the cell wall. As will be shown elsewhere in detail, this low pass filter has two poles. These poles determine the shape of the dark adaptation characteristic of animal vision. This same capacitor is also part of the charging circuit that controls the light adaptation characteristic of animal vision.

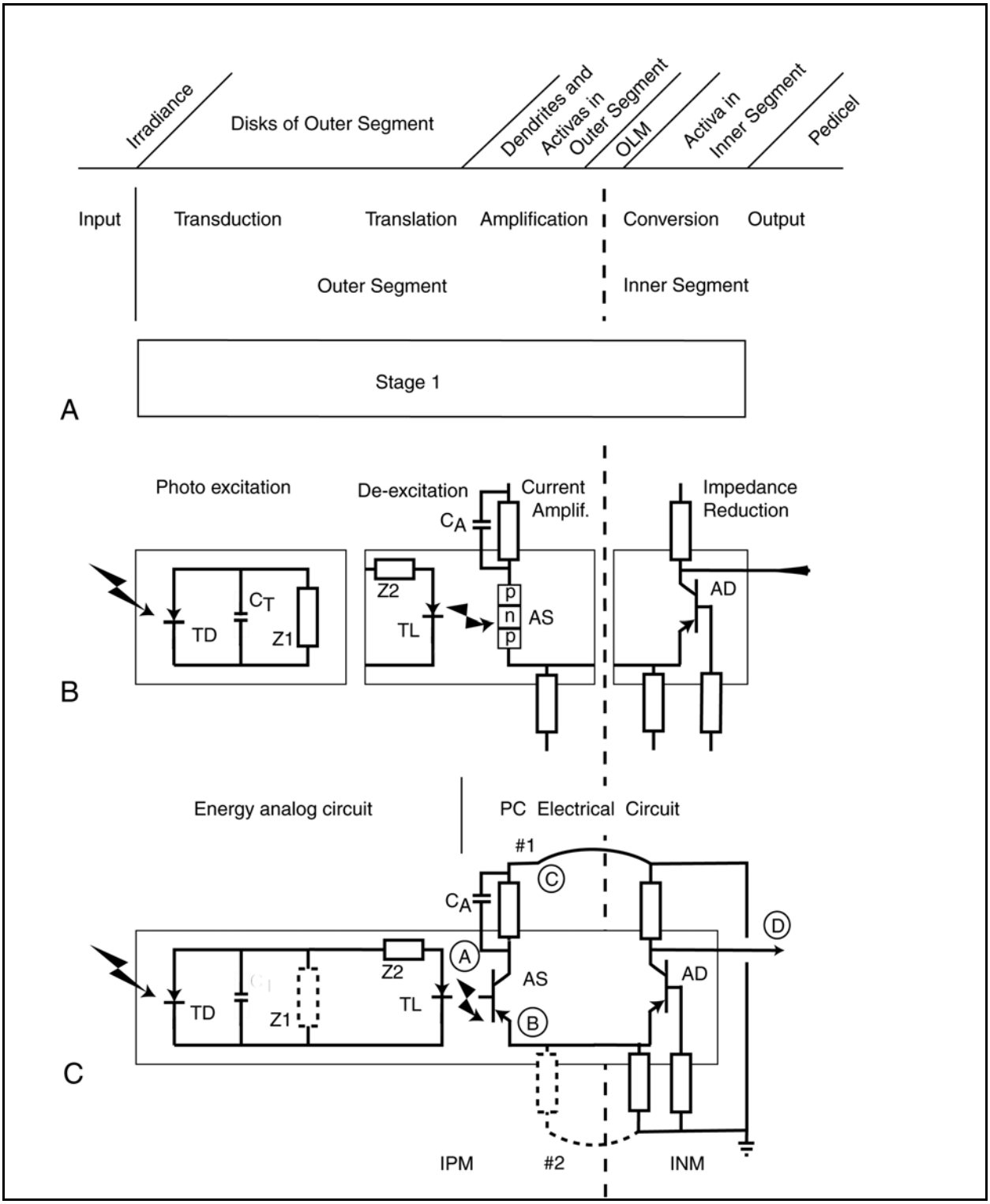


**Figure 12.5.1-1** Nomenclature, block diagram and overall circuit for Stage 1, the photodetection process in vision. (A) The nomenclature in context. (B) The three basic circuit blocks and the transition from energy to electrons as the signal carrier. The Activa of the current amplifier is shown in its bulk (p-n-p) form. (C) The overall circuit diagram expressed in standard symbols.

The Activa on the right in **(B)** is located within the IS of the photoreceptor cell. It is arranged in a common base configuration. The result is that this circuit can act as a unity gain current amplifier with a much lower impedance at its output collector than at its emitter terminal. By passing this current through a suitably sized load impedance, this circuit is able to drive multiple synapses leading to other circuits. Not shown diagrammatically, but extremely important, is the fact that the diode in the collector impedance of this circuit consists of a significant area of the axolemma of this cell. This portion of the axolemma is also coated with electrostenolytic material. As a result, the voltage of the axoplasm is a logarithmic representation of the current through the distribution amplifier and the load impedance. The current supply to the collector terminal of this device is clearly in contact with the INM. Similarly, the poditic supply serving the base terminal and the dendritic supply serving the emitter are also in contact with the INM.

**(C)** merges the circuit elements of **(B)** into a functional photoreceptor cell. The symbols representing circuit elements to the left of the solid vertical line are representations of a quantum mechanical process. The symbols to the right of the line are symbols representing real electrolytic circuit elements. This part of the diagram is not an analog of the visual process. It is ***the*** representation, using human symbols, of the actual process.

> *To the left of the vertical bar*, the description involves an **electrical analog to a physical system**, in this case, a quantum mechanical system. The current flowing in this analog will be used to describe the actual flow of excited electrons which are carrying a quanta of energy. The capacitor symbol will indicate the capability of the $\pi^*$ band to store quanta of energy and the number of charges on this capacitor at any time will indicate the number of quanta of energy available for de-excitation under the proper conditions. The open block in this figure will represent a resistive impedance in the analog. This is not the impedance found in an operating photoreceptor cell. This impedance relates to a potential dissipative process leading to the de-excitatin of the chromophoric material as observed in a laboratory after separation of the OS from the IS. It need not be a resistor, it may be a photon emitting device causing flourescence of the material.
>
> *To the right of the vertical bar*, the description uses man-made symbols to represent an actual electrolytic circuit within the photoreceptor cell. It is not an analog or an equivalent circuit. **It is a real circuit of a real photoreceptor cell.**

When combined in the manner shown, the two Activas share a common emitter terminal. Only one impedance is needed to represent the connection of this terminal to the electrostenolytic supply. Based on the knowledge that the emitter lead of the adaptation amplifier passes through the colax of the IS to connect to the distribution amplifier circuit, it will be assumed for the moment that this single impedance connects to the INM and not the IPM. Therefore, the dotted components on the right can be omitted. The resulting condition is compatible with the generation of an ERG as usually recorded in the laboratory. The impedance $Z_1$ has a much higher value than the combined impedance $Z_2$ and TL when the cell is in-vivo. Therefore, $Z_1$ is usually omitted from the combined figure.

This combined circuit incorporates:

1. A chromophoric photon to “exciton” transducer
2. A static gain control within the chromophoric mechansim
3. An “exciton” to electron-hole translator
4. A dynamic gain control mechanism and first Activa as an amplifier
5. An second Activa acting as a distribution amplifier
6. A current to voltage converter that also acts as a “hard” limiter

The extremely interesting fact is how all of these functions can be accomplished in such a simple combined quantum mechanical and electrolytic circuit. Another interesting fact is how the circuit elements act differently when not connected into a complete stage.

## 12.5.1 The Transduction Block in vision

The transduction function within a photoreceptor is performed by a liquid crystalline material coated onto the external surface of a protein substrate, known as opsin. The liquid crystalline material consists of one of four chromophores with an overall sensitivity to light with a wavelength of between roughly 300 nm. and 675 nm. Each chromophore is sensitive to a region of about 100 nm. within this range.

### 12.5.1.1 Fundamentals of biological transduction in vision

The chromophores are retinoids derived from Vitamin A. However, they are not retinal, retinol or one of these materials associated with the protein, opsin, through a Schiff-base linkage. Whereas both retinal and retinol contain a single polar atom in a conjugated carbon chain, the chromophores contain two polar atoms in a conjugated carbon chain. The optical performance of the compounds with 2-polar atoms is significantly different.

Both retinal and retinol exhibit an absorption spectra related to the length of the conjugated carbon chain they are based on. The peak of this absorption spectra is nominally 500 nm (some investigators have measured 498.3 nm). The absorption spectra of these materials is *isotropic* in dilute solution. The absorption coefficient of these materials is not very high.

The chromophores of the visual process are different. They exhibit a higher absorption coefficient based on the quantum resonance occurring between the two polar atoms. This resonance absorption is only exhibited when the material is in the liquid crystalline state. The spectral peak is not related to the total length of the conjugated carbon chain. It is only related to the length of the conjugated chain, including the polar atoms as termini, between the two polar atoms. Because of the "slow wave structure" found in the liquid-crystal, the spectral response of these materials is highly *anisotropic*. Peak absorption is achieved when the incident light is parallel to the optical axis of the individual molecules. This optical axis is essentially parallel to the mechanical axis of these all-trans molecules. Because of the "slow wave structure," the liquid crystal is most sensitive to a wavelength approximately 250 times longer than the physical length of the molecule.

The transduction block consists of the disks of the OS, more specifically, the chromophoric material, rhodonine, in the liquid crystal form present as a coating over the structural protein opsin. These coated disks are stacked into a column of thin disks. The photons that are intercepted by this column of disks, normally the column is irradiated along its cylindrical axis, are absorbed by the chromophores and cause an electron to be excited into the $\pi^*$ band of the crystal. Whether a photon is absorbed or not is controlled by the absorption cross-section of the OS at the spectral wavelength of the photon. All absorbed photons generate excited electrons. These excited electrons move within the energy band of the liquid crystal until they encounter some mechanism to cause their de-excitation. Normally, this cannot occur within the crystalline structure because of the symmetrical dipole configuration of the chromophores and the inability of the protein structure to absorb energy at these energy levels, approximately 1.0 to 2.5 electron volts. Over an extended period of time, the electrons will be de-excited through second order thermal processes such as interaction with the material found in the inter-photoreceptor matrix (IPM). This secondary process involves time constants on the order of a few minutes to a few hours.

Because of its great significance in vision, the transduction process and the resultant transfer characteristic of the process is treated separately in **Appendix A** and more compactly in **Section 7.2** of this work. The complete transduction equation, presented there as the Photoexcitation/De-excitation Equation (or the P/D Equation) is found to involve a differential equation of the first order with a complex argument. This complete equation can be simplified under a number of different assumptions leading to the correct mathematical form to correlate with the work of many different investigators. The results of this treatment will be utilized beginning with **Section 12.7**.

An analog of the energy circuit for the transduction block is shown in the left portion of **(b)**. This analog consists of a radiation sensitive photoemitter, a capacitor and a resistive element. This circuit can operate without the presence of a power source (a battery). As is discussed in Appendix A, the performance of the photoemitter is a bit specialized in that this circuit analog is isolated electrically from any other source of charges and involves quantum mechanics. The total number of available charges is finite. Therefore, the number of charges generated by the photoemitter, is limited by the number already moved from the bottom of the circuit to the top and stored on the capacitor. The excess charges stored on the capacitor are eventually returned to their original location by the resistive element. The value of this resistive element will become an important consideration in the overall operation of the circuit.

In the case of chordates, the liquid crystalline material of the chromophores is formed on the surface of the disc substrates with the optical axis of the chromophore perpendicular to the surface of the disc. In this configuration, the liquid crystal exhibits a very high absorption coefficient for light passing along the axis of the disc stack. It exhibits essentially no absorption to light passing perpendicular to the stack.

The above situation explains a problem in many laboratory experiments. The spectral absorption measured by micro-reflectometry along the mechanical axis of the OS will exhibit the anisotropic resonance absorption spectrum of one of the four chromophores. The peak will occur at either 342, 437, 523 or 625 nm. for animals at a body temperature of 37°C (98.6° F). The spectral absorption measured using an optical beam passing perpendicular to the mechanical axis of an OS will always exhibit the isotropic (non-resonant) absorption spectrum of the underlying conjugated carbon chain. In this case that chain shows a peak at 500 nm. regardless of which chromophore is actually present. This peak is not exclusive to retinal or retinol. It is characteristic of any simple conjugated carbon chain terminated with at least one polar atom.

### 12.5.1.2 Fundamental quantum-mechanics of biological transduction in vision

**Figure 12.5.1-2** illustrates the quantum mechanical model of the transduction process for a specific chromophore to transfer the energy of an incident photon to the dendrite of the IS for further manipulation. The terminology is discussed in detail in **Appendix A**. Only the highlights will be discussed below. The light shown enterring from the top is parallel to the long axis of the conjugated retinoid forming the chromophore. The typical disc diameter is 2.0 microns as shown on the left. The dimensions of the base region of the distributed 1$^{st}$ Activa within a microtubule of the photoreceptor is much smaller, on the order of 0.1 microns.

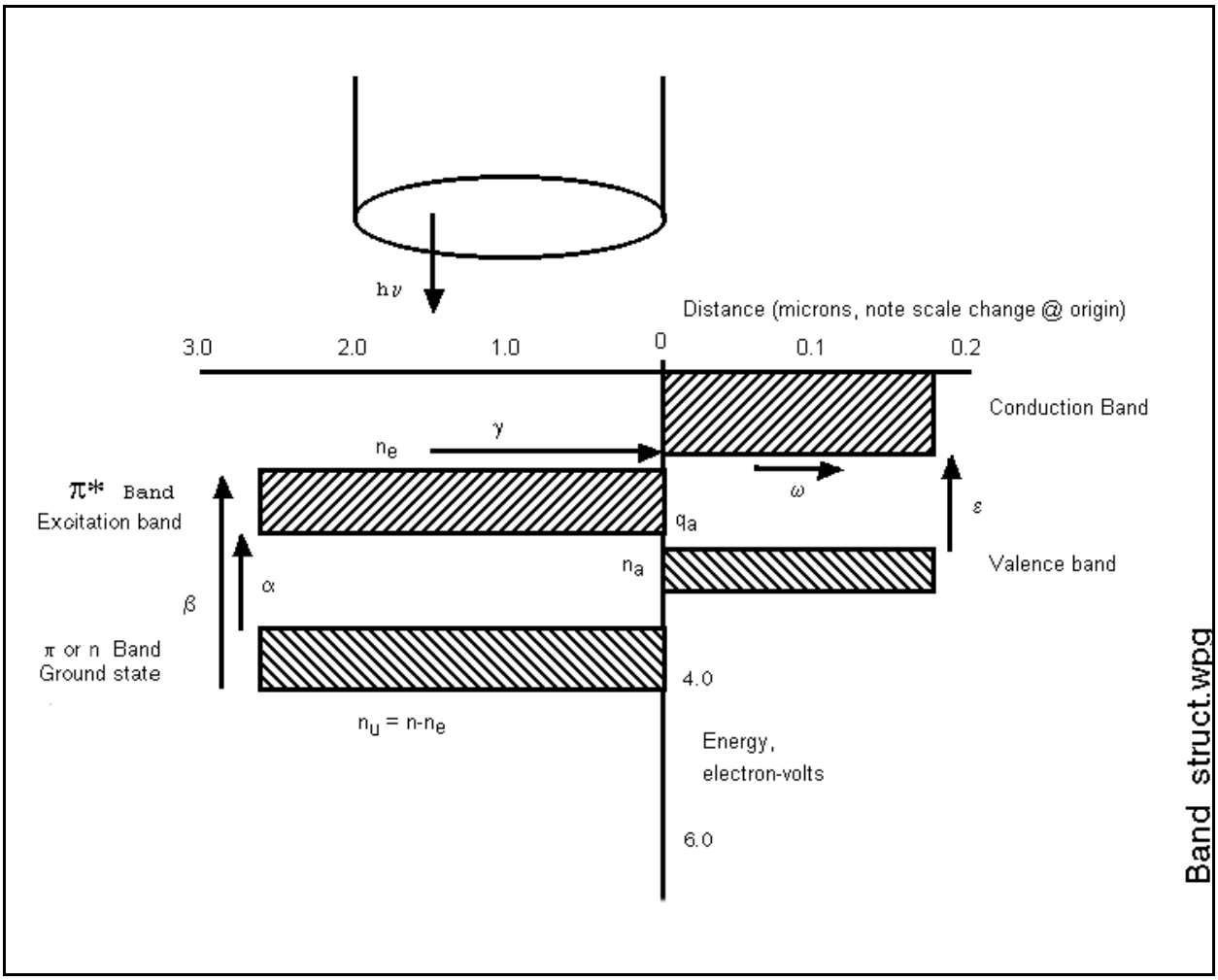


**Figure 12.5.1-2** The quantum mechanical interface ADD between a specific liquid crystalline chromophore and the base region of the associated liquid crystalline semiconductor. The band gap, α, on the left and the maximum energy, β, defines the photon energy that the chromophore will absorb. The band gap of the water-based semiconductor on the right is highly sensitive to temperature. At 37°C, it is believed to be 2.11 electron-volts. Any photon that can be absorbed by the chromophore and has an energy greater than ε will generate a free electron in the conduction band of the semiconductor. See text and Appendix **A** for terminology.

### 12.5.1.2.1 Quiescent operation

Under quiescent conditions, in the absence of illumination, all of the electrons associated with the liquid crystalline chromophore on the discs are located in the quantum mechanical ground state labeled **n**, sometimes **π**, in the left half of the drawing. There are no excited electrons, "excitons," in the **π*** band. No signal is generated within the OS or the microtubule structure of the IS. The transducer material is in quantum mechanical contact with the microtubules of the IS. Note the interface between the bands of the liquid crystal on the left and the liquid crystalline semiconductor device on the right need not overlap. The energy is transferred by a quantum mechanical process, not a conductive one. Note also the horizontal scale change between the two sides of the diagram.

### 12.5.1.2.2 Operation with illumination

Upon illumination by radiation of proper wavelength, each incoming photon with an energy greater than that indicated by **α** and less than that indicated by **β** will cause an electron to be excited from the ground state, **n**, into the

$\pi^*$ band of the liquid crystalline transducer. These excitons appear at a location directly above where the photon was absorbed. This can be anywhere in the 2.0 micron diameter of the crystalline structure shown. These excitons will travel to the quantum junction with the translation circuitry of the photoreceptor cell by one of several means. The important point is that there travel velocity is finite and the resulting ensemble of excited electrons exhibits a finite delay time between excitation and arrival at the boundary where excitation can occur.

The lifetime of excitons in the $\boldsymbol{\pi^*}$ band is very long relative to events associated with vision, i.e., the chromophores incorporating oxygen atoms are not known to fluoresce under physiological conditions.

Upon arrival at the boundary, the excitons are prepared to give up their energy if there is a quantum mechanical opportunity to do so. This opportunity is provided by the input structure of the dendrites. Under normal conditions, each exciton will give up its energy and be de-excited back to the ground state, **n**, in exchange for a free electron (or hole) being released within the junction of the first Activa within the microtubule structure interfacing with the outer segment.

At any given time the absorption coefficient of the liquid crystal associated with a given disc (or possibly a surface of the disc if the coating is fractured along the disc edge), is proportional to the number of unexcited electrons in the **n** band given by $\mathbf{n_u = n - n_e}$

### 12.5.1.2.3 Transient operation

The transient performance of the transducer is quite straight forward. However, it does include a state variable. Upon the application of illumination, the absorption coefficient is directly proportional to the number of unexcited electrons in the **n** band. If the photoreceptor has been in the dark for some time, all of the available electrons are in the **n** band and $\mathbf{n_u = n.}$ If however, the photoreceptor was recently illuminated, it is possible some of the excited electrons have not yet been de-excited. In that case, the number of available electrons is $\mathbf{n_u = n - n_e}$. Once a photon is absorbed, an exciton appears in the $\boldsymbol{\pi^*}$ band within less than a microsecond. The travel time to the boundary is appreciably longer and is a function of how many excitons are in the band. Once at the boundary, de-excitation occurs in less than a microsecond under physiological conditions. The result is that the "attack" transient response of the transducer to illumination, the time to generate excitons in the $\boldsymbol{\pi^*}$ band, has a short time constant and the "decay" transient response, the time to clear the $\boldsymbol{\pi^*}$ band, has a much longer time constant. However, *these are not the time constants of interest in vision.*

In vision, the time constants of interest are related to the boundary situation. The attack time constant related to vision is a function of the travel time between the creation of an exciton and its arrival at the boundary, ready for de-excitation. This time constant is a function of the illumination level. The decay time constant is related to how long it takes to clear the $\boldsymbol{\pi^*}$ band of excitons after the illumination ceases. Normally, this time constant is independent of the prior illumination level. The entire equation of the transient response of the transducer/translation process is given in the Photoexcitation/De-excitation Equation, (P/D) given in Appendix **A**. The attack time constant of the combination is quite variable, extending from less than one millisecond for high illumination to greater than one-half second for very low illumination. The decay time constant is nearly constant at a given temperature. For humans, its value is 0.525 seconds. These are only two of the time constants important in vision. They are essentially independent of any metabolic conditions occurring in conjunction with the active circuitry of the eye.

## 12.5.1.3 The quasi-static transduction process

Eddington, writing in Gennis[20] as late as 1989, attempted to describe the operation of the signal transduction process in terms of a cytoplasmic cascade. His conclusion as of 1989 was that "the details are somewhat murky or unknown." The following and later sections will clarify most of these details. However, the clarification is not compatible with a cytoplasmic cascade.

**Figure 12.5.1-3** highlights the steady-state transfer characteristic of the transduction process. The frame on the left summarizes the functional elements involved. For simplicity, all of the chromophores of a given region of the retina will be considered en masse and (initially) to exhibit a single absorption spectrum described as that of the M–channel.

In this figure, the expression "chromophores en masse" can be interpreted in two distinct ways. It can refer to

[20]Gennis, R. (1989) Biomembranes: molecular structure and function. NY: Springer-Verlag pg. 354

the group of chromophores, of a specific spectral type, in the liquid-crystalline state associated with and appropriately oriented within a single outer segment of a photoreceptor.

Alternately, it can refer to a larger group associated with multiple outer segments exhibiting the same spectral sensitivity within a given unit area of the retinal surface.

The Activa shown can consist of a single Activa within a single photoreceptor or it can represent a group of Activas associated with a group of outer segments as defined above.

In either case, the single base connection to the chromophores en masse shown consists of multiple neurites contacting the chromophore material at the edges of the disc stack(s). These neurites have frequently been described morphologically as dendrites. However, they are more complex than typical dendrites. The morphological label microtubules will be used when speaking of these neurites until their functional role is defined in **Section 12.5.2**.

The excitation photon flux is shown as F photons/sec. The total number of orbitals available for excitation on the surface of a disc will be taken as $A_0$. The exact value of $A_0$ is discussed in **Section 4.3.5.3.5**; The value is on the order of $10^7$ per disc and $10^{10}$ for a complete outer segment of one photoreceptor. Each absorbed photon results in an electron in a $\pi$–orbitals (the ground state) being excited into a $\pi^*$–orbital. The instantaneous absorption coefficient is a variable that depends on the total number of unexcited electrons in the $\pi$–orbitals, $A_0$ –(F-K). The Activa provides a de-excitation mechanism described by K de-excitons/sec. This de-excitation mechanism is represented by a current that is a fixed percentage of the collector current, $I_c$. The reciprocal of this percentage is defined as the amplification of the circuit. Z describes the impedance of the electrostenolytic source associated with the –150 mV supply potential. This Z plays a major role in describing the "dark adaptation characteristic" of human vision (**Section 17.6**). The output signal of the overall circuit is taken as the voltage across the resistor in the emitter circuit of the Activa, AS.

The photon excitation process is described in detail in **Section 5.4.3**. The precise interface between the base current, K, of the Activa and the chromophore, and how it results in the de-excitation of the chromophores, is a more complex quantum-mechanical process than required to understand the overall circuit operation. It will be summarized in **Section 12.5.2**.

The highly sensitive chromophores are surrounded by higher energy (insulating) materials except for the active tissue of the microtubules perpendicular to the edges of each opsin disk. The surrounding material consists of the inter-photoreceptor-matrix, IPM, and not a lemma associated with the inner segment. Further, the excitation process involves the triplet state of p*–orbitals and is peculiar to oxygen. Electrons from this level do not de-excite spontaneously (thermally). See **Section 5.3.1**. Thus, the excitation level of the chromophores is determined by the difference between the level of photon excitation, F, and the level of de-excitation via the base current of the Activa, K.

Frame **A** shows the overall situation for a constant level of de-excitation, K de-excitons/sec. As the photon flux level increases above the de-excitation level, the net excitation level, the number of $\pi^*$–orbitals, within the chromophore increases. As a result, the number of unexcited $\pi$–orbitals is drastically reduced.

Frame **B** illustrates the net absorptance of the chromophoric mass as a function of the photon flux. For fluxes below K, there is no net excitation level and the absorptance coefficient is essentially constant at its maximum value. An absorptance can be described by a relative optical density as shown by the right scale. At maximum absorptance, $A_o$, the optical density of the chromophore mass is high, taken here as a relative density of 2.0 or 100%. As the absorptance decreases, the optical density also decreases. The chromophore mass is said to bleach as a function of the excitation level. This is caused by the failure of the de-excitation flux, K, to equal the potential photon-excited flux.

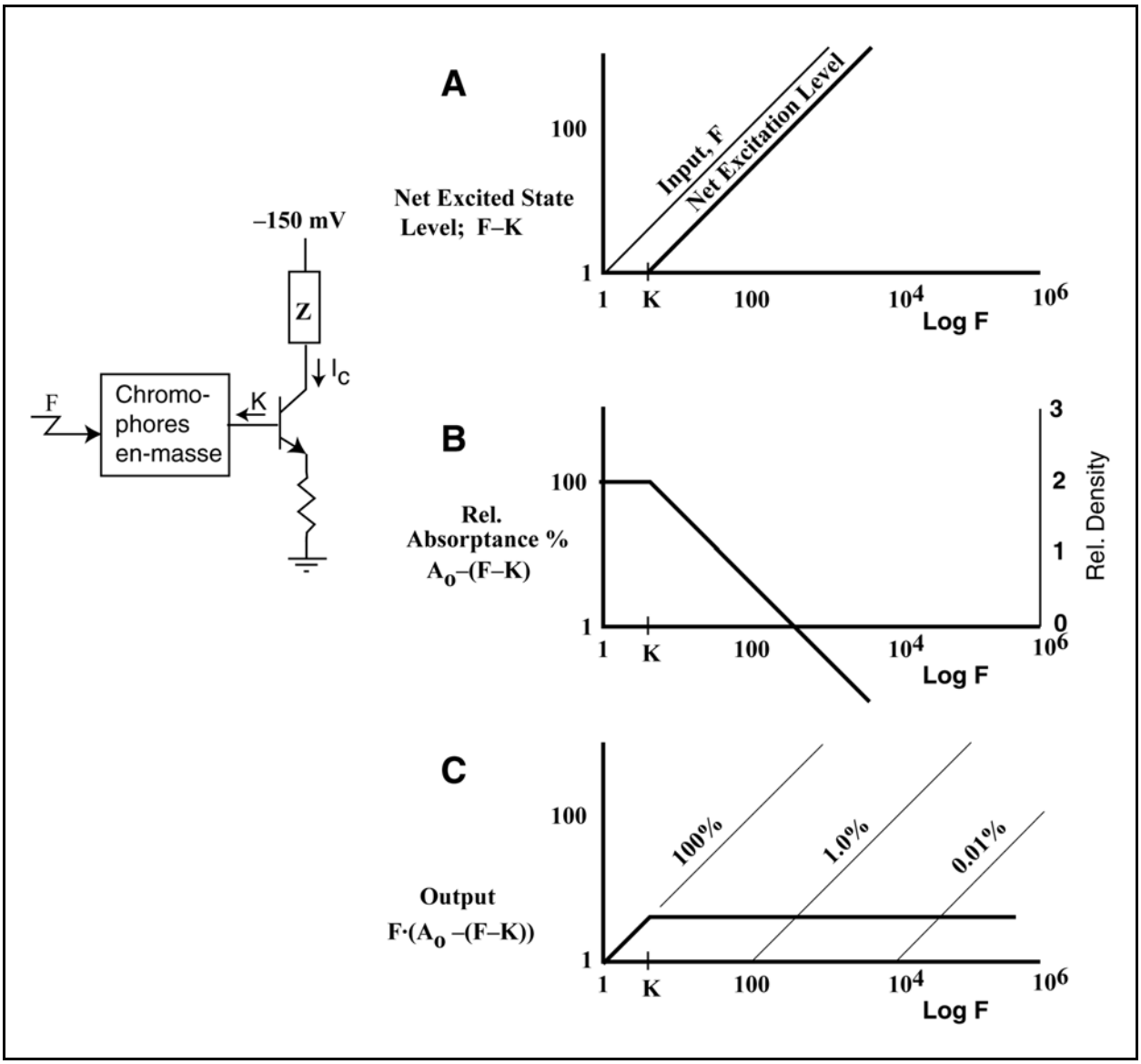


**Figure 12.5.1-3** The quasi-static transduction transfer function. Left frame; a simplified description of the transduction and amplification circuit associated with the adaptation amplifier of the photoreceptor cells. Right frames; descriptions of the parameters associated with the transduction process. **A**; the net excitation level, the reciprocal of "bleaching," within the chromophore coating of a disc rises rapidly with exposure level. **B**; The absorptance of the chromophores continues to decrease along a straight line. **C**; Parametric curves at lower right indicate relative efficiency. The efficiency continues to decrease with exposure level. See text.

Frame **C** shows the average (quasi-steady-state) output of the transduction process as a function of the photon flux, resulting from the reduction in the absorptance coefficient at high photon flux levels. The value of K corresponds to the transition of the illumination level from the scotopic regime into the mesotopic regime. The reduction in the absorptance coefficient can be described as an effective reduction in the quantum efficiency of the overall transduction process. However, note carefully, it is the effective capture cross-section of the chromophores to radiation (since there are fewer unexcited π–electrons per unit volume) that is reduced and not the efficiency of π*–electron creation as a function of photon flux. In the real case, the bulk chromophore represents a series of two-dimensional monolayers on the surface of a finite number of opsin disks. The reduced number of π-orbitals per unit area of the monolayer is the actual cause of the reduction in the capture cross-section.

At very high photon flux levels, the absorptance of the chromophores, and the associated optical density, becomes very low and most photons pass through the outer segment, impinge upon and are absorbed by the RPE. This impingement frequently results in pain.

## 12.5.2 The Transduction and Translation blocks of the photoreceptor neuron

This section will expand substantially on the above overview.

> In the following paragraph, an analogy will be made between the operation of the translation diode, $Q_n$, and the base of an Activa, $AS_n$, and a conventional opto-coupler used in electronic circuits. The analogy is a good one in that it involves quanta. However, it must be pointed out that the quantized energy transfer need not involve a radiative transfer; the transfer could just as well involve a mechanical energy transfer with the quanta of energy involved frequently called a phonon.

### 12.5.2.1 Histology and electrical schematic of photoreceptor neuron outer segment

**Figure 12.5.2-1** expands on the previous figure. It provides many details related to both the transduction and translation mechanisms.

#### 12.5.2.1.1 Histology of the outer segment

Frame **A** highlights the transduction mechanism related to the disc stack portion of the outer segment of a photoreceptor neuron. Four partial discs are shown. The full discs are nominally 2.0 microns in diameter and about 15 nm in thickness. They are spaced at a nominal 25 nm. The range of the thickness and spacing are summarized in **Section 4.3.5**, along with many other parameters such as the number of discs in a typical outer segment.

The opsin substrate is typically 16 nm thick with a ballooning at the edge of each disc raising the thickness to about 22 nm according to **Table 4.3.5-1** As shown the disc to disc pitch is nominally 25 nm. These dimensions suggest the chromophores forming a liquid crystalline monolayer on the surface of each opsin substrate is 1.5 nm (15 Angstrom) in length and nominally 0.5 x 0.5 nm (5 x 5 Angstrom) in cross section. A figure in **Section 4.3.5.1** illustrates the resulting configuration in greater detail.

> An important note regards the nature of these dimensions. When working at the nanometer level in determining the dimensions of atoms and molecules, it is important to realize that the outer electrons associated with these structures form an electrical field (labeled a cloud). This cloud is a statistical distribution of where the electrons of elementary physical chemistry are actually located. In more advanced studies, it becomes clear that the peak density of the statistical distribution is used to specify the radius and/or diameter of the structure. Two atoms separated by the sum of their published radii still can couple together through their cloud of electrons. This is also true of biological structures, particularly with respect to lemma.

With this physical chemistry background and these dimensions, the liquid crystalline monolayer of each disc is in molecular contact with the adjacent disc, at least in the ballooned edge of the disc. Similarly, the edges of the discs are in quantum-mechanical contactwith the lemma of the microtubules. These potential contacts are critically important in evaluating the question of adaptation within the transduction/translation mechanism (and the phenomenon of “bleaching”).

As indicated, the stimulating photon flux is applied axially to the disc stack. This also applies the stimulation along the axis of the individual chromophoric molecules coating the discs. This is also critically important to the operation of the chromophores. Their anisotropic absorption characteristic requires the stimulating photons to be applied parallel to the axis of the chromophore (between the two oxygen atoms of the individual Rhodonine molecule). This requirement is discussed more fully in **Section 5.3.5**.

The interface between the discs of the outer segment and the microtubules connecting to the inner segment through the ciliary collar is described in greater histological detail in **Section 4.3.5.5**.

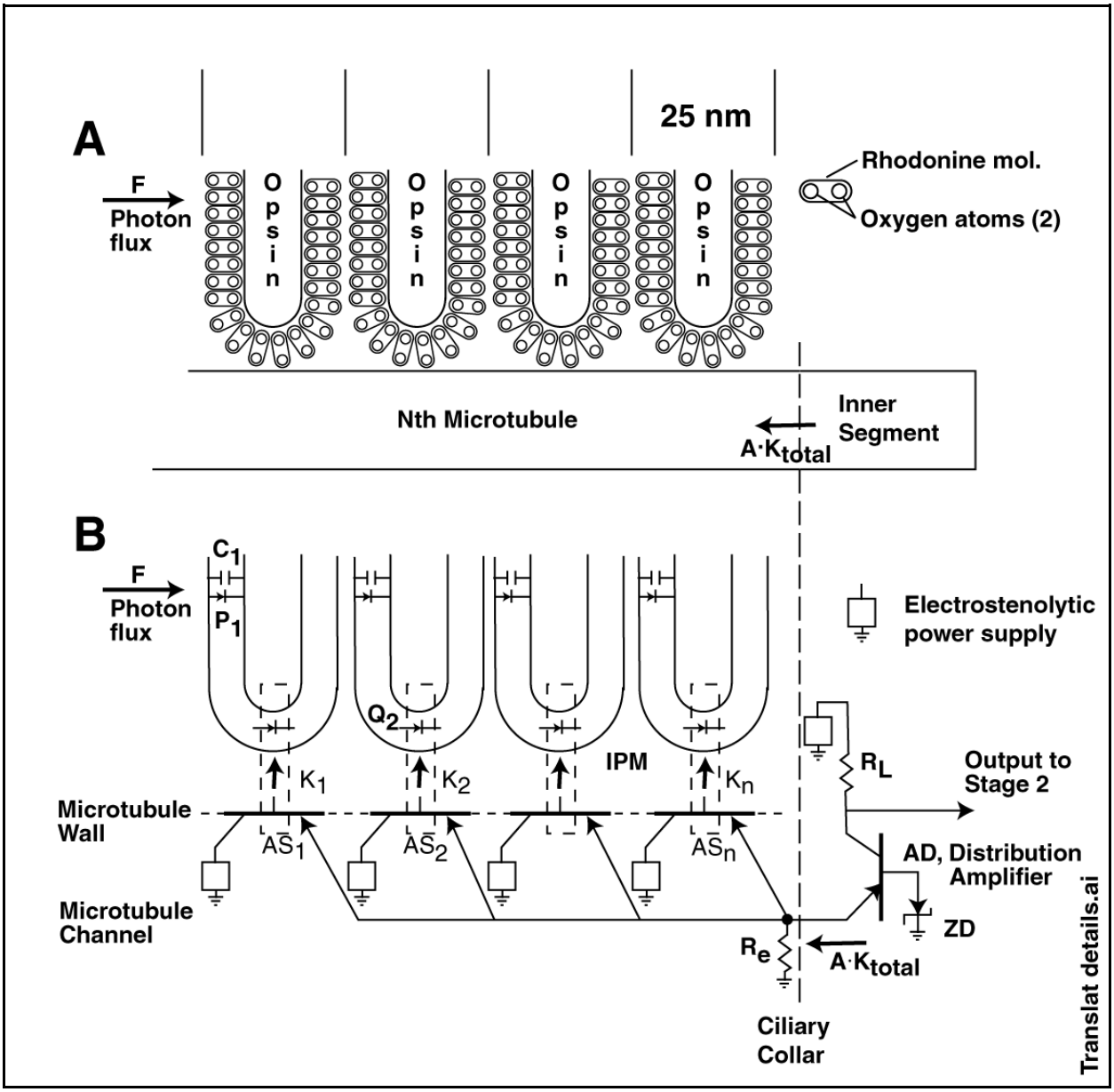


**Figure 12.5.2-1** Graphic details of the photo-detection mechanism of stage 1. **A**; Histological representation of the disc structure of the outer segment and its interface with a microtubule. Each disc is 2 microns in diameter. There are typically nine microtubules surrounding each disc stack. **B**; The quantum-electrical representation of the mechanisms of frame **A**. The dashed boxes enclosing the diodes, $Q_n$ and the arrows, $K_n$ are expanded vertically for clarity. The base terminal of each Activa, $AS_n$, is in intimate contact with the quantum-mechanical diode, $Q_n$. See text.

It is also important to note the presence of the alternate layers of low index of refraction protein opsin and low index of refraction fluids forming the Inter Photoreceptor Matrix, IPM, between the monolayers of Rhodonine. This arrangement reduces the bulk index of refraction of the disc stack and essentially eliminates any internal reflections at the surfaces within the stack. This is a familiar technique used in waveguide technology to absorb energy without introducing reflections within the waveguide (**Section 4.3.5.3.4**).

*In this work, the chromophore, Rhodonine() when present as a monolayer on the surface of the protein substrate, opsin, results in a package labeled Rhodopsin().* The content of the parenthesis identifies the

chromophore present and its absorption spectrum. Historically, rhodopsin has been defined as only the protein substrate (that does include a minuscule amount of retinol/ retinal–this retinol may act as a seed for the formation of the protein molecule (**Section 5.1.4**). The molecular weight of one ligand of retinal is 284 while the protein portion of bovine opsin is 41159. The retinal is only 0.68% of the total molecular weight of the composite molecule. *No one has ever described how this simpler package acts as a photoreceptor within the outer segment of the photoreceptor neuron. Nor has any investigator every shown that this simpler package supports an anisotropic absorption characteristic in the visual wavelength of vision.* Dratz & Hargrave have noted the axis of the retinol ligand is nominally perpendicular to the stimulating radiation (**Section 5.1.4.1**).

*The axis of the Rhodonine() molecules are nominally parallel to the stimulating radiation and form a liquid crystalline surface intercepting the radiation that is 100% chromophore* (**Section 5.5.8**).

In the upper part of frame A, transduction of the photon flux, F, into excitons occurs in the chromophore coating consisting of Rhodonine molecules. The individual molecules are each capable of a single conversion of a photon to an excited state. After that conversion, the molecule is transparent to further irradiation. However, the presence of these molecules in a liquid crystalline state of matter means that their exciton is free to move within the excited energy band (the $\pi^*$ band) of the whole coating of a single disc and their exciton is readily returned to the ground state by action occurring elsewhere in the coating. This de-excitation occurs at the coating interface with the microtubule shown.

The interpretation of $A \bullet K_{total}$ will be addressed below.

### 12.5.2.1.2 Schematic of the outer segment

Frame **B** of describes the quantum-mechanical and electronic mechanisms associated with the histological package of frame **A**.

To understand the details of this frame, the reader must have a significant background in quantum- mechanics and semiconductor physics. Lacking that background, the reader is directed to the critically important material in **Chapter 10**, that relies upon the details of these subjects addressed in discussions in **Chapter 8** and **Section 9.2. Section 10.8.5** focuses on the photoreceptor neuron.

The most important feature in this material is the ability of the lemma of a neuron, in conjunction with its internal reticulum to form an active semiconductor device labeled an Activa. This device is analogous to a man-made transistor of the PNP type. In this frame, two are shown, the adaptation amplifier, AS, and the distribution amplifier, AD. The adaptation amplifier is shown as a distributed device, $AS_1$, $AS_2 \ldots AS_n$ along the surface of a microtubule as described above. The darkened horizontal lines form the base(s) of the distributed device, AS as shown. The emitters (shown with arrowheads contacting the bases) of these distributed devices are all connected in parallel to the emitter of the second Activa within the distribution amplifier, AD. The collectors of these same distributed devices are shown connected to individual electrostenolytic power sources (**Section 8.6**).

The details of the quantum-mechanical mechanism appears in **Section 5.4**. In frame **B**, The total photon stimulating photon flux generating excitons within the excited energy band of the liquid crystalline chromophores is labeled **F**. The sum of the charges seeking to de-excite these excitons by quantum-mechanical means is labeled $K = K_1 + k_2 \cdots \cdot + K_n$ where n is the number of disks in direct quantum-mechanical contact with one of the nominally nine microtubules.

Note, because of the liquid crystalline nature of the chromophores of each disc and the quantum-mechanical contact between discs, it is possible for excitons to be generated in the coating of a disc not in contact with a microtubule, those excitons to travel within the excited energy band to another disc that is in quantum-mechanical contact with a microtubule, and thereby be de-excited back to its ground state.

Any individual chromophore molecule can capture a photon traveling parallel to its axis and raise an electron from its ground state to an excited state, per **Section 5.4**. In this frame, the photodiode labeled $P_1$ and the excited energy band, diagramed using the conventional capacitance symbol labeled $C_1$, represent this individual chromophore. It is one of an astronomical number of chromophore molecules coating each disc. More specific numbers will be described in subsections below. Note that once excited, the excitons associated with $C_1$ are free to travel within the

common excitation band of the disc, and through quantum-mechanical coupling to other discs within the outer segment.

> This sharing of excitons within a nominally common excitation band runs squarely into the Pauli Exclusion Principle (**Section 5.4.2**). This Principle leads to a broadening of the axial spectral characteristic of the outer segments of photoreceptors that is proportional to the total effective number of chromophores within the discs of that segment. This broadening complicates the calculation of the spectral characteristic of a given outer segment but is accounted for in the spectral bandwidths reported in **Chapter 5**.

An important fact illustrated in frame **B** is that the first, or the Adaptation, Activa, AS, of a photoreceptor neuron is in distributed form. Distributed transistors are common in man-made semiconductor devices and should not raise alarm within the Biosciences. In this case, the combination of the outer lemma, a thin layer of water (hydronium), and a reticulum within the microtubule forms an Activa with either a continuous base layer or a segmented base layer as shown. As also shown, each distributed PNP type Activa operates in the high gain common-emitter mode. A current gain (amplification factor) of between 100 and 200 would be expected for these devices (laboratory verification is urgently needed, but may be difficult to instrument).

It is most likely a distributed power supply serves all of the distributed Activa, $AS_1$, $AS_2$ . . . $AS_n$ of a single microtubule as shown. The data of Baylor et al[21]. in their 1979a paper supports this distributed character. The details of the electrostenolytic power supply appear in **Section 8.6**.

The second Activa, AD is shown at right. It is a conventional PNP Activa, where the word distributed is used in its function context, not a histological context. This Activa is operated in the common base configuration. This configuration operates at a nominal current gain of 1.0 but offers a much lower output impedance than the common collector configuration. Because its "signal in" is a current and the "signal out" is a voltage, this type of amplification is given the name *transconductance*. The low output impedance allows many stage 2 neurites to connect to the pedicle of each photoreceptor neuron without any performance degradation.

The adaptation amplifier, AS, and the distribution amplifier, AD, form an asymmetrical differential amplifier. This circuit is widely used in operational amplifiers throughout the electronics world. Here, they are used in a special manner; the input connection to the base(s) of AS are physically left floating, unconnected to any other physical circuit element. These input connections are shown immediately below the vertical arrow. While not connected to the diodes shown within the lower region of each disc, they are sensitive to the quantum-mechanical energy provided by these stimulating diodes, $Q_n$ (similar to modern light emitting diodes, but operating at a different wavelength).

As noted in discussing frame A, the photon flux stimulating the Rhodonine chromophores, causes an exciton to be raised into the *shared excitation band (*the $\pi^*$ band) of the liquid crystalline monolayer coating formed of Rhodonine molecules. When each of these excitons comes into the vicinity of the stimulating diodes, they are de-excited into their ground state and their energy is transferred to the base of the adjacent Activa, resulting in a free electron being formed within the semiconductor forming the base. Thus a de-excitation mechanism, K, is available to counter the excitation **F** mechanism.

The free electron released into the base of a PNP Activa connected in the common-collector configuration (also known as the emitter-follower configuration) results in approximately 20 to 40 electrons to pass between the emitter and collector of the Activa. This is the amplification factor, A, of the individual sections of the AS (and of the total AS as well). This amplification factor is well controlled biologically within a narrow range. However, at this time, there is no known data on the semiconductor material involved (basically water in a liquid crystalline form, and called hydronium in some circles). These electrons are all collected and delivered to the common load shown as $R_e$. Through the common emitter connection, any incipient change in the voltage across this load, causes an opposing current from the emitter of the distribution amplifier, AD, to oppose this change. This emitter current in AD is associated with an equal current in the collector of AD. Although the current gain of this circuit is less than or equal to 1.0, it is believed able to output a current of up to 20-30 pA under steady state conditions. This current is converted to a voltage due to the impedance of the electrostenolytic power supply to AD.

The output voltage of AD is proportional to the logarithm of the applied current and becomes the signal voltage at the pedicle of the photoreceptor neuron. The maximum signal swing of this voltage does not exceed 130 mv (under what is called Large Signal Conditions. After adaptation, the signal amplitude at the output of AD is generally in the

---

[21]Baylor, D. Lamb, T. & Yau, K.-W. (1979a) Responses of retinal rods to single photons. *J Physiol* vol. 288, pp. 613-634

few mv range (the Small Signal Condition). The logarithmic character of the signal under Large Signal Condition is due to the input characteristic of any Activa or man-made transistor. This input characteristic is determined by the fact that it is associated with the diode forming the PN junction of a PNP semiconductor device.

> At an earlier time, the symbology for a transistor was drawn as two back-to-back diodes. Later there were heated discussions within the IEEE over which way the arrow should point on the emitter lead to define the type of transistor involved in the symbol finally adopted.

Under Small Signal Conditions, a limited range of the diode input characteristic can be approximated by a linear resistor.

Although the schematic shown above is compatible with the composition of the membrane associated with all neurons, it does not require the physical movement of any atoms or ions through any lemma of the neuron, physical movement is limited to electrons "holes" (the absence of electrons in the lattice of a crystalline semiconductor).

### 12.5.2.2 Polarity, signal amplitude & Impedance of the photoreceptor amplifiers

To work effectively, the differential amplifier enclosed in every inner segment (including the microtubules) of every photoreceptor must be properly biased electrically. While any electrical potential within a chemical theory of the photoreceptor is of little importance; in the Electrolytic Theory of the Neuron, it is critically important.

> ***It is important to remember Ben Franklin's biggest mistake here. The conventional current he defined flows from the positive to the negative terminals of a battery (in the external circuit). The actual electron flow is in the opposite direction; electrons flow from the negative terminal to the positive terminal. Care must be taken when talking of transistor devices and Activa to distinguish between the "current flow" and the "electron flow".*** The terms are frequently used interchangably by scientists familiar with this situation.

It should be obvious based on the above discussion that when F = 0, no excitons are formed in the *shared excitation band (*the $\pi^*$ band) of any disc within the OS. Without any excitons to de-excite, and the subsequent production of free electrons in the base of AS, the electron flow from the electrostenolytic power supply through the Activa will be zero (except for a very small leakage current). In this case, any voltage across the resistance $R_e$, must by provide by the distribution amplifier, AD. The breakdown voltage of the zener diode, ZD, is chosen to insure such a voltage across $R_e$ exists. This voltage typically stabilizes at less than a few millivolts. At this voltage, the electron flow through AD will be small and the quiescent value of the collector voltage will be only a few millivolts below the –154 millivolts of the electrostenolytic power supply.

When the photon flux is raised above F = 0, the sum of the electrons flowing through AS will attempt to increase the negative voltage across Re. However this increased negative voltage at the emitter of AD will cause more electron flow through AD and the load resistor, $R_L$. The voltage drop across $R_L$ will lower the negative collector voltage. This reduction in the negative voltage at the collector will constitute a positive going output signal at the pedicle leading to stage 2. The collector voltage of AD can only be reduced until it approaches its emitter voltage at that time, typically at –20 mV. The result is a maximum output signal voltage at the pedicle of the photoreceptor of less than +130 mV = –20 – (–150). Signal voltages approaching this magnitude have been frequently reported in the literature. However, outside of the laboratory and under realistic conditions, the maximum signal voltage is less than 100 mV

The impedance of neural circuits is remarkably high, and not found in man-made electronic circuits prior to the development of very high density printed circuits. For a 130 mV to appear across $R_L$ with only 30 picoamperes passing through AD, the value of $R_L$ would be about four megohms. And this value is used in a distribution amplifier requiring a low output impedance. Smaller neurons will be found to have output impedances of 100 megohms and above. This is particularly true of small neurons below the resolution of light microscopy.

### 12.5.2.3 The photoreceptor neuron from a different physiological perspective

**Figure 12.5.2-2** shows an alternate schematic of the stage 1 photoreceptor neuron (expanded from frame **B** of **Figure 12.5.1-1**, allowing other features to be illustrated.

The photo-excitation (transduction) mechanism consists of a Rhodonine molecule (a chromophore) acting as a

photon-to-exciton converter. For each photon absorbed, one electron is moved from the ground state to the π* excitation band of the liquid-crystalline lattice of the outer segment, OS. The symbols, $C_T$ and $Z_1$ are used to define the decay time constant of these excitons. Because of the unique properties of the oxygen atoms of Rhodonine molecules (**Section 5.3**), the life time of these excitons is very long in the absence of any discharge mechanism. Conceptually, when an individual Rhodonine molecule is excited, it is no longer subject to excitation and appears transparent to the photon flux. Within the liquid-crystalline lattice, the electronic energy bands are shared, and a reduction in absorption cross section for the entire lattice results from the net increase in excitons as a function of time.

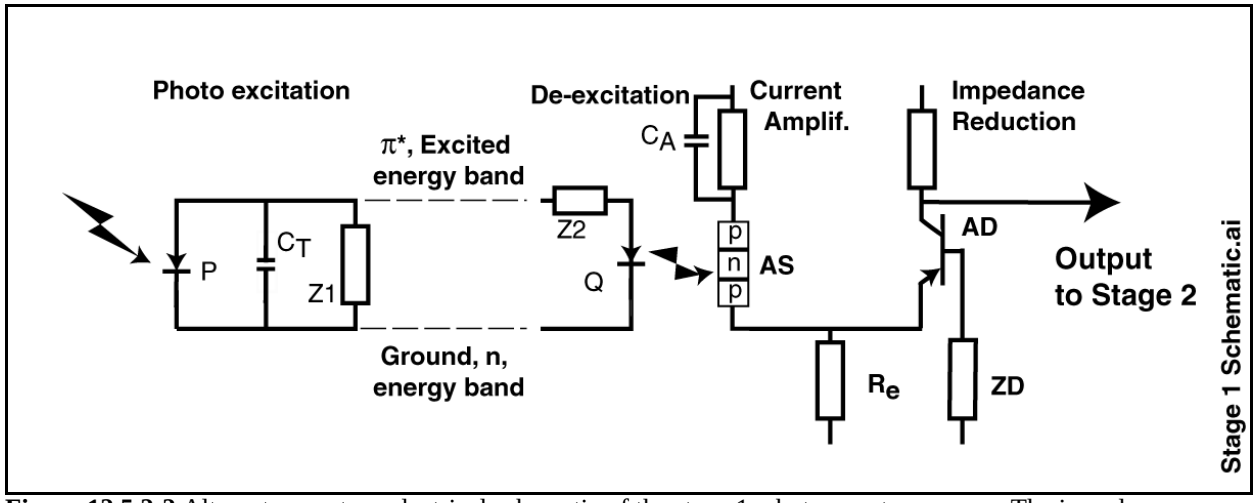


**Figure 12.5.2-2** Alternate quantum-electrical schematic of the stage 1 photoreceptor neuron. The impedances shown above the two Activa, AS & AD, include individual electrostenolytic power sources. The resistive element, Re and the zener diode, ZD are connected to the local electrical ground formed by the inter-photoreceptor matrix, IPM. The symbol at far left represents incident energy within the spectral band of the chromophore of the photoreceptor. The similar symbol between Q and the N-type region of the first Activa, AS, represents a quantum-mechanical energy transfer. The impedances shown in the collector lead of the Activa include separate electrostenolytic power sources. The impedances along the bottom all connect to a common ground (the matrix surrounding the neuron). See text.

The photon/chromophore stimulation mechanism is described in detail in **Section 5.4**. It is common to virtually all light sensitive processes.

The π* and n energy bands shown are continuous within the liquid crystalline lattice formed by the monolayer of chromophores on each disc. These bands may be shared between adjacent discs. Excitons in the π* band are known to travel at a finite speed within the π*. $Z_2$ is a essentially a delay line reflecting the time for an exciton to travel from its point of origin to its point of de-excitation. The average of this time delay is the dominant delay term in the (photo) excitation/de-excitation equation, P/D Equation, of **Section 7.2**.

This delay term can be addressed mathematically[22] and it is a function of the electric field created within the discs, i. e. the delay is inversely proportional to the number of excited electrons present at any given instant. The higher the excitation rate, the stronger the electric field created, the shorter the transport delay. The equation in this case involves a first order Bessel function of the first kind to describe the unit delay involved. It is incorporated in the delay term of the photoexcitation/de-excitation process of **Section 7.2.4.2.1**.

On arriving at the edge of the disc, the exciton becomes involved in the de-excitation mechanism between the chromophore coating and the wall of the microtubule where the Activa, AS, is located. The de-excitation mechanism involves a quantum-mechanical process where the exciton is returned to its ground state, and a free electron is produced within the N-type material of the base of the Activa, AS. With the return of the Rhodonine molecule to its ground state, it is again susceptible of capturing another photon arriving within its absorption spectrum.

[22]Goldman, S. (1949) Transformation calculus and electrical transients, Chap 10. NY: Prentice-Hall

There is an energy threshold related to the first Activa of the neuron; on the order of 2.11 electron-volts in human endotherms **Section 12.5.2.4**). This threshold affects the de-excitation of excitons resulting from absorption of long wavelength photons, at wavelengths longer than about 0.587 microns. This threshold requires the summation of the energy from more than one exciton within the chromophore to generate one free electron in the base terminal lead of the first amplifier of the neuron (a 2-exciton mechanism).

The electrostenolytic power supply cited in the caption will be described in **Section 8.6**.

The translation of energy between Q and the N-type material of the Activa. are diagramed in **Section 4.2.2** and in exploded view in **Section 4.3.2**. For short wavelength photons and high photon fluxes, this element can be considered a network having a transfer function characterized by a constant gain, wide frequency response and zero time delay, i. e. it can be ignored.

The current amplifier, labeled AS in this figure, is also labeled the adaptation amplifier, or first amplifier of a stage 1 neuron elsewhere in this work. It is truly the first amplifier containing an active device—Activa—within the visual modality of the neural system. Connected as a common emitter device, it offers high gain, on the order of 40:1 but potentially 200:1, similar to man-made transistors of the junction type. It is not directly associated with the adaptation process (**Section 7.2.6.1.2**). The adaptation process is found in the chromophores of the outer segment of the stage 1 photoreceptors (**Section 12.5.3**)

The distribution amplifier, labeled AD in the figure shares a common emitter terminal with the first amplifier, thus forming an asymmetrical differential pair. The purpose of the distribution amplifier is to reduce the impedance of the signal source at the pedicle of the photoreceptor neurons. It does this by converting the signal from a current at the output of the first amplifier to a voltage at the collector of the second amplifier. This allows the distribution amplifier to interface efficiently with the multiple neurons of the stage 2 signal processing neurons within the retina.

### 12.5.2.4 The *special* case of the long wavelength visual channel(s)–a 2-exciton process

As indicated in **Section 12.5.4**, there is a special situation that is frequently found in the long wavelength chromophoric channel of the visual system. It is virtually identical to the phenomena found in modern silver halide photography where a "dye" similar to the rhodonine family (a conjugated carboxyl-ion system) is used to coat the silver halide crystals. By coating the crystal in this way, the spectral sensitivity of the silver halide emulsion is extended to wavelengths beyond the band gap limit of the crystal itself. In that trade, the dye is usually labeled a "coupler."

Specifically, the dye is deposited as a liquid crystal on at least a portion of the surface of the silver halide crystal. The incident photon excites the chromophore and an electron is transferred to the $\pi^*$ band of the chromophore just as described earlier. However, this excited electron does not have sufficient excess energy to cause the release of a free electron at the interface with the silver halide crystal.

Here again, the process is quantum-mechanical and the correct method to handle this problem is a probabilistic one. The question becomes; what is the probability that one or more excited electrons, acting in consort at the interface, can cause a free electron to be created in the silver halide crystal. This action would involve the summing of the energy of individual excited electrons. The equation could be written as follows: P(free) = P(1) + P(2|1)*P(1): i.e., what is the probability that a free electron will be released as a result of the action of one excited electron acting alone, P(1), plus (or) the action of a second excited electron P(2|1) acting essentially simultaneously with the first, or another excited electron, P(1). **Figure 12.5.2-3(left)** describes conceptually the probability that a single exciton, with the energy of the photon that generated it, can generate a free electron at the disk-microtubule interface. The assumption is that the band gap of the liquid crystalline water of the Activa is 2.2 electron-Volts. An electron-Volt equals $1.6 \times 10^{-12}$ ergs. In chemical terms, 1 electron-Volt per mole is about 23,000 calories per mole.

In this work, liquid crystalline water has been called hydronium, a term used in many contexts but not generally as used here. In this context, the liquid crystalline water is a state of matter between the liquid state and the solid state (ice in one of over a dozen specific configurations). The liquid crystalline state is most often encountered in water at a temperature between zero and a few degrees centigrade. It is also frequently found as a boundary layer (the Helmholtz double layer) at an interface between bulk water and a container wall in the absence of stirring. It is often found in a confined space measured in nanometers.

The figure is conceptual; both the terminology and equations of probability theory become very complex very fast. It is the concept that is important here, not precise values. As an example, the band gap of water in the

liquid crystalline state (employed in the Activa of the neural system is unknown. Based on the work of Sliney in an earlier era, it can be deduced that the band gap of interest is less than 2.34 electron-Volts. However, how much less is an important question. The lack of any unaccounted for notches in the long wavelength skirt of the scotopic Luminous Efficiency Function, LEF or R'(λ), would suggest the band gap on interest is less than 2.2 electron-Volts.

In photography this logic can actually be carried to the third and fourth terms in a similar equation and positive results are obtained in practice at wavelengths out to about 4 times the band gap of silver halide. Moreover, the same silver halide crystal retains its inherent isotropic spectral sensitivity as well. Thus, the coated silver halide crystal exhibits two distinctly different spectral absorption bands.

In the above equation, we have already seen that the value of P(1) is virtually zero for photons with less energy than the band gap of the semiconductor. For photons with more energy than the semiconductor, their probability is quite close to 1.0. This is particularly true in the outer segment where a photon presented parallel to the axis of the outer segment that fails to excite a chromophore coating the first disc is pretty certain to excite one of the following few thousand chromophore coatings in a single outer segment. However, the value of the term P(2|1)*P(1) is relatively high, and the process is useful. The effect is to generate a exponential relationship that is graphically similar to the square law relationship, $Y = X^{½}$ between the number of free electrons produced and the number of excited electrons producing them. This relationship is illustrated conceptually in **Figure 12.5.2-3(right).**

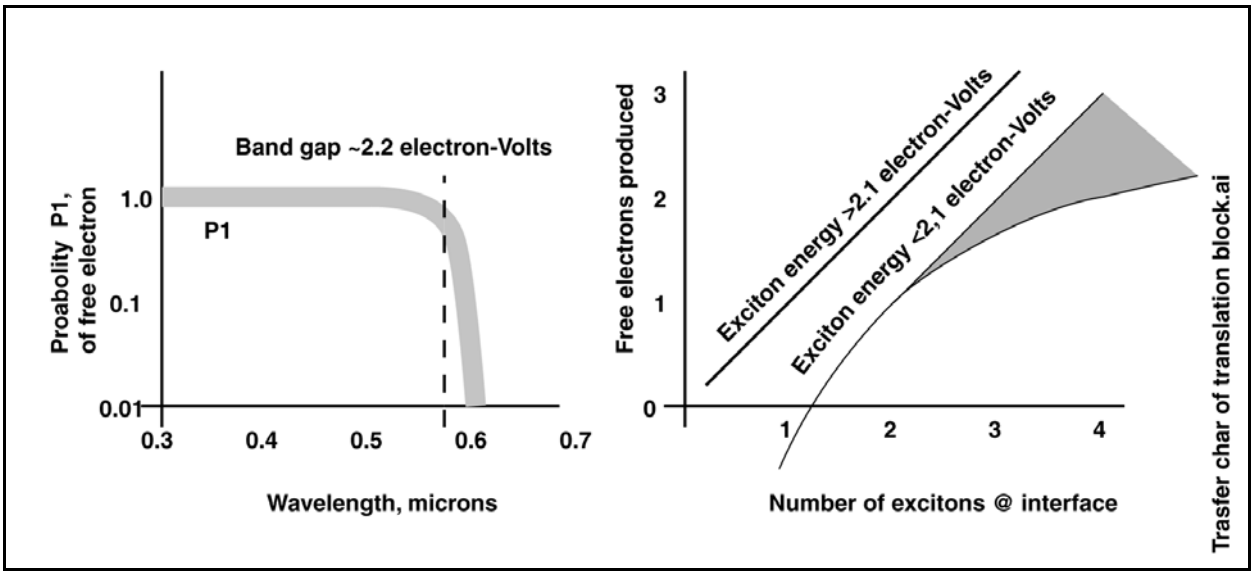


**Figure 12.5.2-3** Conceptual probabilities of translation from exciton to free electron in the base of the Activa. Left; Probability of translation as a function of wavelength for an endotherm with a band gap in the first Activa of 2.2 electron-volts. In humans, the best estimate of the band gap is 2.11 electron volts at 37°C. Thus P1 applies to all UV–, S– & M– spectral bands. For exotherms, the band gap increases at lower temperatures and the dashed line moves to the left. Right; The probability of a free electron being produced in human endotherms with a bandgap of 2.11 electron volts. Upper line corresponds to UV–, S– & M – spectral bands. Lower line corresponds to the L– spectral band. The gray area is an estimate in the absence of solving the precise probability equation. The two slopes are believed to be parallel over an extended range above 2 excitons at interface simultaneously. However, the long wavelength response goes below zero at one exciton at the interface at a given moment. See text.

Note that this "Square Law" process is not what is commonly referred to as a "2-photon" process. In this case, it is two excited electrons, or excitons, that are involved. It will be referred to as a *2-exciton process*. These excitons are not moving at the speed of light, have a relatively long life expectancy at one location and are subject to the affects of electrical fields. Thus, the chance of interaction between, or joint action by, two excitons is considerably higher than for two photons.

The probability function is correlated to what photography specialists describe as the "gamma" of their films. A gamma of 1 is associated with the slope of the density of the free silver after chemical development versus the intensity of the illumination. A gamma of 2 is associated with a coupler supporting a 2-exciton

mechanism. A gamma of 3 or four is associated with infra-red sensitive films with couplers employing a 3-exciton or 4-exciton mechanism. A gamma of 3 can be associated with a "Cube Law" and a gamma of 4 can be associated with a "Fourth Power Law."

Sliney, et. al.[23] have provided data on the spectral absorption of the L-channel in human vision extending out to 1.060 nm. The photon energy at this wavelength is only 1.17 electron-volts. This would indicate that the energy threshold of the neural system of vision at body temperature is not more than twice this number, 2.34 electron-volts, or a three-exciton process would necessarily be required in human vision. Unfortunately, he did not attempt any measurements near 1.7 microns to refine the energy threshold value.

2-exciton and 3-exciton mechanisms are currently being found in the field of dye lasers[24] and have been known in photography since the 1940's (See Mees & James, 1966). Prasad used a 1.3 micron photon source to pump a dye that generated a 0.43 micron laser radiation at very high efficiency. Interestingly, Naka & Rushton[25] made the comment in one of their 1966 papers that "*they would not find it surprising if this process, from the photographic field, should be found in vision as well.*" It is in fact a major mechanism found in the L-channel of the visual modality of endotherms, including humans.

Arkhipov & Bassler have recently discussed the multiple-exciton event in the context of conjugated polymers similar to those of the visual chromophores[26]. While valuable, their discussion did not proceed to a definitive conclusion. They describe a sequential, quasi-instantaneous process. This process may involve excitation to a higher $\pi$-level on the excitation side of the barrier, or the accumulation of energy in the coarse of transfer across the barrier.

- - - -

As in the photographic process, the characteristics of the process in vision is a function of the energy of the excitons relative to the n-electron ground state and the minimum energy threshold of the translation block. In the human visual system, the process involves the L-channel excitons, energy of approximately 2.1.1 eV and the translation block threshold at a temperature of 37 degrees Celsius. This effect is reported at a number of places in the literature. It is more clearly reported[27] in the case of the median ocellus of the horseshoe crab, *Limulus polyphemus*. This eye incorporates two photoreceptors, one with peak sensitivity at 360 nm. in the ultraviolet and a second with peak sensitivity at 530-535 nm, corresponding to the M-channel. There is no reported photoreceptor sensitive to the intervening region normally occupied by the S-channel at 425 nm. Because of this "space" between the channels, it is much easier to distinguish the basic difference in sensitivity between the channels.

The paper by Chapman & Lall is very insightful and this work confirms theoretically nearly all of their hypotheses. Thei work was clearly exploratory and using very primitive equipment for the 1967 time period, 20 nm FWHA filters and *paper tape* data storage.

They assert, "Not only is the UV channel more than 200 times more sensitive to light than the M-channel, the M-channel exhibits a 'gamma' of one half that of the UV channel." This is illustrated in **Figure 12.5.2-4.** The inset illustrates the fact that the sensitivity in the M-channel changes faster than in the UV-channel. The effect becomes important at a shorter wavelength in the *Limulus* than in man because of its lower operating temperature. This lower temperature causes the threshold energy, or energy gap, of the translation block in *Limulus* to be higher[28] than in man. A band gap of less that 3.3 electron-volts (equivalent wavelength of 375 nm) at room temperature appears

---

[23]Sliney, D. Wangemann, R. Franks, J. & Wolbarsht, M. Visual sensitivity of the eye to infrared laser radiation. J.O.S.A. vol.66 No. 4 April 1976

[24]Prasad, P. (2002) Dye Lases by Three-Photon Excitaton NY: University of New York at Buffalo. In Photonics Spectra, April 2002, pg 22

[25]Naka, K. & Rushton, W. (1966) An Attempt to Analyse Colour Reception by Electrophysiology page *J Physiol* vol 185, pp 556-586 page 584

[26]Arkhipov, V. & Bassler, H. (2003) Exciton dissociation in conjugated polymers *In* Nalwa, H. & Rohwer, L. *eds*. Handbook of Luminescence, Display Materials and Devices, Volume 1: Organic Light-Emitting Diodes. NY: American Scientific Publishers Chapter 5

[27]Chapman, R. & Lall, A. (1967) Electroretinogram characteristics and the spectral mechanisms of the median ocellus and the lateral eye in *Limulus polyphemus*. *J Gen Physiol* vol. 50, pp. 2267-2287

[28]Millman, J. & Halkias, C. (1972) Integrated electronics: analog and digital circuits and systems. NY: McGraw-Hill pg. 29

appropriate. Recall that biological operations do not follow Avogadro's Law. Biological operations generally are limited to a temperature range from the freezing point to about 60 Centigrade. 3.3 electron-Volts at 23 C is equivalent to 2.1 electron-Volts at 37 C.

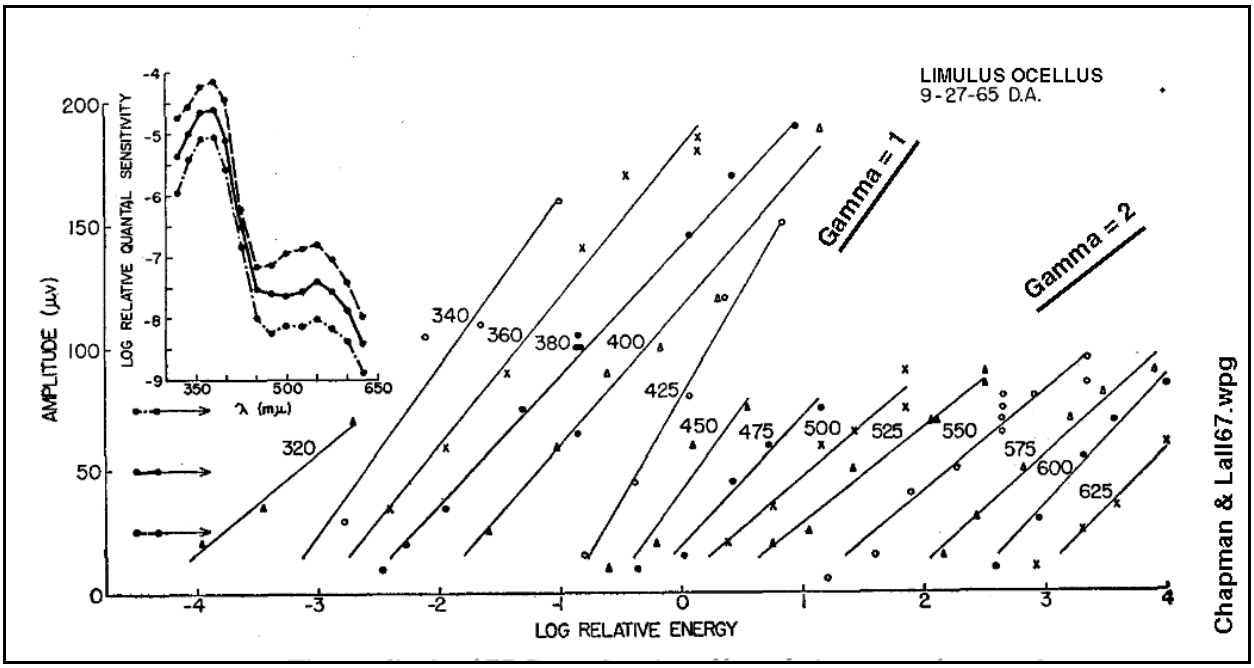


**Figure 12.5.2-4** Data suggesting a 2-exciton mechanism in the Limulus median ocellus. The data is from ERG recordings with the probe contacting the cornea of the ocellus. The individual spectral responses were arbitrarily displaced along the abscissa. Note the change in slope with wavelength. The slope in the long wavelength region is one half the slope in the short wavelength region. The "Gamma" are for illustration only, showing these trends. The slopes in the 320 nm and in the mid wavelength region ( 425 -500 nm) are distorted by averaging due to the 20 nm filters employed. From Chapman & Lall, 1967.

### 12.5.2.5 The *general* case of multiple spectral channels affected by temperature–a 2-exciton process

During 2019, this investigator became aware of a unique paper relate to the visual performance of the simple eye of Limulus, an exothermic animal of ancient origin. It broadens the application of the 2-exciton mechanism.

#### 12.5.2.5.1 The UV & mid-wavelength visual channels in an exotherm–*Limulus*

The fact the band gap of liquid crystalline water is temperature sensitive introduces an unexpected but well documented situation relating to *Limulus*[29], [30]. *Limulus* exhibits only two spectral bands in the ocellus eye, the UV– and the M–channels (Chapman & Lall, fig. 8, 11 & 12).

Because *Limulus* is exothermic, its body temperature is typically between 10 to 25 Celsius. The band gap of liquid crystalline water reflects a higher value as the temperature is reduced over this range. As a result of the higher band gap, the M–channel chromophore must operate in a 2-exciton mode in order to stimulate the first activa (a situation only found in the L–channel of endothermic animals). It can be expected that all exothermic chordates can be expected to exhibit the 2-exciton mechanism in both their M– and L–channels. Below 20°C, exotherms can be

[29]Millecchia, R. & Mauro, A. (1969) The ventral photoreceptor cells of Limulus. J. Gen. Physiol. vol. 54, paper II-pp. 310-330 and paper III III-331-351

[30]Chapman, R. & Lall, A. (1967) Electroretinogram characteristics and the spectral mechanisms of the median ocellus and the lateral eye in Limulus polyphemus. J. Gen. Physiol. vol. 50, pp. 2267-2287

expected to employ a 2-exciton mechanism in the S–, M– & L–channels.

### 12.5.2.5.2 The proposed band gap of liquid-crystalline water versus temperature

The band gap of the N-type semiconductor material used in a PNP Activa (liquid-crystalline water) is a very important parameter when the Activa is used in a sensory neuron. **Figure 12.5.2-5** is a first known estimate of the band gap for liquid-crystalline water employed throughout the neural system of animals in general, including the primitive *Limulus*, and both exothermic and endothermic members of *Chordata*. The values given are crudely determined from the 2-exciton mechanism found in a majority of eyes. In endothermal animals, the value at 37 Celsius is near 2.1 electron-Volts. In exothermic animals, at 23 Celsius, the value is closer to 3.3 electron-Volts.

There has been virtually no research on water as a semiconductor when in the liquid crystalline form, at any temperature. There is one paper that has suggested a value of 2.1416 eV at 37°C.

**Section 8.1.3.3** will seek to understand the semiconductor properties of liquid-crystalline water based on such phenomenon as *glacial* blue ice, as opposed to common blue ice found in sea water..

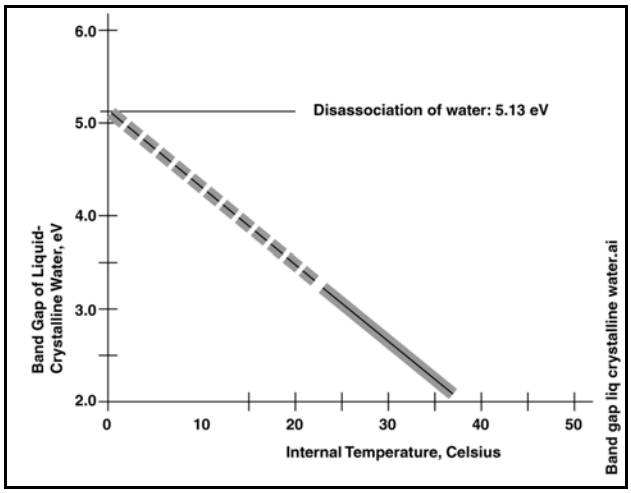


**Figure 12.5.2-5** Estimate: Band gap of liquid crystalline water. The black line is the best estimate and the gray band is the potential range in this value. This estimate is based on endothermic animals (primarily humans) plus the data from Limulus. Disassociation of bulk water normally occurs at 5.13 eV.

### 12.5.2.5.3 The impact on visual discrimination of the 2-exciton mode of photodetection

When this new relationship for the transfer characteristic of the translation block is introduced for the long wavelength chromophoric channel of humans and other endotherms, the results are significant in at least three ways. These will be discussed exhaustively in **Section 13.5.3**. Briefly, for endothermic animals they result in,

1. Gamma Differences among the L– and M–channels of vision at specific light levels.

2. Decrease in long wavelength channel sensitivity relative to the other channels to broadband illumination

3. Loss in spectral discrimination in the region between the M- & L- channel with lowered broadband illumination

Item one is the probable cause of the fascination of humans with a flickering fireplace.

### 12.5.2.5.4 The impact on the P/D Equation of the 2-exciton mode of photodetection

The variation in the band gap of the Activa of the adaptation amplifier (the first) with temperature appears to be similar to the variation in the P/D Equation describing the performance of the chromophores of the outer segment of each photoreceptor. The P/D Equation, describing the current injected into the neural system by a single disk in response to an impulse stimulus. It is presented in **Section 7.2** and supported in detail in **Appendix A**.

In the current situation, the variation in the band gap relates to the minimum energy exciton that can be transferred to the base of the first Activa. While closely related morphologically, the mechanisms appear to be totally unrelated except for their variation with temperature.

A comparison with the sensitivity of the band gap in Silicon and Germainium[31] might be informative.

For Silicon, the equation is $E_G(T) = 1.21 - 3.60 \times 10^{-4}T$ $E_G(300°K) = 1.1$ eV
For Germanium, it is $E_G(T) = 0.785 - 2.23 \times 10^{-4}T$ $E_G(300°K) = 0.72$ eV

In both these cases the band gaps are becoming smaller with rising temperatures. The decrement is on the order of $3 \times 10^{-4}$ per degree.

The estimate of the negative band gap change is about 300 times larger in the biological situation, ~ $-8.6 \times 10^{-2}$ eV per degree within the biological range of zero to 160°Celsius.

When initially plotting the data for [**Figure 12.5.2-5**] and comparing the data to that associated with the P/D Equation, it became obvious that the band gap of the biological Activa could not be extended below zero degrees centigrade because of the disassociation of bulk water at an energy of 5.13 eV. By assuming the band gap of interest was 5.13 eV at zero Celsius and the most accurate data point was for endothermic humans at 37°C the band gap assumed for exotherms at 3.3 eV at 23°C would become 3.22 eV. This is a very small change recognizing that there was no precise measurement of the room temperature in the laboratory reporting the temperature.

Based on the revelations discussed above, the equivalent equation for the biological band gap when restricted to greater than zero degrees Celsius would be,

In Biology, the equation is $E_G(T) = 5.13 - 1.9 \times 10^{-2}T$ , T > 273°K $E_G(300°K) = 3.22$ eV

This proposed band gap equation is significantly different from the values for intrinsic semiconductors. It should probably be compared to binary semiconductors like Indium Antimonide ($E_G$ = 0.17 eV at 300°K) or Gallium Arsenide ($E_G$ = 1.43 eV at 300°K). These materials are considered III-V semiconductors based on their positions in the Periodic Table. A broader band gap material is Aluminum gallium indium phosphide, AlGaInP, with a band gap varying between 1.8 eV and 2.0 eV at 25°C (298°K). The gap varies with the composition of the material resulting from a complex deposition process, known as heteroepitaxy.

Aluminum gallium indium phosphide has a crystalline structure usually described as the Zinc blende Structure. The complexity of Aluminum gallium indium phosphide as a crystal might be compared to the liquid-crystalline water forming the N-type material in **Section 8.4.2.3**. The atoms of the water molecules might be deposited on the polar groups of the lipids and result in an effective band gap in the range described above. The result would be a quantum-mechanical situation beyond that of an intrinsic or binary semiconductor.

The connection between the band gap and the disassociation energy of (bulk) water, and its exhibition of both a hexagonal and tetrahedral crystalline form has not been investigated here.

### 12.5.2.5.5 Potential impact on the sensory modalities of exothermic animals

*If the variation in the band gap of sensory neurons in animals is confirmed, it will provide new and significant understanding of the exothermic animals. It may also explain why some fish, including at least some sharks are able to achieve an endothermic state when needed.*

As the band gap rises in proportion to the drop in temperature within the biological temperature range, the spectral wavelength, where the 2-exciton mechanism is required, rises. It moves from an estimated wavelength of 590 nm in endotherms at 37°C to an estimated wavelength of 427 nm at 27° and 354 nm at 20°C (68°F) in exotherms. This means that the chromophores of the S–, M –, & L–channels will all rely upon the 2-exciton mechanism at 20°C. As the light level falls below the sunset level, these exotherms will be virtually blind.

***This fact, if confirmed, readily explains why it is so easy to hunt frogs with a triton tipped spear after sunset.***

***It also may explain why sharks would seek to warm the retina of their eyes when in cold waters.***

This induced restriction on the quantum-mechanical processes within the eyes is likely to also be present in the auditory, vestibular and and some tactile sensory neurons of exotherms.

---

[31]Millman, J. & Halkias, C. (1972) Integrated Electronics: Analog & Digital Circuits & Systems. NY:Mcgraw-Hill page 29

## 12.5.3 CRUCIAL MECHANISM: Adaptation of the outer segment–the phenomenon of bleaching

This sub-section addresses the quiescent, or steady, state of adaptation only. The transient, large signal light and dark adaptation (which involve different time constants) are addressed fullly in **Section 7.2.2**. Small signals generated by photoreceptors examining a scene do not affect the state of adaptation of the eye. Adaptation affects all of the photoreceptors in a local area of the retina on a spectral channel by spectral channel basis.

The net number of Rhodonine molecules in the ground state at any moment is indicative of the sensitivity of the total coating to stimulation. This sensitivity is also indicative of the *state of adaptation* of that OS. The number of molecules of Rhodonine per disc is very large. For a 2 micron diameter opsin substrate coated on both sides by a monolayer of Rhodonine molecules (neglecting the edge regions of coating), there are approximately $2 \times 10^8$ molecules of potentially excitable chromophore (**Section 4.3.5.5**) per outer segment, OS.

After a period measured in tens of seconds following the cessation of stimulation, all of the molecules of an outer segment, of an operational neuron, will be in their ground state and the OS will be at maximum sensitivity. Upon stimulation, the sensitivity will be given by the recent state of excitation, F, minus the recent state of de-excitation, K. The availability of charges to de-excite the chromophore molecules is usually less than required by the flux, F. As a result, the sensitivity of the OS decreases until a balance is achieved between the photon flux, F, and the de-excitation, K. This is the extremely important mechanism of adaptation. As a result of this mechanism, the average sensitivity of the OS becomes inverse to the average incident flux, F. The product of the average incident flux, F, times the average sensitivity is therefore a constant. Any short term change in the incident flux causes the value of K to vary accordingly, and this variation becomes the output signal delivered to the distribution Activa of the inner segment. This short term mechanism is termed the (photo) excitation/de-excitation mechanism in this work and its description is the Excitation/De-excitation Equation, the E/D Equation. The reason “photo” is in parentheses is because this same equation has been found to apply to all sensory modalities in the neural system of *Chordata*. The overall operation of the transduction mechanism is addressed in Appendix A.

With the large number of chromophore molecules per OS (about $2 \times 10^8$), the number of chromophore molecules in the ground state can easily drop to less than 1000. This would reduce the sensitivity of the OS by a factor of $2 \times 10^5$, a value commensurate with the dynamic range of vision. This is without factoring in the additional dynamic range (~10:1, **Section 2.4.7**) provided by the iris of the eye. A value of $10^6$:1 is compatible with the known adaptation range of the human eye (**Section 7.2.4** and **Section 17.6.1**, particularly **Figure 17.6.1-6**). This dynamic range is compatible with the white area of figure 2.1.1-2 in **Section 2.1.1.1**. Outside the white area the performance of the visual modality is limited by a broad range of factors.

*Note the incredible fact; the operating efficiency of the individual OS, under photopic condition is less than 0.001% compared to its scotopic operating efficiency. This means the level of bleaching under photopic conditions is also on the order of 0.001% of its unbleached condition. These numbers cannot be plotted realistically on linear scales. The level of bleaching is estimated to reach 99.999% before the lower edge of the photopic regime is reached (*$3 \times 10^{+3}$ cd/m$^2$).

**Figure 12.5.3-1** provides a caricature of the crucial adaptation mechanism, the ability of the chromophores within the outer segment of each photoreceptor to deliver a constant output signal to the inner segment under virtually any state of excitation. It is the ability of the chromophores of vision to maintain the product of illuminance and the adaptive state (the sensitivity) over a very wide range of stimulation. The abscissa is shown with two separate relative scales. The photon flux is the preferred scale as it is independent of the number of photons as a function of wavelength and color temperature which is not true of the illuminance scale. Similarly, the ordinate scale applies to two separate parameters.

The output signal range about the mean varies between about 0.1 to 10 mV positive, with a 20 mV positive signal resulting in some saturation at the pedicle of the photoreceptor neuron.

For levels of F below K, the available base current is sufficient to de-excite all of the excitons produced in real time. This situation maintains the sensitivity of the disc (or all of the discs of the outer segment, at maximum. In this regime, the output to the Activa follows the incident photon flux faithfully. At some high, but undetermined , photon flux, the pool of ground state electrons will be so depleted that the sensitivity of the disc will approach a vertical asymptote. This situation will cause the output to go to zero. Except under these two extreme conditions, adaptation is remarkably well behaved over many orders of magnitude of photon flux.

At average illuminance level significantly below K (two or more magnitudes), the information extraction engines of stage 4 restrict the bandwidth of the signaling channels and information processing channels to make optimum use of the information available

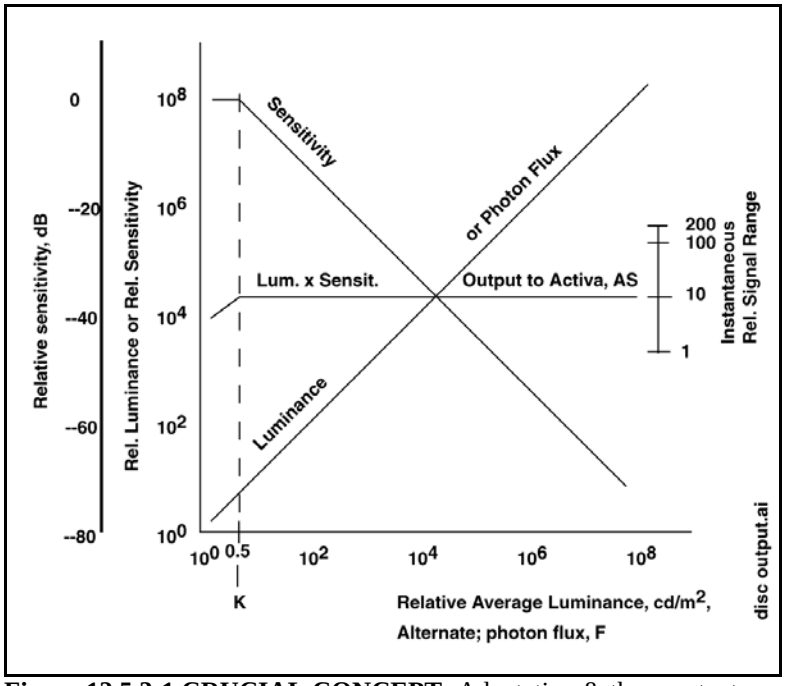


**Figure 12.5.3-1 CRUCIAL CONCEPT:** Adaptation & the constant signal output of discs of photoreceptors. K; the maximum average electron flow available from the base terminal of the first Activa, AS. Except at illumination levels (or photon flux, F) below the scotopic regime, the product of the average photon flux and the sensitivity equals a constant. Short term photon flux changes about the average constitute the output signal delivered to the base of the first Activa, AS. See text.

In summary,

**It is important to note** the visual modality operates as a nominally constant quiescent signal amplitude system beyond stage 1. This appears to be true for all operating modalities within the neural system. The nominal quiescent signal amplitude, for bipolar signals, throughout the neural system is nearly constant.

**It is similarly important to note**, stage 1 of the visual modality does not utilize high signal amplification except that of the 1st Activa, of all sensory neurons. The current gain of the 1st Activa is between 40 and 200 based on similar man-made transistors **and** the few data points in the literature relating the pA currents through the base and emitter leads of the 1st Activa.

**To maintain this nominally constant signal amplitude** throughout the neural system, the adaptation mechanism is primarily a signal reduction mechanism in the presence of very high intensity luminance. It operates over a loss range of 0 dB to greater than –80 dB. 0 dB is the fully dark adapted condition.

## 12.5.4 Effect of dis-assembly in the laboratory

It is very instructive to take a moment to examine the characteristics of the overall photodetection process, Stage 1, in the visual process developed here and to examine the observable characteristics of the various components in the laboratory.

### 12.5.4.1 Probing

As indicated elsewhere, the process of probing the photoreceptor cell in the laboratory is an awkward process, although useful information can be and is obtained. The size of typical probes is 10-25 microns, much larger than the 0.1 to 2 micron structures involved in the smaller neurons used in the stage 2 signal processing and stage 4 &5 information extraction activities related to vision. Therefore, attempting to obtain electronic signals that are not contaminated by the probing process is difficult and time consuming, essentially a probabilistic process in itself.

At impedance levels of 100 megohms associated with the smaller neurons, the capacitance associated with the output pedicle is frequently at or below five picofarads. Loading the output circuit of the neuron with an electrical probe exhibiting an equal or higher capacitance leads to problems. Such loading of a neuron will usually produce a highly distorted output on an oscilloscope. The investigator must makes a careful choice of electrical probes. In these situations, an open-gate MOS type of transistor most likely must be used as the very tip of the probe.

### 12.5.4.2 Dissection

If the "battery" powering the neural portion of the photoreceptor cell is disconnected from the neuron, the resting potential and the output waveforms associated with the cell will be grossly affected. Even penetrating the cell membrane has the potential of changing the resting potential and hence the overall performance of the cell.

> Removing one or more neurons and placing them in a petri dish requires careful attention to the chemical environment surrounding the neurons. If the environment does not include glutamic acid at a concentration of a few %, the electrostenolytic "battery" on the surface of each neuron will be deprived of its source of energy. ***Any Ringer's Solution must contain glutamic acid (****at a nominal 3% concentration****) if the neurons are to be kept functional.***

As shown in the pipette isolation technique, the total current into and out of the OS can be measured during irradiation by sucking the OS of an otherwise complete cell into a pipette which is connected into an electrical measuring set. Breaking the connection between the OS and the IS immediately terminates the electrical response to irradiation. The OS can still be bleached but it will not return to the unbleached condition except after an extended period of time. The OS is not a stand-alone photoreceptor. It must be attached to the IS for proper operation.

Similarly, the output of the IS, as measured at the pedicel, does not respond to irradiation in the absence of a proper connection to the OS via the microtubules passing through the cilium.

### 12.5.4.3 Extraction of the chromophores of vision–the Rhodonines

> ***The conventional process for extracting the visual chromophores in the laboratory does not lead to the extraction of the original material nor does it preserve the necessary and specific configuration of the chemical material that gives it its unique properties.***

To date, the method of extracting the active chromophores of vision has assumed they are contained *within* the discs of the outer segment of the photoreceptor neurons. The fact that electron-micrography has shown there is an important material coating the *outside* of the discs has been ignored. The goal has been to strip away all of the material surrounding the discs themselves using very coarse laboratory techniques that have routinely stripped away the actual chromophoric material and generally destroyed both its liquid-crystalline state of matter (**Section 5.5.15**) and its molecular structure by exposing the material to oxidative processes.

If the chromophoric molecules extracted above are now treated with an oxidizing agent, which most detergents are, in order to speed up the extraction process, another significant change takes place; the delicate chromophoric molecules are now oxidized by the detergent and they lose one or both of their heavy atom terminal groups--to be replaced typically by a hydrogen or a methyl group. The effect of this action is to transform the Rhodonines into a retinene or a similar fragment that is no longer a chromophore in the visual spectrum. The remaining material can no longer by characterized as a visual chromophore but only as a chromogen.

If any of the original chromophoric material remains in the aliquot preserved by the investigator, any oxygen associated with the chromophoric material will be excited into its triplet state. As a result, the chromophoric material becomes transparent with a relaxation time measured in tens of minutes to hours. The material will almost certainly be solubilized and lose its resonance properties associated with the liquid-crystalline state of matter.

As a result of this mishandling, the investigator is left to analyze the protein material forming the discs. Lo and behold, the dominant proteins of the disc is opsin *and* opsin does include a negligibly small ligand of retinol,

probably acting as a seed in opsin formation. Individual ligands of retinol are isolated and not photosensitive at the wavelengths of the known chromophores. The size of the retinol compared to the opsin protein is so small that the capture cross section of the combined molecule is negligibly small.

If the chromophoric material is diluted in order to continue extracting it from the protein material of the discs, the ordered and shared state of the $\pi$ band is disturbed. This has three effects; the individual molecules of the chromophoric material now exhibit very narrow absorption bands at visual wavelengths, measured in angstroms, as appropriate to such molecules at room temperature. The Pauli Exclusion Principle is no longer invoked as it is in a liquid-crystalline, and crystalline, state of matter. Secondly, the anisotropic, and highly focused spectral sensitivity of the chromophores is lost. Third, the absorption coefficient of these materials drop by several orders of magnitude since the slow structure associated with liquid crystalline materials no longer exists and the molecules are no longer quantum-mechanically resonant at visual wavelengths.

***Extracting the liquid-crystalline chromophores of vision from outer segments using a detergent, inevitably destroys the chromophores. The chromophoric material suffers one of two fates.***

***1. It is solubilized and discharged down the laboratory drain.***
***2. It is converted to a different chemical form by reaction with the detergent.***

***In either case, the investigator is left with a non-functional material as his residue.***

If a more benign laboratory procedure is used to isolate the chromophores on the surface of the opsin substrates, the investigator will be richly rewarded. *No oxidizing detergents can be used*. It is probable that the most effective approach will be to solubilize the material on the surface of the discs and then re-crystallize the chromophoric material by conventional means (**Section 5.5** and **Section 2.1.4** of "The Neuron and Neural System"). If the chromophores from multiple outer segments are processed simultaneously, a method of differential re-crystallization will be required. The various Rhodonines will re-crystallize separately due to their physical shapes at the molecular level.

If chemical analyses of the chromophoric material are planned, recall that most chemical references will not recognize the existence of a carboxylic acid "system" where the two oxygen atoms are part of, but separated by, a conjugated carbon molecular chain. They will certainly not recognize that this carboxylic acid system can be present within a retinoid containing other, non-functional, chemical groups. Do not rely upon an outside laboratory to analyze the recovered chromatic material.

## 12.6 (Reserved)

## 12.7 The Transfer Functions of Stage 1–Based on the P/D Equation

The complexity of the mechanisms and circuitry of stage 1 makes it difficult to describe its performance by a single transfer function. However, the transfer function can be described by breaking the discussion into several elements.

Besides the adaptation mechanism discussed in **Section 12.3.1**, the complete transfer function employs the photoexcitation/ De-excitation, P/D, Equation. This equation has been found to be universally applied to the sensory neurons of a sensory modalities. As a result, the equation is more appropriately known as the Excitation/De-excitation, E/D, process and/or Equation. It is developed in detail in Section 7.2 of Chapter 7. The complete P/D Equation is presented in **Section 7.2.4.2.1**.

### 12.7.1 The Large Signal Model

**Figure 12.7.1-1,** reproduced from **Section 17.2.2.**2 shows such a conceptual representation of the performance under a fixed condition of adaptation. The operating regions are correlated with the luminance level based on the values in **Section 2.1.1**. The ordinate is arbitrary but will be related to the Value scale of Munsell as the discussion proceeds. The figure will be definitized further by specifying the size of the isolated test target used to acquire the data in the figure.

The goal of the human visual system is to maintain the neural signals within the visual modality within a dynamic range of less than 200:1. This is the range from about 0.2 to 40 using the ordinate scale of this figure. The dashed line through the center of the "normal operating range" describes a neutral gray in the middle of the instantaneous dynamic range. If the *average* incident illumination does not fall on this dashed line so as to achieve a nominal value of 3 on the ordinate scale, the adaptation mechanism will cause the absorption cross section,$\sigma$, of the P/D Equation to decrease as discussed earlier in this chapter. The adaptation mechanism is very robust as indicated by

the diagonal lines in this figure. Under very bright illumination (the hyperopic regime), the absorption cross section can decrease by 80 dB, a value of nominally $10^4$:1. If the average illumination still does not conform to a brightness value of about 3, the visual system will saturate and enter a condition normally associated with "snow blindness." The perception of scene contrast will be reduced to near zero. For illumination levels below the photopic regime, full dark adaptation will be approached. Usually, the scene contrast is greatly reduced in this regime, with starlight the dominant natural source. Th result is a reduced signal level in the brightness of the neural signal.

- - -

The solid curved line intersecting with the dash-dot line labeled compression can be expected to describe the overall response of the visual system to a luminance stimulus in the absence of any adaptation mechanism. If the feedback employed by the sensory neurons was 100% effective in limiting the growth in the neural signal above a specific cut-in value, the curve labeled 100% adaptation asymptote would be achieved with the introduction of adaptation. However, the feedback employed in vision, like in hearing, is not designed to provide a hard limit on the brightness response. It is designed to expand the brightness range associated with a given luminance range over a limited operating range known as the photopic region. The result is the dashed line through the middle of the shaded box labeled "Normal Operating Regime." The following material will attempt to quantify the scales of this figure more completely.

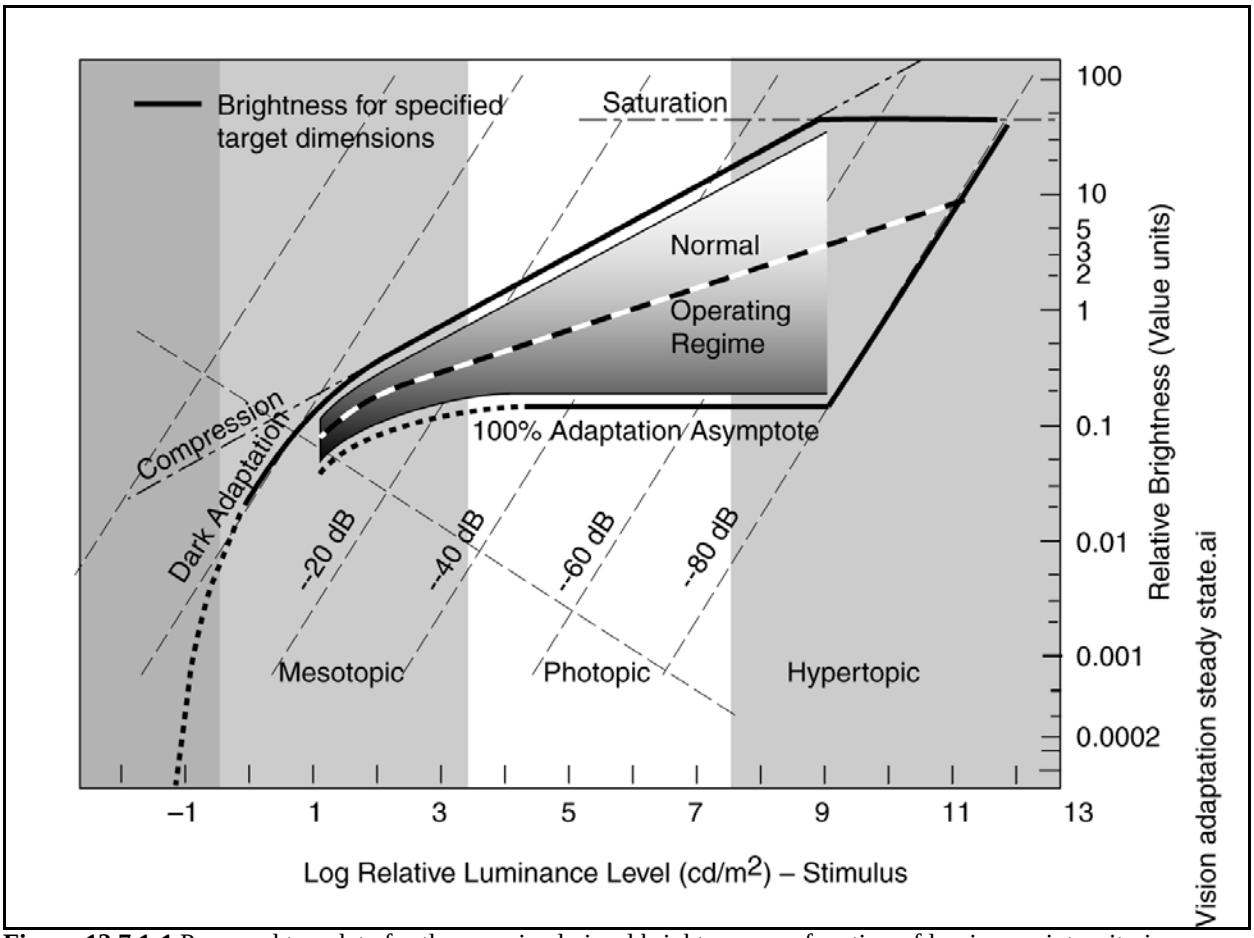


**Figure 12.7.1-1** Proposed template for the perceived visual brightness as a function of luminance intensity in humans ADD. The dashed line within the Normal Operating Regime is called the terminal brightness locus by Stevens & Stevens. The Compression line is called the Dark adaptation line by them.

The large signal model must be evaluated in terms of the temporal characteristics of the input signal. If the signal is at a constant level with respect to time, changes in the scene contrast will be handled differently. **The adaptation mechanism has a limited response time usually measured in seconds.**

### 12.7.1.1 Short term large signal model– milliseconds duration

For short term stimuli, such as those illustrated in Section 12.8.1-4A, the adaptation mechanism remains frozen during short duration stimuli. Thus the dynamic range of the 1st Activa (in the adaptation amplifier) is usually controlling. The figure shows a hard saturation at the 20 picoampere level within a fraction of a second following the P/D response. The signal labeled 7.8 photons/micron$^2$ was handled by the 1st Activa well (a dynamic signal level of 243:1) but saturated at a signal level of 16 photons/micron$^2$ (a dynamic signal level of 500:1).

### 12.7.1.2 Longer term large signal model– seconds or longer duration

For longer term stimuli, lasting more than a few seconds, the adaptation mechanism is controlling. Within the time constant set by the 1st Activa electrostenolytic power supply, the adaptation mechanism will re-establish the nominal brightness value of 3 as described above. Until it has had time to do this for increases in illumination (which may take many time constants for illumination changes of a decade or more), the system will saturate, and generally cause pain to be reported to the brain. This is the situation encountered on leaving a movie theater in the middle of the afternoon on a clear day. For significant reductions in illumination, the adaptation mechanism also requires time to change the sensitivity (to raise the absorption cross section, $\sigma$). This is the situation when you enter a movie theater from outside on a bright clear day.

- - - -xxx

Based on the observed characteristics in the referenced test data and the literature, the large signal dynamic range of the photoreceptor is quite enormous. It is a photon counter at low irradiances and its maximum signal level is limited, according to the P/D, by the availability of n-electrons in the chromophoric liquid crystal of the OS (the total of all discs which are in electronic communications within a single OS). The maximum sustained signal level, $i_o$, may also be limited metabolically by the ability of the IS to support the necessary supply current under long term conditions; this would introduce another time constant into the overall "Adaptation Equation".

The instantaneous dynamic range of the photoreceptor is much smaller. As shown by the test data, the maximum output current available from most photoreceptors is in the 20-30 pA range and it clearly exhibits the logarithmic characteristic of the diode at the input to the amplifier stage. Whether it is appropriate to describe the diode circuit as a clamp depends on the values of the resistors involved. But clearly, for large instantaneous signal changes, the signal level is clamped to $i_o=i_s$.

It should be noted that the overall dynamic range of the eye is essentially linear until the number of available n-electrons is depleted. However, the instantaneous dynamic range is effectively limited to a range on the order of 100:1 and the output is a very accurate logarithmic function of the input.

## 12.7.2 The Small Signal Model

The small signal model of the photoreceptor is straight forward based on the graphic above and the complete P/D equation. This equation is differentiable and an exact output can be obtained for any input condition. The P/D equation remains a linear equation under all small signal conditions and the 1st Activa does not saturate.

Within the dynamic range of the 1st Activa (about 200:1) and the adaptation mechanism, The perceived scene contrast will be faithfully reported to the brain (stage 5 of the visual modality). As noted above for low scene illumination, the scene contrast may be low. As a result, the perceived scene contrast reported to the brain may also be low. The stage 4 information extraction engines of the visual modality appears to make certain algorithmic modification under these conditions to optimize the information provided to stage 5.

## 12.7.4 The transient state transfer function EMPTY

[Work in Devoe 1966 including the circuit diagram shown in Armington 1974]

Note also Crone page 190 and the mathematical problem with this description

## 12.8 Comparison with data in the Literature

This section may appear superfluous since much of the most important literature has been utilized in the development and justification of the overall model. However, there are more comparisons to be made.

It is necessary to show how the model developed here applies to all types of animal vision. Thus, it must be shown to apply to *Arthropoda* and *Mollusca* (basically all invertebrates with vision) and to *Chordata* (the vertebrates and some of their ancestors) and possibly a few unusual cases such as *Limulus* (which may have a unique photoreceptor cell, known as the eccentric cell) and *Annelida*.

Reference will be made to the Photoexcitation/De-excitation Equation (P/D Equation) developed in **Section 16.3**. It describes the electrical waveforms generated within the outer and inner segments of the photoreceptor cells. After some modification, the P/D Equation appears as the "generator waveform" at the pedicle of a photoreceptor cell. Reference will also be made to **Section 11.1.5** where a variety of waveforms were defined by Class. **Figure 12.8.1-1** offers a modified diagram annotating the relationship of these waveforms to the photoreceptor cell. The electrostenolytic supply for the adaptation amplifier (on the left) has been shown explicitly because of its importance to the discussion of **Section 12.8.1. 2** & **3**. The details of this circuit, its relation to the vascular supply of the retina and its impact on adaptation mechanism will be detailed in **Sections 12.5.3.2.1** & **16.4.2.1**. The Class A waveform path is shown dashed because there is no known technique for contacting the open connection to the base region of the Activa within the adaptation amplifier. However, using the Faraday cage technique of Baylor et al., the signal current of the Class C waveform has been found to equal the Class A signal waveform. Effectively, all of the important waveforms of the photoreceptor have been recorded in the laboratory as will be discussed below.

The area between the RPE and the inner segments of the photoreceptors is chemically unique. It is an area free of oxygen and dopamine and filled with the discs of the outer segments. Oxygen must be excluded to avoid oxidation of the chromophore material on the discs in liquid-crystalline form. The discs are immersed in a solution of chromophores and chromophore carriers, IRBP's. The solution also contains glutamate as the neural system fuel and GABA as a waste product of electrostenolytics. Bruck's membrane is well documented as the outer surface of the RPE farthest from the pupil of the eye. Verhoeff's membrane is less well documented and may not be a physical membrane. Alternately, it may be a highly cribiform surface of limited structural strength.

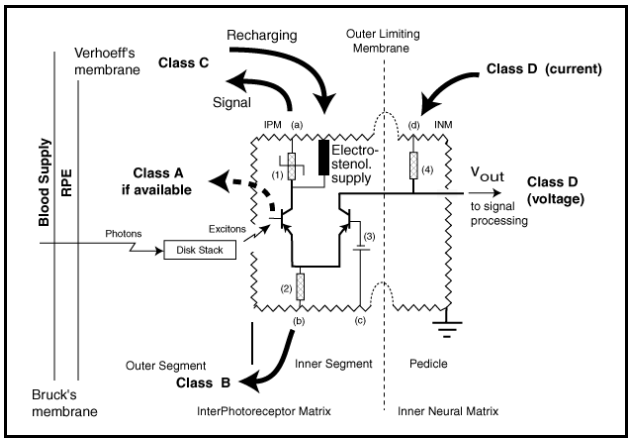


**Figure 12.8.1-1** Waveforms associated with the photoreceptor cell. The photons are shown arriving at the disc stack of the outer segment from the wrong direction for simplicity. The electrostenolytic supply to the collector of the adaptation amplifier Activa has been shown explicitly. See text.

### 12.8.1 The outer segment and the suction pipette technique

The Baylor team has been studying the photoreceptor cell for many years using a technique where a single operational OS is sucked into a Faraday cage in the form of a micropipette. In the more recent experiments, this pipette has had a thermocouple mounted near the tip of the pipette to provide precise temperature information. By moving the OS into the Faraday cage gradually, it is possible to determine the source of the current emanating from the OS. The current is very uniform as a function of the length of the OS. This technique essentially isolates the selected OS from the IPM. Therefore, the collected current is returned to the system through the ground connection provided by the experimenter. In this way, a Class C waveform is obtained but the return path is not via the ground bridge between the IPM and the INM. The waveform is usually measured as a current because of the extremely high impedance level.

If measured as a voltage, the Class C waveform can be considered the result of a second order physical system if the capacitance associated with the collector is significant. Therefore, the waveform is not discontinuous, as in the Class B waveforms, where the amplitude departs abruptly from the baseline. It would depart with a small amount of curvature after the intrinsic delay of the P/D Equation. Other considerations may apply, see **Section 16.4.1.1.8**.

The circuit under test will remain functional for some time. It can continue to operate because of the electrostenolytic materials stored within the furrows of the disc stack and surrounding the OS.

Baylor provides some interesting data when applied to this model[32]. Under totally dark conditions, the adaptation amplifier Activa is essentially cutoff except for the noise current due to both the chromophore and the Activa itself. Under this condition, the Class C waveform is dominated by the impedance of the electrostenolytic supply and the capacitor, $C_A$. Because of this, the waveform is band limited to approximately 3 Hz at the half power point in monkey. In the dark, the RMS noise floor for this same waveform had a variance of about 0.03 $pA^2$. This waveform is not associated directly with the signal path in vision which is generally regarded to have a bandwidth of at least 50 Hz. However, its noise spectrum does define the first time constant of the dark adaptation portion of the light adaptation function in monkey. This 3 Hz low pass filter in the feedback path of the adaptation amplifier becomes the lower frequency limit of the high pass network contributing to the actual signal path bandwidth of 3 to >50 Hz.

In spectral experiments, the same school has provided data they did not expect using the micropipette approach. During the 1970's they worked with turtles at 20C[33]. They isolated photoreceptors with spectral peaks reported as 460, 550 and 630 nm. (accuracy limited by the 15-20 nm. width of the spectral filters) using axial illumination. They also reported two cells with a peak response near 515 nm. During the 1980's they attempted similar experiments with turtles using the new technique. Based on their experience, they attempted to measure the spectral response of a variety of "cones," both red and green. In these micropipette experiments, they illuminated the OS in the transverse direction. As a result, they recorded spectrums, they interpreted as red cones, with a peak spectral response in the region of 498 +/-2 nm. They have not offered an explanation of why they have been unable to record the expected chromatic spectrum. By illuminating the OS from the side instead of from along its axis, they have recorded the isotropic (non-operational) spectrum of the chromophore material instead of its anisotropic (operational) spectrum. It is assumed here that the two cells reported to have a peak near 515 nm. in the 1970's experiments were misalligned relative to the incident illumination. The result was a spectrum representing a mixture of the isotropic and anisotropic spectrums.

Beginning in 1990, the Baylor school began applying the stimulus axially with regard to the outer segment. As a result, the operational spectra of photoreceptors were recorded. In one of the L-channel chromophore recordes, they reported its peak near 640 nm instead of the 625 nm used in this work.

*The very useful recordings of the responses related to the P/D Equation by the Baylor team during the 1970's are explored fully in an accompanying work, Chapters 2 & 8 of "The Neuron and Neural System[34]."*

### 12.8.1.1 The Class C voltage waveform at the outer segment

Theoretically both the potential change related to, and the current flow from, the confines of an individual outer segment should be measurable and compared to that predicted by the P/D Equation. However, the potentials related to the dendrites of the outer segment are difficult to probe. Baylor & Hodgkin presented voltage data on what they believed was a single photoreceptor of the turtle. **Figure 12.8.1-2** shows their data overlaid with the predicted P/D Equation. They discussed their results in terms of a peak near 644 nm (the discussion was based on their measurements at a wavelength of 644 nm as well as 400 and 805 nm). Note the range bars. Eleven responses were averaged at 644 nm, 14 at 805 nm and 11 at 405 nm. The vertical scale does not reflect the voltage measured at a common excitation. It has been scaled to estimate the voltage generated per photon absorbed (not applied) at three different wavelengths. This required the intensity of the stimulus to vary. They did report a resting potential of -43 mV and a maximum response to light of -23 mV at 22.2 Celsius. The stimuli were applied axially to the outer segment and the resulting spectrum is that of the anisotropic absorption of a L–channel photoreceptor. The expected peak absorption would be at a wavelength of 625 nm. It was not possible to define the exact location of the probe relative to the cell in that era. The diameter of the probes frequently exceeded the diameter of an individual cell. These values suggest the probe was contacting the interior plasma associated with the common emitter terminal of the inner segment of the photoreceptor rather than the axoplasm. If true, the response represents a Class B

---

[32]Baylor, D. Nunn, B. & Schnapf, J. (1984) The photocurrent, noise and spectral sensitivity of rods of the monkey, *Macaca fascicularis*. J. Physiol. vol. 357, pp. 575-607

[33]Baylor, D. & Hodgkin, A. (1973) Detection and resolution of visual stimuli by turtle photoreceptors. J. Physiol. vol. 234, pp. 163-198

[34]Fulton, J. (2008) The Neuron and Neural System *online* https://neuronresearch.net/neuron/ and updated through 2019

waveform. The time response did not vary significantly between the wavelengths used because the product of absorption and stimulus intensity, $\sigma \cdot F$ was held constant.

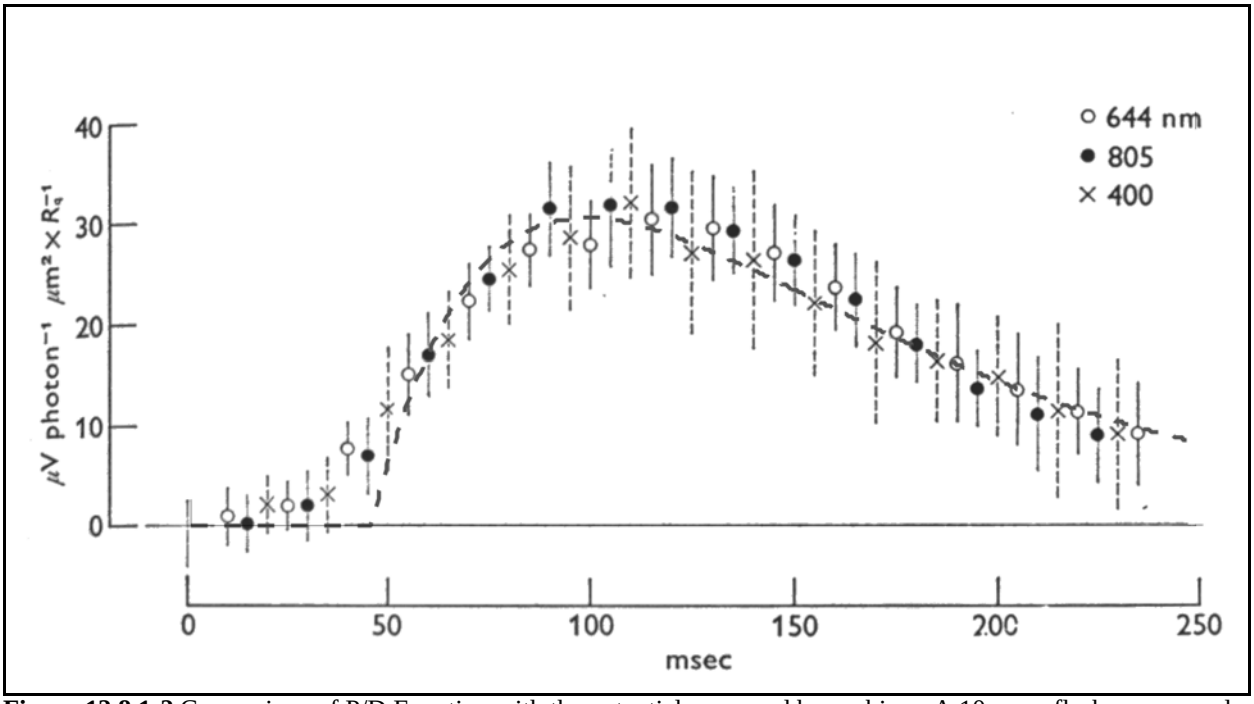


**Figure 12.8.1-2** Comparison of P/D Equation with the potential measured by probing. A 10 msec flash was passed through a narrow band filter. The impulse form of the P/D Equation is shown as the dashed line for a $\sigma \cdot F$ value of 175. An absolute delay of 46 msec is shown. The data is from Baylor & Hodgkin, 1973.

Using the overlay, the peak in the amplitude of the data can be equated to $0.55 \cdot \sigma \cdot F = 96.25$/msec based on a time constant of 80 msec at 22.2 Celsius. $\sigma \cdot F \cdot \tau = 2.2$. When referenced to 37 Celsius, the effective time constant of the P/D mechanism of turtle is 12.5 msec. Since this is the same time constant as man, this suggests that the identical mechanism is employed.

Neither the theory or the measured data suggest any crossing of the horizontal axis (an undershoot) at this point in the signaling path of turtle. The absolute delay of 46 msec. was not analyzed as to the portion due to the intrinsic delay in turtle, the delay in the adaptation amplifier and any instrumentation delay.

## 12.8.1.2 The Class C current waveform at the outer segment

Collecting the total current from within the confines of a single outer segment provides the best opportunity to measure a waveform directly related to the Photoexcitation/de-excitation mechanism. The Baylor team demonstrated the collection of the current from a single outer segment using a Faraday cage as a collection device. Their initial focus was to obtain the response at very low stimulus levels (seeking the response from a single photon). **Figure 12.8.1-3** shows their data overlaid with the performance predicted by the P/D Equation.

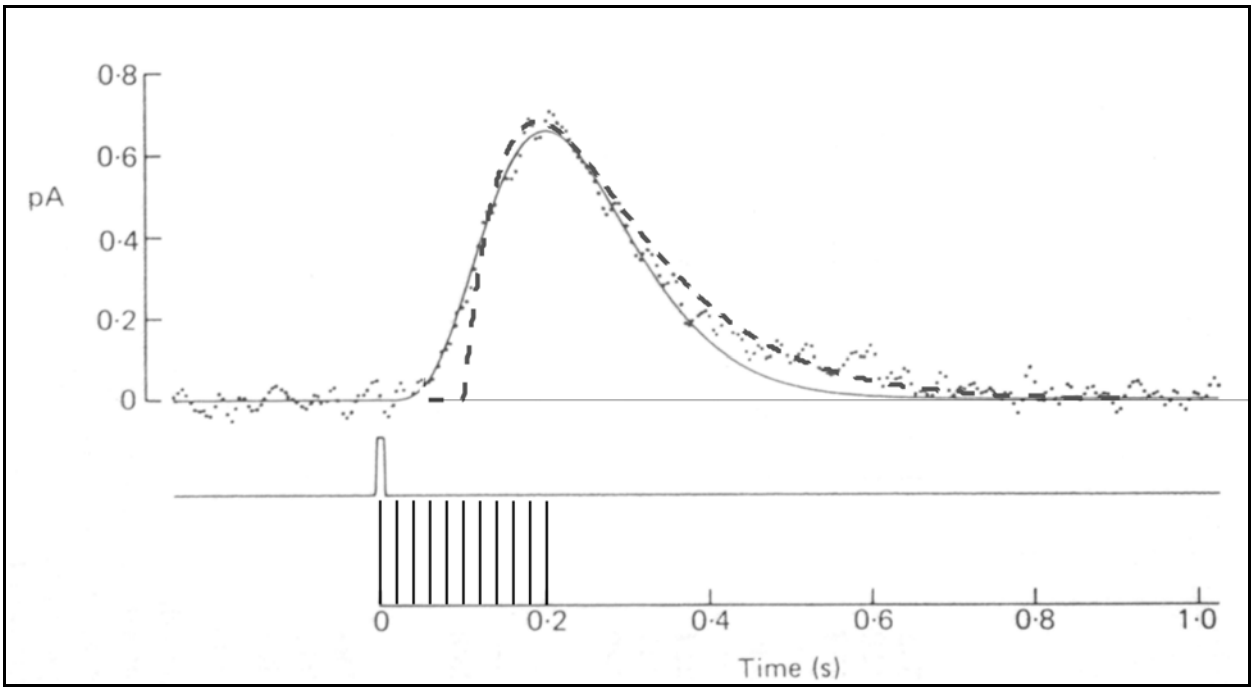


**Figure 12.8.1-3** Comparison of P/D Equation with current collected by a Faraday cage. The data points and the solid line are from Baylor, Nunn & Schnapf, 1984. They used a six stage filter to create the solid line. They noted the response did not match the data points adequately near 0.2 seconds and between 0.4 and 0.7 seconds. The heavy dashed line is the P/E Equation for $\sigma \cdot F \cdot \tau = 0.60$. The fit is better in both regions. The data shows considerable sinusoidal interference unrelated to the signal. If this interference was of a different phase, the fit to the dashed curve at 0.06 to 0.08 seconds would be even better. It is not clear if the interference is related to their filter. If so, the filter may have introduced a delay of 0.1 seconds. This delay is larger than the 5 ms initial delay predicted by the P/D Equation. See text. From Baylor, Nunn & Schnapf, 1984.

Baylor et. al used six identical low pass filters in series (but presumably isolated from each other–see Fourtes & Hodgkin, 1964) to emulate their data. They noted that the resulting curve was not as narrow as desired near 0.25 seconds and did not fit the data well between 0.4 and 0.7 seconds. They also noted that the data from other cells deviated even further from their proposed curve.

The P/D Equation of this work (**Section 7.2**) provides a better fit to the data set presented in the figure. The Equation was drawn for $\sigma \cdot F \cdot \tau = 0.56$, $\tau = 0.70$ seconds and $\sigma \cdot F = 8$ (heavy dashed line). At these values, an intrinsic delay, following the start of the impulse, of 5.2 ms is predicted. It provides an excellent fit to the data after time = 0.1 seconds (See **Section 16.4.1.1.8** for a discussion of the deviation in this area for low values of $\sigma \cdot F$). By increasing $\sigma \cdot F$ slightly, the P/D Equation can fit data sets with a longer tail as described by Baylor, et. al. Neither the data as measured or the P/D Equation exhibits any negative component under the above conditions.

Bearing the subject of **Section 16.4.1.1.8** in mind, the long time constant of 60-70 ms in the eye of monkey may be

significant. If this value was confirmed for higher levels of $\sigma \bullet F$, it would suggest a significant difference between humans and the Macaca family. Such a long time constant compared to the 12.5 ms of humans would suggest much less capability in analyzing fine detail quickly. This capability is critical in reading (other than for the large block characters usually used in learning experiments with monkeys ).

More experimentation is needed in this area to further refine the instrumentation and separate the data into additional classes if necessary. Establishing mean values and range bars for each class of data would allow further perfection of the theoretical model.

The data of figure 3 of Baylor, Lamb & Yau (1979a) provides very important data concerning the class C current waveform. **Figure 12.8.1-4** reproduces their data for the Class C current of the toad, *Bufo marinus*, using the suction pipette technique and transverse stimulation of a "red rod." Temperature was poorly controlled to the range of 18-25° Celsius. The peak absorption was at 500 nm as expected for the intrinsic absorption of the Rhodonines when the outer segment is subject to transverse stimulation. Frame A shows the data as collected, including significant saturation at 20 pA output current. Below 20 pA output current, the waveform faithfully reproduces the theoretical P/D response. Frame B shows the expected performance of the first Activa under these operating conditions. A nominal electrostenolytic supply voltage of -154 mV is assumed. A nominal electrostenolytic supply impedance of 7 megohms is also assumed. Under these conditions, the instantaneous output current, $i_c$, is proportional to the excitation current, $i_b$, for output current levels below 20 pA. The output current is outgoing from the cell to the pipette wall. As the excitation current increases, the output current increases proportionately in accordance with the load line, until the load line, $R_L$, intersects the saturation line. At this point, the Activa stops exhibiting "transistor action" since the collector potential is below the saturation potential. This is the reason for the hard saturation in frame A.

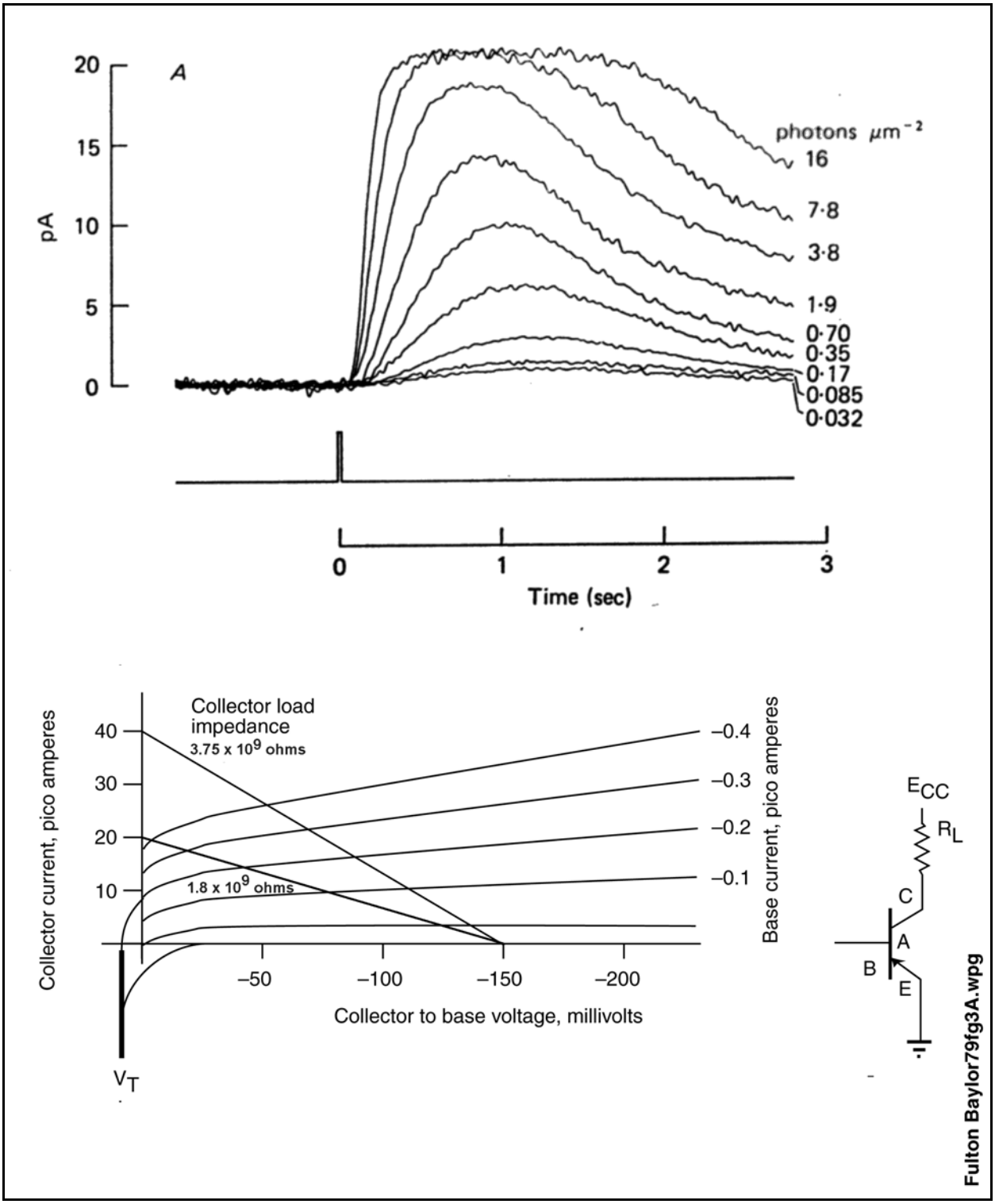


**Figure 12.8.1-4** The Class C current waveform using suction pipette techniques. A; The collected Class C current showing saturation. From Baylor et al., 1979a. B; the current-voltage characteristic of the associated first Activa. Note the magnitude of the load impedances, thousands of megohms.. See text.

It is clear from frame A that the maximum output current is 20 pA regardless of the particular impedance of the assumed load line. The load line shown was chosen to give a 25 mV saturation voltage in accordance with other available data. The first Activa of this PC has gone into saturation at a current of 20 pA.

### 12.8.1.3 The Response of the OS according to Schnapf et al.–Inadequate protocol

The current waveforms presented in Figure 1 of Schnapf, Kraft & Baylor[35] for the human and Figure 1 of Baylor, Nunn & Schnapf[36] for the monkey appear to represent the Class C current waveform measured using the micro-pipette technique. This waveform is at the collector terminal of the Activa within the dendrites associated with the outer segment. The waveforms can be analyzed in terms of a forward current due to the application of the Class A waveform to the base of the Activa. and a reverse current due to the recharging of the capacitor associated with the collector of the Activa after the end of the Class A waveform. It is the recharging current that causes the "undershoot" noted in the measurements of Schnapf, et. al. In the first paper, the labeling of the putative types of photoreceptors should be studied carefully. ]

Schnapf et al. presented data gathered from a human retina that purports to show the response of two "cones" to light flashes of unspecified duration and a wavelength of 500 nm limited by a 10 nm filter. The Schnapf et al. paper was presented as a Letter to Nature magazine of only 3 pages. It did not describe its methods carefully, citing instead Baylor et al., 1979a.

The technique was to dice into small pieces, of about 100 microns across, the enucleated eye of a living subject. No details were provided as to where on the retina, the dices pieces originated. The retina was diced initially during exposure to dim red light, suggesting the state of adaptation was not controlled. The responses for their red cones in figure 1 shows saturation at their maximum exposure level. The green cones, exposed to a lower maximum level, did not exhibit saturation.

Part of the data from figure 1 in the Schnapf et al. paper, top, and the P/D Equation, bottom are compared in **Figure 12.8.1-5** with the aid of an inset related to the histological situation.

The measurements were made *in-vitro* at 37 Celsius on tissue from a human retina using transverse illumination. The data was band-limited to 50 Hertz. Only the data for the "green" photoreceptor is shown. The other data involves a higher degree of saturation and complicates the analyses. By collecting data at 500 nm, they also show the difference in spectral absorption between the two photoreceptors documented. In the first case, the traces are the average of eleven individual traces. In the second case ("Green"), the number of traces averaged was a variable. Neither case provides range bars on the data sets.

The bipolar waveforms in their figure 1 of the 1987 paper are distinctly different than the monopolar waveforms of the Baylor team during the 1970's and as late as 1984. The bipolar waveforms appear to resemble the ERG's discussed in **Section 12.8.2**. This similarity to other bipolar waveforms questions the test equipment configuration used by Schnapf et al. Specifically where the return lead was connected to the pieces of diced retina described. Individual outer segments were drawn into a metallized micropipette acting as a Faraday Cage similar to that of the Baylor team more than eight years earlier. It was difficult to make measurements at the picoampere level in the 1980's. It appears likely that the return lead was influenced by signals from the stage 2 signal processing circuits orthodromic to the outer segment of the PC in stage 1. A delay of 52 ms between the initial P/D response and the inverted response that was added to obtain the net response is shown in the bottom frame. This would suggest the delayed response originated within stage 2.

The delayed response may have been positive-going and monopolar. In that case it would have been inverted at the input to the differential amplifier of the test equipment shown in the inset. It could have been acquired through the signal return lead if the "ground" was located too close to one of the stage 2 neurons within the ~100 micron die. Note also the 30 Hertz sinusoidal interference signal probably acquired through the one-half wave rectifier in the power supply of the test equipment. It appears throughout the data recording interval in all traces.

---

[35]Schnapf, J. Kraft, T. & Baylor, D. (1987) Spectral sensitivity of human cone photoreceptors. *Nature*, vol. 325, pp 439-441

[36]Baylor, D. Nunn, B. & Schnapf, J. (1987) Spectral sensitivity of cones of the monkey *Macaca fascicularis, J. Physiol*. vol. 390, pp 145-160

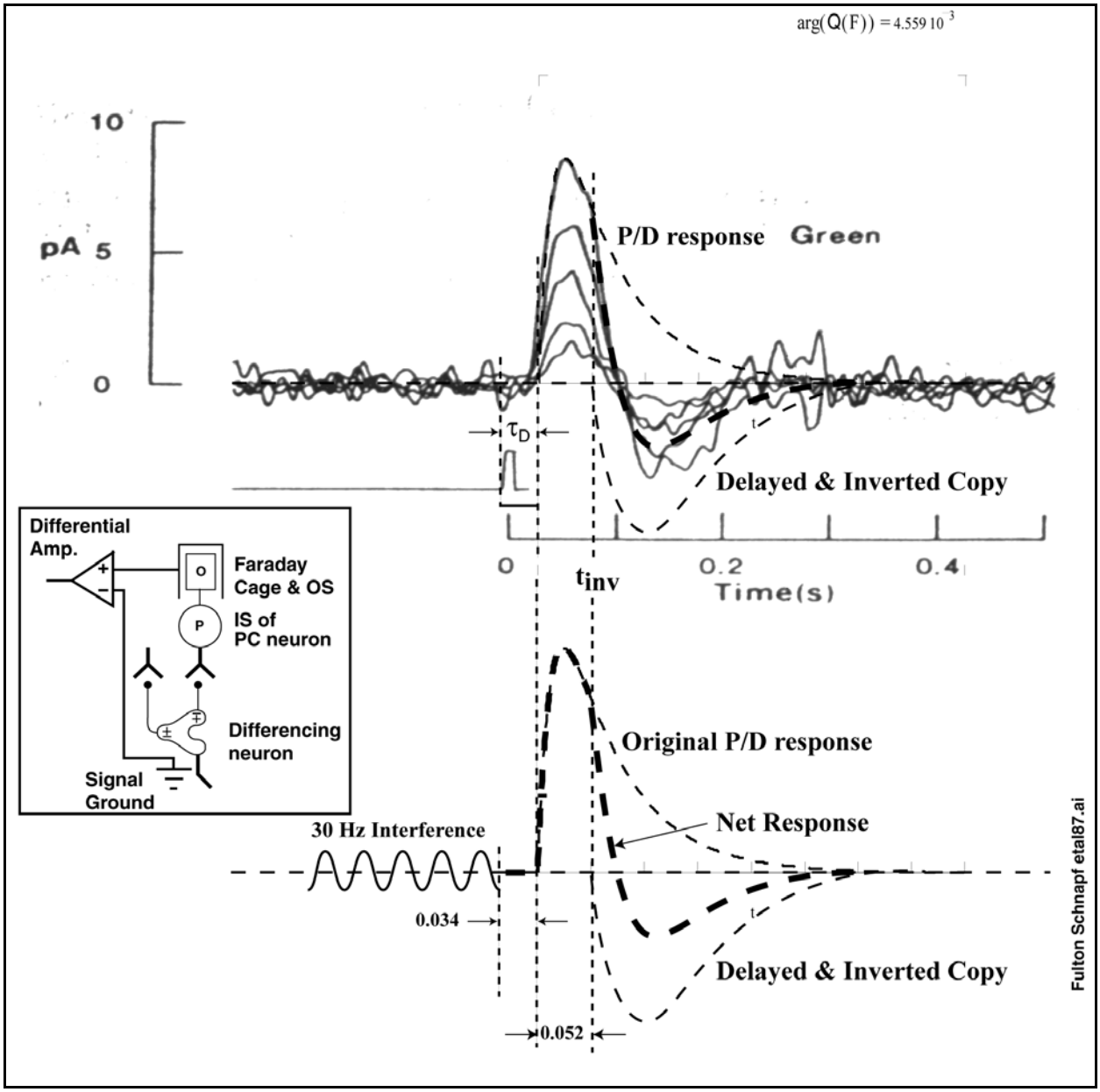


**Figure 12.8.1-5** Comparison of the P/D Equation and a delayed & inverted copy with published measurements. P/D Equation plotted for $\sigma \cdot F=18$, $\sigma \cdot F \cdot \tau = 0.25$, $\tau = 12.5$ ms. Measurements by Faraday cage micropipette *in-vitro* at 37 Celsius. Micropipette was connected to the positive input of a differential amplifier. A connection to the negative input was used as a signal return lead. Note significant 30 Hz sinusoidal interference throughout laboratory data.. See Text. Data points from Schnapf, Kraft & Baylor, 1987.

The P/D Equation in the lower frame is plotted for an absorbed photon flux, $\sigma \cdot F = 18$, a temperature of 37 Celsius and a time constant of 12.5 ms. $\sigma \cdot F = 18$ appears to represent their stimulus of 2,542 photons/ micron$^2$ quite well. The P/D Equaton allows the precise state of adaptation, related to $\sigma$, to be calculated. The P/D Equation predicted an intrinsic time delay of $\tau = 46$ ms. This is slightly longer than the 34 ms measured relative to zero on the graph of the original publication. The difference, 16 ms, may be impacted by the (unspecified) width, and quality of the pulse used. The initial delay, $\tau_D$ is measured from the beginning of the stimulus. The origin of the time scale is taken as the center of the pulse shown. Theoretically, it should be taken at the initial point of the stimulation.

In the top frame, the P/D function (upper thin dashed line) overlays the upper curve so well, it is difficult to see the features in the data curve. Both curves rise, peak and begin to descend along identical loci. At the time marked $t_{inv}$, there is a distinct discontinuity in the measured curve. It is at this time that the delayed and inverted copy of the P/D response becomes significant. Becuase of the 50 Hz bandpass filtering and the filtering within the inner segment of the PC, the time course of the filtered and delayed copy is estimated. The instantaneous difference between the P/D response and the delayed copy is shown by the heavy dashed line through the data set. This line, when combined with the P/D Equation prior to $t_{inv}$, traces the expected path for a noise free response to the stimulus as measured in the laboratory.

> In the above figure, a case can be made for an $\alpha$-wave and a $\beta$-wave as in ERG recordings. However, it is obvious that a choice must be made as to where the transition occurs; it can be taken as the start of the delayed representation at $t_{inv}$ or it can be taken at the point the net response crosses the horizontal axis. Using $t_{inv}$ as the transition point eliminates the amplitude of the delayed response from affecting the transition.

### 12.8.1.3 The peak Class C waveform at different positions along the outer segment

**Figure 12.8.1-6** provides the results of the suction pipette technique developed by Baylor, et. al[37]. using the suction pipette as a Faraday Cage enclosing a portion of a photoreceptor cell. The procedure involves the isolation of a single in-vivo PC by sucking it into a Faraday cage. All of the current emanating from the PC along that part of the cell enclosed by the Faraday cage is collected and measured. The PC was from a toad, *Bufo marinus*. They speak of "red" rods (their terminology and emphasis) however all of their data exhibits a peak wavelength at 500 nm because of the use of illumination presented transverse to the axis of the outer segment. Test were performed at room temperature.

The data suggests that in the toad, the microtubules extend the length of the outer segment. The current collected in their experiments changed by 0.7 pA/micron for their average outer segment.

The peak current decayed from 26.8 pA on the first of two measurements to 22.4 pA on the second suggesting a lack of glutamate in their Ringer's solution. They did not describe their Ringer's solution which is normally glutamate-free.

The current profile is quite similar to the voltage profile measured earlier by Penn & Hagins[38] in bulk retinal membranes. This profile suggests that the IPM is a resistive medium but the simple electrical model developed by Hagins for the photoreceptor cell is too simple[39]. A more comprehensive model will be provided later in this work.

---

[37]Baylor, D. Lamb, T. & Yau, K.-W. (1979) The membrane current of single rod outer segments. J. Physiol. vol. 288, pp. 589-611

[38]Penn, R. & Hagins, W. (1969) Signal transmission along retinal rods and the origin of the electroretinographic a-wave. Nature, vol. 223, pp. 201-205

[39]Hagins, W. (1965) Electrical signs of information flow in photoreceptors. In Symposia on Quantitative Biology, vol. XXX Long Island, NY: Cold Spring Harbor Laboratory

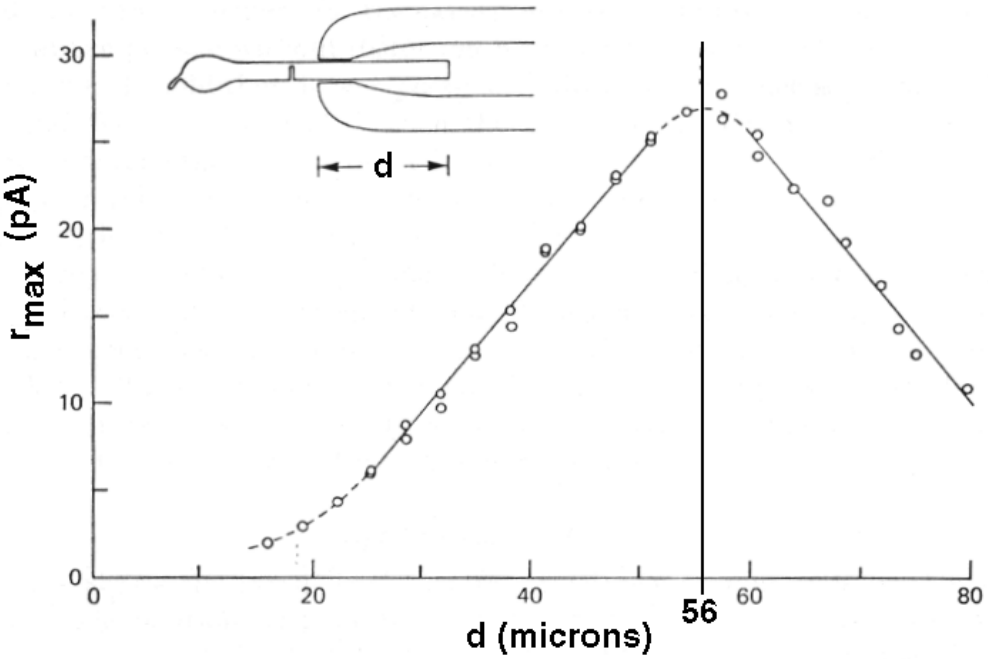


**Figure 12.8.1-6** Current captured by a Faraday Cage surrounding the Outer Segment and Inner Segment of a photoreceptor cell as a function of position. Ordinate is response to a diffuse 20 msec 500 nm flash delivering 64 photons per square microns, a saturating light. Abscissa is distance from electrode tip to distal tip of outer segment (see Inset). The cell was expelled and drawn in twice, and most points are averages of two measurements. During the experiment, the response at the optimal position (d=58 microns) decayed from 26.8 to 22.4 pA and all points have been scaled to give 26.8 pA at this position. Curve fitted by eye. This cell was completely isolated from the retina. From Baylor, Lamb & Yau (1979).

Both Baylor, et. al. and Penn & Hagins employed transverse illumination in their early experiments. Thus, their data does not reflect the operational (anisotropic) spectral sensitivity of the photoreceptors to axial light. Later Baylor work has employed axial illumination.

## 12.8.2 ERG compared to inter-neuron-probe data of the photoreceptor output

There is an open question that keeps reappearing in the literature. Is the photoreceptor output of *Chordata* of opposite polarity to that of either *Arthropoda* or *Mollusca*? The confusion is compounded by the variety of data acquisition techniques used, the presentation convention used, and frequently the presence of a β-wave that is larger and of opposite polarity than the α-wave.

Armington[40] has shown how the polarity of the ERG signal depends on where and how it is acquired. His waveforms can now be interpreted in greater detail based on the P/D Equation. It appears many of his waveforms were acquired using AC-coupled test instrumentation.

### 12.8.2.1 ERG data–An inverted summation of the P/D response + delayed copies

*There is no logical connection between the polarity of a conventional ERG signal and the polarity of the signal generated by a photoreceptor neuron.* The ERG traditionally used an electrode contacting the cornea or sclera of the eye and an indifferent electrode contacting somewhere else. Any representation of the actual

[40]Armington, J. (1974) The Electroretinogram. NY: Academic Press page 174 & 175-179

neural signal from a photoreceptor neuron should reflect the polarity of that signal at the pedicle of a photoreceptor neuron with an indifferent electrode contacting the inter-photoreceptor-matrix, IPM.

*The typical ERG consists of a faithful but inverted P/D signal from a photoreceptor (the α-wave) contaminated by a delayed copy (β-wave) of opposite polarity. The delay is nominally 18 ms in the data of Breton et al., 1994.*

Many records are ERG based with one electrode contacting the outside of the eye and the second contacting an "indifferent location". Frequently in ERG work, the investigator will be talking about the β-wave since it is much larger than the α-wave (and of course of the opposite polarity). Therefore, it is necessary to be sure that the comparison is carefully made. **Figure 12.8.2-1** illustrates the ERG data available from a number of sources. Whereas Devoe[41] plotted his data for the wolf spider with the initial edge going upward on the paper, his caption to the figure says "Negativity of the cornea of the illuminated eye with respect to the indifferent electrode is upwards". The data is for a long pulse of irradiance. Hamasaki[42] provides a variety of ERG recordings for the Octopus due to pulse irradiation, all of which show an initial response proceeding in the negative direction. There is a lot of this data available and the general conclusion is that in the protostomic animal, the ERG begins with a negative going waveform called the α-wave (which is followed by a larger positive going β-wave in many protostomic animals).

**Protostomia–**That large class of bilaterally symmetrical animals generally characterized by a notochord located along the *ventral* surface of the animal.

**Deuterostomia–**That large class of bilaterally symmetrical animals generally characterized by a notochord located along the *dorsal* surface of the animal.

Because of the importance of the *Limulus* in vision research, it is important to determine if this ancient animals visual system conforms to the above finding. Chapman & Hall[43] provide very compelling data in this regard. They show ERG waveforms for both the compound lateral eyes and the simple median eyes of *Limulus*. Whereas the data for both eyes is plotted as upward going waveforms in their Figure 1, they indicate in the text that "the corneal surface became negative with respect to a reference elsewhere". It is concluded that *Limulus* conforms to the protostomic norm.

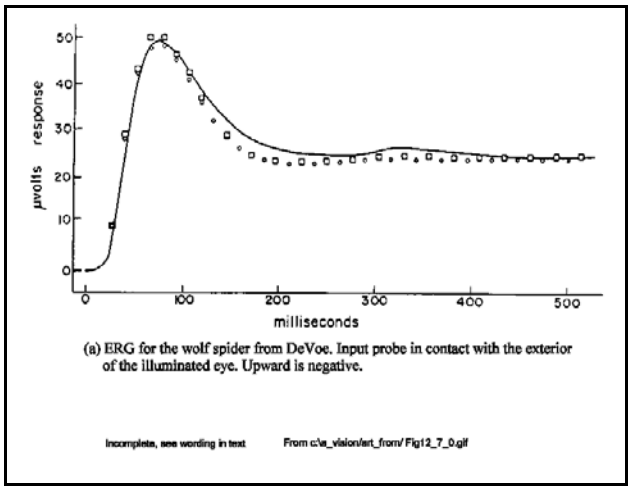


**Figure 12.8.2-1** ERG showing a pure photoexcitation/de-excitation response to a step change in illumination. As in all ERG's using the surface of the lens as a source, the response is *inverted*. The trace shown suggests no other delayed signals were combined with this initial signal. From DeVoe, 1965.

Breton et. al.[44] provide a large volume of ERG's for humans, concentrating on the a-wave but showing the b-wave clearly. They used a contact lens with a metallic ring to contact the eyeball and the "indifferent electrode" was contacting the temple area. All of the recordings show an initial rising waveform which is negative going. Rubin & Walls[45] discuss the historical aspects of the human ERG extensively with respect to the a-wave and waves b through d. Their examples all show a negative going a-wave. Dowling & Wald[46] show a wide variety of ERG's recorded during their

---

[41]Devoe, R. (1965) A non-linear model of sensory adaptation in the eye of the wolf spider. In The functional organization of the compound eye, Bernard, C. editor. NY: Pergamon

[42]Hamasaki, D. (1968) The ERG-determined spectral sensitivity of the Octopus. Vision. Res. vol 8, pp 1013-1021

[43]Chapman, R. & Lall, A. (1967) Spectral mechanisms of Limulus eye. J. Gen. Physiol. vol. 50, pp. 2267-2287

[44]Breton, M. Schueller, A. Lamb, T. & Pugh, E. (1994) Analysis of ERG a-wave amplification and kinetics in terms of the G-protein cascade of phototransduction. *Inves. Ophthalm. & Vis. Res.* vol. 35, no. 1

[45]Rubin, M. & Walls, G. (1969) Fundamentals of visual science. Springfield IL: Charles C. Thomas

[46]Dowling, J. & Wald, G. (1958) Vitamin A deficiency and night blindness. Proc. Nat. Acad. Sci. vol. 44, pp.648-661

investigations of vitamin A deficiency in rats. They take pains to show an enlarged view of one of the ERG's to emphasize that the initial response is the negative going a-wave followed by a larger positive going b-wave.

Smith & Lamb present a human ERG based on a well characterized experiment using only "blue" light (peak wavelength of 450 nm, Lee # 195, but no definition of the cutoff wavelength).

The literature clearly indicates that the leading edge of the a-wave captured by ERG is negative going in *Chordata*.

Based on the available data, with the input electrode contacting the eye surface, the **ERG's of *Chordata* and both *Arthropoda* and *Mollusca* begin with a negative going a-wave.** *The ERG a-wave is an inverted replica of the actual P/D response at the pedicle of the photoreceptor neurons.*

### 12.8.2.1.1 The ERG based on Ganzfeld illumination of Breton et al.–1994

Breton et. al.[47] have provided a largely theoretical derivation of the response of the photoreceptors of the human eye without the benefit of any schematic of the eye or retina, or any consideration for the stage 2 signal processing incorporated into the human retina. They employ a modified contact lens to measure the electrical potential of the cornea with a reference electrode placed on the temple and a ground electrode on the forehead. The reference electrode suggests they were using a differential amplifier as the principle electrical input circuit. They used a Ganzfeld sphere to illuminate the entire field of view simultaneously as the result of a short flash introduced into the sphere.

> Their null hypothesis is based on a chemical theory of vision. They outline a very complex series of chemical events occurring in succession following a short flash of light. The flash initiates a G-protein cascade of phototransduction that results in a neural signal (of unknown character). They assume their measured electrical response, *a(t)* in microvolts, is *proportional* to their calculated response *R(t)*. *R(t)* is a normalized photoresponse, $1 - F(t)$ where *F(t)* is the cGMP-activated current as a fraction of resting ((dark) level, Φ, citing their equation 5.
>
> They predict that each member of the family of responses, *a(t)*, when normalized, should generate "a delayed gaussian function of time," whose width from $t_{eff}$ (at any criterions response amplitude) should be inversely proportional to the square root of the number of photoisomerizations produced by the brief flash. It appears their delayed gaussian is a Michelis Equation, also known as the Logistics Equation.
>
> Their equations predict a maximum rate of rise for their delayed gaussian at intensity Φ is given by the square root of A•Φ/e. They then note, "Experimentally, it is found that the maximum rate of rise of the a-wave does not increase indefinitely but saturates a high intensity, although such saturation is not predicted by our equations."

The assumption that their measured voltage is generated by their G-protein cascade, and that the failure of their equations to predict ***a clear saturation in their data are enough to falsify their null hypothesis***. But there is more, their model only applies to the initial rise in the phototransduction response. ***Their delayed gaussian function creates a highly improbable step response to an initial impulse***, However, **their collected data may be useful when related to The Electrolytic Theory of the Neuron**.

The analysis of photo-transduction by Breton et al. based on a putative G-protein cascade can be ignored!

The recent work of Breton et. al.[48] deserves special attention in light of the electrolytic model proposed here for several reasons.

First, with the P/D Equation of **Section 7.2** shown to describe the total response measured at the OS as a function of irradiance, including both the rising response and the trailing response; it is possible to subtract an appropriate set of

---

[47]Breton, M. Scheuller, A. Lamb, T. & Pugh, E. (1994) Analysis of ERG a-wave amplification and kinetics in terms of the G-protein cascade of phototransduction. *Invest. Ophthalm. & Vision Sci*. vol 35 #1 pg 295-309

[48]Breton, M. Scheuller, A. Lamb, T. & Pugh, E. (1994) Analysis of ERG a-wave amplification and kinetics in terms of the G-protein cascade of phototransduction. *Invest. Ophthalm. & Vision Sci*. vol 35 #1 pg 295-309

these waveforms from their figure 3 and thereby obtain a new set of waveforms related to the rest of the signaling system subsequent to this interface**. Figure 12.8.2-2** shows their original Figure 3(A) and the same figure in frame B after the portion of the waveforms occurring after 30 ms hav**e** been removed.

Second, it should be noted that the data of Breton et. al. is not taken from a single photoreceptor in a suction pipette; the waveforms shown in **Figure 12.8.2-2** are the cumulative waveforms obtained when a single flash of light is applied to virtually all of the photoreceptors in the eye simultaneously. To obtain a plot as they do that still faithfully follows the predicted response of a single photoreceptor, even after averaging the result of two to four flashes, strongly infers that all of the active photoreceptors of a specific spectral response in a given retina are basically identical under threshold conditions--identical in sensitivity, amplification, bias potentials, and axon lengths etc.

Third, if the wavelength of the stimulating flash is not restricted to stimulating only one chromatic channel, the signals recorded by an ERG will contain highly confusing traces after about 20 ms; By proper choice of wavelength, 494 nm or 572 nm, it may even be possible to cancel the modified a-wave traces added to those traces in the b*-wave interval defined below. Such cancellation calls for the suggested wavelengths by adhered to within ±1 nm.

- - - -

Looking at frame **A** of the Breton figure, the traces labeled the so-called a-wave are recognizable as an inverted set of waveforms described by the P/D Equation of this work, out to about 16 ms for the trace with the greatest slope and out to about 25 ms for the lowest slope trace. Each exhibits a delay after the initial flash, exhibit an initial slope that is a function of the intensity of the flash, reaches a peak, and then begins to return to the baseline. After those periods, the traces, consisting of the b-wave set, become more and more confused until they reach 45 ms. However, if the b-wave set of traces in frame **A** is truncated as shown in frame **B**, the confusion is reduced. Note the numbering of the a-wave traces and their counterpart numbering in the b*-wave interval.

> Armington (1974) has defined the late interval of the b-wave, the c-wave. In the process, he also attempted to show a single ERG that has features associated with both the photopic and scotopic regime.

Trace 1 before 17 ms, appears to be a fairly conventional P/D Equation waveform. At about 17 ms, trace 1 now consists of the continuing return of the original trace 1 to which has been algebraically added and delayed, inverted and scaled version of the original trace 1. The delay is approximately 17 ms. The scaling is on the order of 62%. There is an additional negative going segment added algebraically to trace 1 between 17 and 19 ms.

Trace 10 follows the same pattern. However, since it was caused by a much lower intensity initial flash, it begins after a more significant delay, reaches a lower maximum at 17 ms after a lower slope rise (all as predicted by the P/D Equation) At about 24 ms, it too encounters a significant change. At about 24 ms, trace 10 now consists of the continuing return of the original trace 10 to which has been algebraically added and delayed, inverted and scaled version of the original trace 10. Like in trace 1, there is an additional negative going segment added algebraically to trace 10 between 18 and 23 ms.

Traces 2 through 9 follow the same pattern within the limits set by trace 1 and trace 10.

Based on this analysis of the traces, the inverted traces were added to the original traces at between 17 and 19 ms from when they departed from the baseline initially. This is too long for the electronic signal generated by the P/D mechanism in the outer segments of the photoreceptor neuron to travel to the distribution amplifier. However, it is not too long for the signal to travel to the first Activa of the stage 2 signal processing neurons (with or without traveling through a bipolar neuron. See **Section 13.1** for the morphology and **Section 13.2 for the electrical schematic supporting these assertions.** Both a horizontal neuron and an amercine neuron are exhibit differential inputs and are quite capable of generating the inverted copy of the initial waveform.

The complexity of the potential routes through the stage 2 signal processing after 30 ms, as described in **Section 13.2**, indicates that ERG experiments will not likely be a profitable avenue for analyzing stage 2 signal processing.

- - -

The use of Ganzfeld illumination in ERG experiments and then trying to explain the unknowns relating to summing all of the neural paths to form a single trace following a flash stimulation appears awkward. An alternate would be to stimulate only the 1.2° diameter foveola in one set of experiments and then stimulate the fovea out to about 8° diameter while excluding the foveola. The resulting data should provide a more manageable and interpretable framework. The lengths of the axons of stage 1 photoreceptors in the foveola are known to be significantly longer than the axons of these same photoreceptors located in the fovea outside the foveola.

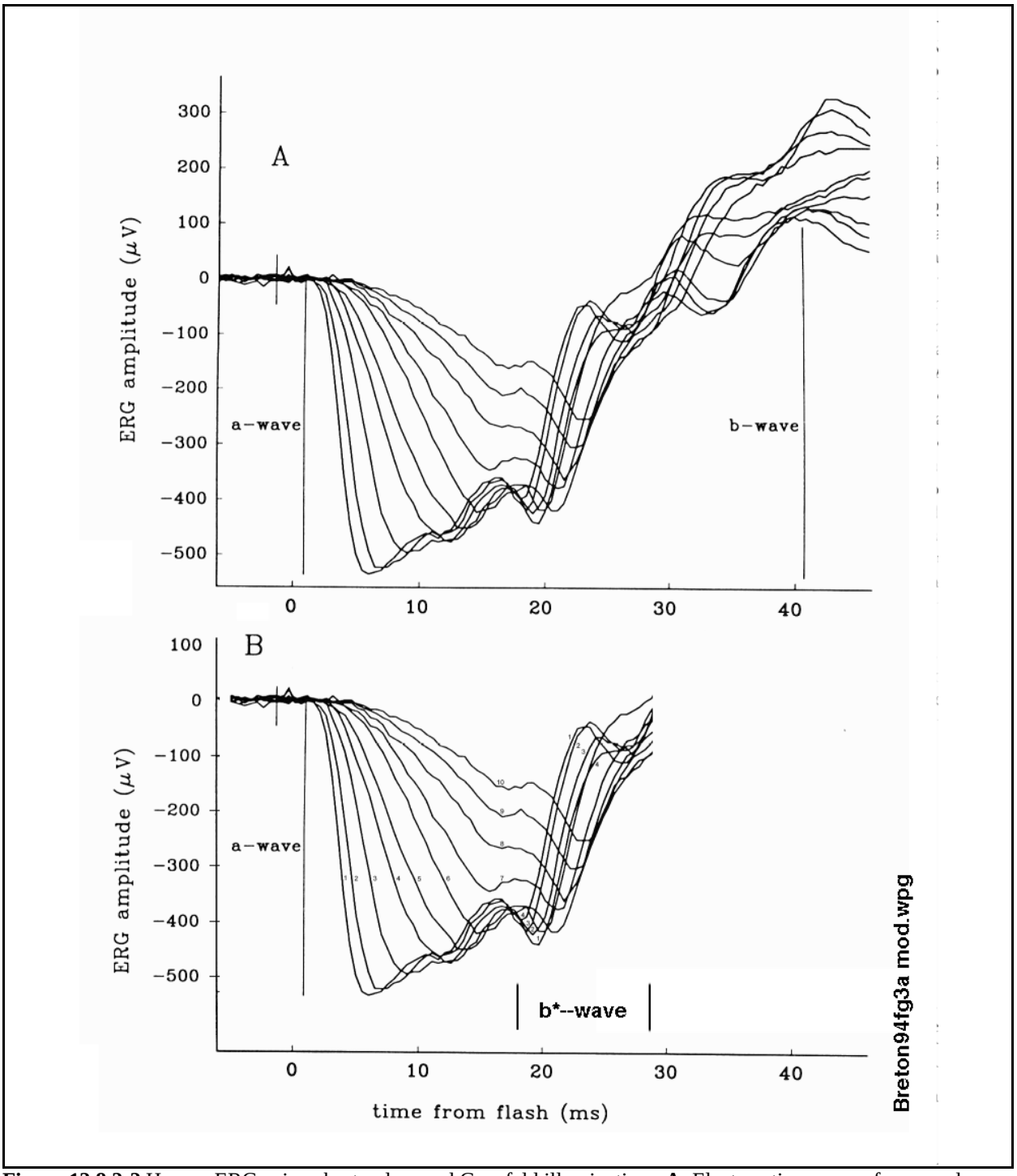


**Figure 12.8.2-2** Human ERG using short pulses and Ganzfeld illumination. **A**; Electroretinograms of a normal observer recorded in response to brief flashes. Each trace is the average of four flash presentations, except for the highest intensity, which is the average of two. The recording bandwidth was 500 Hz, and the digitizing interval 0.5 ms. **B**; A truncated version of **A** to emphasize the repeat nature of the b* wave. The traces and initial tick indicating the time of the flash are aligned, but the time scales are marginally aligned. Note the numerics associated with each trace in the a-wave that is repeated in the b*-wave. The traces in the b*-wave set are delayed and scaled copies of the a-wave set. See text. From Breton et al., 1994.

### 12.8.2.1.2 Double pulse ERG exploring rabbits–Bornschein, 1964

Bornschein & Gunter[49] provided useful test data that can be used to quantify the P/D Equation in that species and potentially disentangle the short term and longer term effects and parameters discussed in **Section 12.7.1**. Their 50 msec pulses of light were effective in emulating an impulse and resulting in a P/D impulse response. The voltage calibration in figure 3 indicates clearly that their probe was not equalized adequately for their purpose, and suggests their waveforms need to be corrected for droop in their test configuration.

### 12.8.2.2 Comparing probe data from *Chordata* and other *Orders*

When probe data is examined, the same confusion is found as in the ERG data. However, another variable associated with technique appears; during the period prior to the 1970's, the probes used to measure waveforms in the retina were grossly larger than the individual cells. This led to confusion between extracellular and intracellular waveforms and also confusion as to whether the cell contacted was in the Outer Nuclear Layer (a true photoreceptor cell) or the Inner Nuclear Layer (most likely a horizontal or amercine cell). In more recent time, the probes have become much smaller and the technique of sucking a single photoreceptor cell into a pipette has raised the precision of the experiments immensely.

In 1962, Hagins provided some excellent data concerning the P/D process in *squid* for a temperature of 5-10C. He measured the potential of the inter-photoreceptor matrix at different locations relative to a very small illuminated area. The results were complimentary to the suction technique of Baylor at a later time. However, Hagins' figure 8 used a very poor scaling technique. By ignoring the variable delay and variable slope of the P/D process as a function of illumination, and re-scaling the measured waveforms individually to align their rising phases, the figure suggests that lower illumination levels produce higher sustained output voltages. Re-plotting this data, or reviewing the original data shows that the squid photoreceptor cell employs the same P/D process as do chordates and other animals.

In 1983, Ottoson attempted to put the question of polarity at the electrical probe level to rest by publishing side by side figures attributed to an invertebrate and a vertebrate. Unfortunately, this presentation is not satisfying for a number of reasons;

+ he attributes the left hand figure to the horseshoe crab which can be confusing to the student since the waveform is not from the crab family of zoology but from *Limulus*, a member of a virtually extinct and separate family, *Xiphosura polyphemus* of *Arthropoda, Chelicerata*.

+ the left hand figure is not in the paper to which it is attributed. The right hand figure is a highly stylized version of the original, apparently for the purposes of a textbook.

+ the left hand figure has been redrawn from the original with the voltage scale changed implying that the pulses crossed the zero level. In the original, the baseline was labeled zero and there was no guarantee by the original author that the baseline was at -50 mV.

+ the figure on the left is the response to a finite duration *pulse* and on the right is the response to a shorter *impulse*.

+ the use of probe data from the unusual eccentric cell from *Limulus* to represent all invertebrates is open to question. It leaves the impression that the photoreceptor cell in *Arthropoda* generates pulses, a function usually found in the ganglion cells of *Chordata.* A better interpretation would be that the left figure represents a ganglion cell of the type found in *Limulus*.

+ other authors report electrotonic waveforms in eyes of *Arthropoda* distal to the eccentric cell which more likely relate to the invertebrate photoreceptor cell.

Schneeweis & Schnapf provided good data on the photoreceptor responses of macaque monkey[50]. Some of their photoreceptor outer segments were illuminated axially. Others were illuminated transversely. They provided both voltage and current waveforms under patch clamp conditions. Their figure 1 stresses the difference in the

---

[49]Bornschein, H. & Gunter, R. (1964) the Double-flash Erg in Retinal Ischemia *Vision Res* vol 4, pp 423-432.
[50]Schneeweis, D. & Schnapf, J. (1999) The photovoltage of macaque cone photoreceptors: adaptation, noise and kinetics *J Neurosci* vol. 19(4), pp 1203-1216

waveforms to be expected under these different conditions. In their discussion of figure 1, they appear unaware that the voltage waveform represents the derivative of the current waveform. Both waveforms show the same delay following the stimulus. However, the voltage waveform, being a derivative, necessarily reaches its peak before the current waveform. Saturation plays a major role in their current waveforms as a function of stimulus level. Comparing their voltage waveforms of figure 2 with the current waveforms of figure 4 is quite instructive. Note their responses were recorded using amplifiers with passbands extending down to DC. They did not describe their criteria when they noted, "Responses of red and green cones were indistinguishable." It would be expected that the responses would be different in amplitude for the same axial stimulus level in accordance with the absorption characteristic of each photoreceptor. For transverse stimulation, they might easily be indistinguishable. The sentence appears in a paragraph unrelated to their chromatic tests.

### 12.8.2.3 Probe data for non-chordates

Looking at more general data for the protostomic group of animals, Shaw[51] indicates the scope of the difficulty in specifying the nature of the initial response. His Figure 10 for the Locust, shows initially positive going waveforms from a retinula on the left and initially negative going waveforms from a lamina cell on the right; both responding to a pulse over roughly 5 orders of magnitude. The left hand figure shows definite signs of temporal band limiting by the impedances involved--and may not represent a true intracellular signal. His Figure 15 provides a similar dual picture for the same animal and without any obvious bandlimiting. Which structure corresponds to the photoreceptor cell of the deuterostomic eye?

Zuker in 1996 **[[check his ref 21** before adding this reference. he was working in chemistry ]]shows initially downward going *current* waveforms in his Figure 3 for the "photoreceptor cells" of the compound eye of *Drosophila*. These waveforms are very clean and correspond in shape very well to the P/D Equation of this work. However, in the text, he says "(Drosophila photoreceptors, like most invertebrates, depolarize as opposed to hyperpolarize in response to light)" Whether his drawings conform to the normal convention of negativity being indicated in the lower portion of a graph and his words are a cop-out **OR** Vice Versa is hard to confirm. He does not specifically indicate the polarity of his data.

Trujillo-Cenoz[52] shows a different set of circumstances and uses different notation in examining the unicorneal (simple) eye of the spider, *Lycosa*, and the compound eyes of two flies, *Sarcophaga* and *Lucilia*. Meinertzhagen[53] provides a further description of the visual pathways of the insect as does Laughlin[54].

By combining their notation and pictures, from both conventional and electron microscopes to develop a closer parallel to the deuterostomic eye. From his discussion, it is possible to draw up a correlation list;

| *Arthropoda* | *Chordata* |
|---|---|
| Rhabdom | Retina |
| Rhabdomere | Outer Segment |
| Microvilli | Discs |
| Photoreceptor Cell (Retinula) | Photoreceptor Cell (Inner Segment in this work) |
| Monopolar Cell | Bipolar Cell |
| Eccentric Cell | Horizontal (or Amercine) Cell |
| Lamina | |
| Medulla (retinula #1-6) | Magnocellular region (luminance signals) |
| Medulla (other levels for retinula #7-8) | parvocellular (chrominance signals) |

This list can be expanded to include *Mollusca* and *Insecta* but the variety of eye configurations becomes unmanageable.

---

[51]Shaw, S. (1968) Organization of the locust retina. *in* Invertebrate receptors. Carthy, J. & Newell, G. editors. London: The Zoological Society of London by Academic Press pg. 149

[52]Trujillo-Cenoz, O. (1965) Some aspects of the structural organization of the arthropod eye. Cold Spring Harbor, NY:Cold Spring Harbor Biological Laboratory vol. 30, pp. 371-382

[53]Meinertzhagen, J. (1977) Development of neuronal circuitry in the insect optic lob. *in* Soc. for Neurosci. Symp. II. (Cowan, W. & Ferrendilli, J. eds.) Bethesda, MD: Soc. for Neurosci., pp. 92-119

[54]Laughlin, S. (1981) Neural principles in the visual system. *In* Handbook of Sensory Physiology, Vol. 7/6B, (Autrum, H. ed.) NY: Springer-Verlag. pp. 133-280; pg 262

Some authors speak of a laminal cell in the protostomic eye, others appear to consider it part of the brain. The distinction is trivial for the purpose at hand. In several cases, they speak of laminal cells as of opposite polarity to more distal cells which would indicate they involve signal inversion as in the case of horizontal and amercine cells. Whether inversion is involved brings us to the crucial question, is the output of the retinula cell of opposite polarity to that of the photoreceptor of the deuterostomic eye?

It is absolutely mandatory to go back to primary sources to answer this question. Many authors of secondary material, textbooks, reviews and articles in related disciplines, generally quote material at hand on this question--and without attribution. Furthermore, many of these secondary authors speak of a signal as depolarizing synonymously with a positive going leading edge. It is important to note that in all cases reviewed, there was no quiescent value given for the waveform that would indicate a negative resting potential.

**Figure 12.8.2-3** from Laughlin, although quite obsolete, particularly with regard to the outer segments (his retinula and cone), can be instructive. With modification, it provides the answer to the question of polarity. Frames (b) and (c) are taken directly from his paper except for the dotted line in the upper probe of (b). As indicated below, it can be argued that the probe tip was actually extracellular when the waveforms were recorded. It is proposed here that the probe tip was extracellular in (b) and further, the waveform recorded from a retinula depends on where it is probed. The cartoon in frame (a) has been added to provide another perspective. In this case, the probe is shown near the proximal end of the retinula and the recorded waveform is shown with a negative going leading edge. There is significant laboratory work reported in the literature that says the output waveform from the insect eye is hyperpolarizing and the resting potential is given. Goldsmith[55], working with the compound eye of the worker honeybee presents his data with the summarizing statement: “When light strikes the compound eye of a worker bee, an electrode in the superficial layers of the retinula records a monophasic, negative retinal action potential.” In the caption to Figure 4 of his paper, he specifies for both the compound eye and the ocelli: “an upward deflection signifies negativity of the electrode in the illuminated eye.”

[55]Goldsmith, T. (1959) Wavelength discrimination in eye of honeybee. in Sensory Communication, Rosenblith, W. ed. Cambridge, MA: MIT Press pg. 366 (similarly in many other papers)

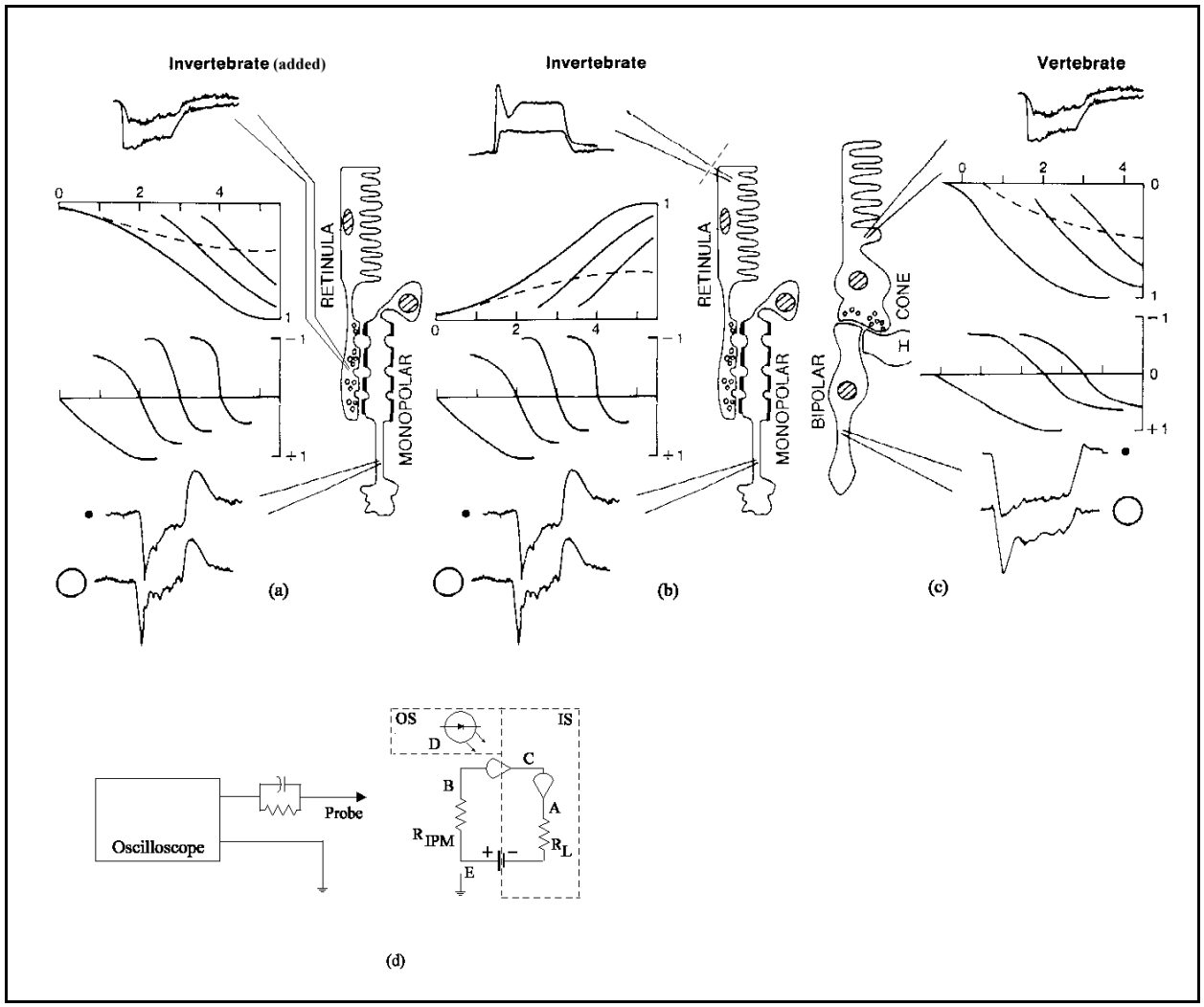


**Figure 12.8.2-3** Photodetection waveforms for Invertebrates & Vertebates. From Laughlin (1981) .

Upon reviewing much of the literature, it appears safe to conclude that it is possible to obtain two different action potentials from the retinula of the invertebrate eye, depending on where you probe. The waveform measured extracelluarly near the distal end of the retinula does not generally exhibit a quiescent level consistent with the interior of a retinula cell and the leading edge is positive going. *In the absence of a non-zero quiescent value, it is not appropriate to speak of depolarization.* The waveform measured intracellularly near the proximal end of the retinula does exhibit a quiescent level of typically -50 mV and does exhibit a negative going leading edge (hyperpolarization).

If one looks at the electrical situation in the region of the retinula, it is possible to rationalize the various primary reports in the literature. Looking at (d), which is based on both the data reported in the literature and the model defined in this work, the basic circuitry found in both retinula of protostomic animals and photoreceptors of deuterostomic animals is shown. As shown above the table correlating the terms used for the different eyes, the stack of discs correspond to rhabdomeres, the discs correspond to microvilli, and in both cases the dendritic structures are too small to be recognized and labeled (except in the case of the deuterostomic eye where they can be seen in the region of the cilliar collar and are described in that region as the cilia. (d) presents a simplified version of the detailed circuitry developed earlier in Chapter 12. However, it shows that there are three main regions from the electronic point of view;

+ the OS contains two important structures, the disc stack and the (8 or 9)dendritic structures that

surround and are laid into the grooves in the disc stack

+ the IS contains the rest of the circuitry associated with the photoreceptor

The disc stack consists of basically organic material which is non-conductive of conventional electrical currents and is extracellular with respect to the photoreceptor cell. The dendritic structures are intracellular but of extremely small dimensions, on the order of 50-100 Å in diameter (or less in the grooves). They do contain a conducting channel, the inside of a microtubule, and their exterior wall is basically a continuous energy sensitive transistor (although shown here as a discrete device for simplicity). The IS contains, in its neural portion, the activa. This is the active device, one or more of which are found in every neuron. It provides the amplification associated with the nerve, this amplification can result in either electrotonic amplification or switching which generates the action potentials. The activa is in communications with the dendritic structure, the surrounding medium (the Inter-Photoreceptor-Matrix or [IPM] similar designation) and the axon of the nerve. It also obtains prime power and maintenance from the housekeeping portion of the cell surrounding it.

If one attempts to use a probe and recording device to obtain waveforms from this photoreceptor, it is possible to probe a variety of different environments within the overall structure. If one attempts to record a signal at D, the environment is basically non-conductive and the signal will be minimal and mostly consist of capacitive pickup from surrounding structures. If one attempts to record a signal from C, the mechanical difficulties are large because the structures are so small--unless it is accomplished near or within the cilia collar. The impedance is also very high in this area. The easiest places to acquire a signal are at B and A.

The signal at B is quite diffuse over an area surrounding the disc stack. Because it is diffuse along each dendrite surrounding the disc stack, it is difficult to capture a significant portion of the current unless the micro-pipette suction technique is used. However, it can be probed successfully, although the extremely high impedance level frequently limits the obtained waveform to the low frequency components. The signal at B does not involve a intracellular resting potential. Therefore, *the waveform at B cannot be described as depolarizing.* It can be described as having a positive going leading edge. If the observed signal waveform does contain a DC level, it is more likely to be due to the voltage at the location of the reference lead compared to the IPM.

The signal at A is at a much lower impedance than at B. It also involves a larger and more accessible structure. Since the electronic system in vision is typically DC coupled, this waveform does exhibit a quiescent or resting potential at any point where it is encountered ( a variable with temperature but typically -50 mV). The signal associated with this point in the circuit has a leading edge which is negative going and typically saturates at a level of about -70 mV. -70 mV is the nominal supply voltage provided by the cell wall of the photoreceptor cell. *The waveform at A is the true and typical electrotonic output waveform of the photoreceptor* which is frequently called the generator potential. It is generally described in this work as a result of the P/D process and described by the P/D Equation (frequently without regard to the DC bias associated with it.

The features of the circuitry associated with the photoreceptor cell are be addressed fully elsewhere in Chapter 12 and the Appendices. The answer to our question is straightforward: The output signal (A) from all photoreceptor cells in the animal kingdom consists of a signal waveform exhibiting a negative going leading edge (the so-called generator potential) and associated with a -50 mV bias level. There is available in the proximity of the OS or Rhabdomere an alternate signal (B) that has a 1:1 amplitude relation to the output waveform. However, it is inverted and does not exhibit a resting potential indicative of a intracellular recording. This signal exhibits a positive going leading edge.

This model is completely compatible with the suction micro-pipette technique developed by Baylor et. al.[56] even with regard to their breaking of the cell at the cilia collar. Specifically;

+ they were able to collect all of the diffuse current surrounding the OS at B. The waveform of the current collected can be described very well using the P/D Equation.

+ the "Light flashes evoked transient outward currents." in the region surrounding the OS.

+ they were able to show that under saturating conditions the maximum current was about 27 pA.

+ they were able to show that if the OS was separated from the IS at the cilia collar, the current obtained was the same as the saturation current above, demonstrating that the maximum current

---

[56]Baylor, D. Lamb, T. & Yau, K.-W. (1979) The membrane current of single rod outer segments. J. Physiol. vol. 288, pp. 589-611

available was given by the fraction, $E_D/R_D$, in the model (by collecting essentially all of the current at C, the impedance of the IPM was not involved).

+ they also showed that the peak current went up in a linear manner as more of the OS was moved into the micro-pipette, indicating the combined optical absorption (photoexcitation) and de-excitation profile was quite uniform over the length of the OS.

+ they showed that the current profile decreased uniformly with distance after the cilia collar was moved into the micro-pipette--indicating that the current passing through the battery $E_D$ and the resistor $R_D$ was obtained over a continuous region of the IS cell wall.

They also calculated the current emanating from a one micron circular ring of the OS of 0.75 pA/μ. Thus a probe in this area with a 1.0 μ collecting area would only pick up a small fraction of this total current around the ring. This is why the measurements at point B are usually low pass limited. The impedance is extremely high and the current is extremely low. The overall probe circuit exhibits a low pass characteristic under these conditions. The impedance of the IPM in series with the capacitance shunting the probe contact (or compensation circuit) limits the frequency sensed to below
$1/(C * R_{IPM})$ hertz. It is difficult to observe system noise under these conditions and the reported waveforms are usually smooth as in Laughlin's figure for the waveform at B in the invertebrate.

In this case, as in the ERG case, *Limulus* represents a special case. Davson[57] indicates that the retinula cells each have a fiber emanating from them but these fibers do not exhibit action potentials and they may or may not be nerve fibers in fact. He indicates that the eccentric cell may be regarded as the true neural pathway from the ommatidium and that the structure passing up through the central axle of the rhabdom is the dendrite of this eccentric cell. The axon of this eccentric cell does exhibit action potential impulses. {His words clearly reflect the time period of their original preparation, when electrotonic signals were not recognized as true signal waveforms in the retina.} No lamina cell is indicated in his discussion of the *Limulus*. Behrens & Wulff[58] obtained electrical signals from both retinula and eccentric cells in Limulus. **[[ need this paper ]]** They report a electrotonic wave with small spikes associated with the retinula cells and a slow wave with large spikes associated with the eccentric cell. This would appear to define the retinula output as that of the photoreceptor and the eccentric cell as a (nearly) conventional ganglion cell. If this is correct, the initial output of the photoreceptor cell upon irradiance in *Limulus* is { +/- }going .

The data related to the electrical response of the photoreceptors in deuterostomic animals is immense and quite compelling, especially the data of the last 20 years. It invariably shows an initially negative going voltage response at the output of the photoreceptor cell; and this applies to both warm blooded and cold blooded members of this group. See any of the papers in this time period from Hodgkin, Baylor, Fuortes, Lamb, Etc.

## 12.8.3 Earliest descriptions leading to the P/D Equation of photoreceptors–Hagens, 1965

Hagins[59] provided carefully calibrated transient response of squid photoreceptor outer segments using the instrumentation of the period. **Figure 12.8.3-1** shows his data. The instrumentation was not adequate to capture the actual rise times of these traces or the initial delay predicted by the P/D Equation, and actually measured in subsequent experiments. He also made a number of unsubstantiated assumptions.

[57]Davson, H. ( 1990 ) Physiology of the eye, 5th ed. NY: Pergamon Press pg. 280

[58]Behrens, & Wulff (1965)

[59]Hagins, W. (1965) Electrical signs of information flow in photoreceptors *In* — Sensory Receptors. Cold Spring Harbor Laboratory on Quantitative Biology vol XXX, pp 403-418

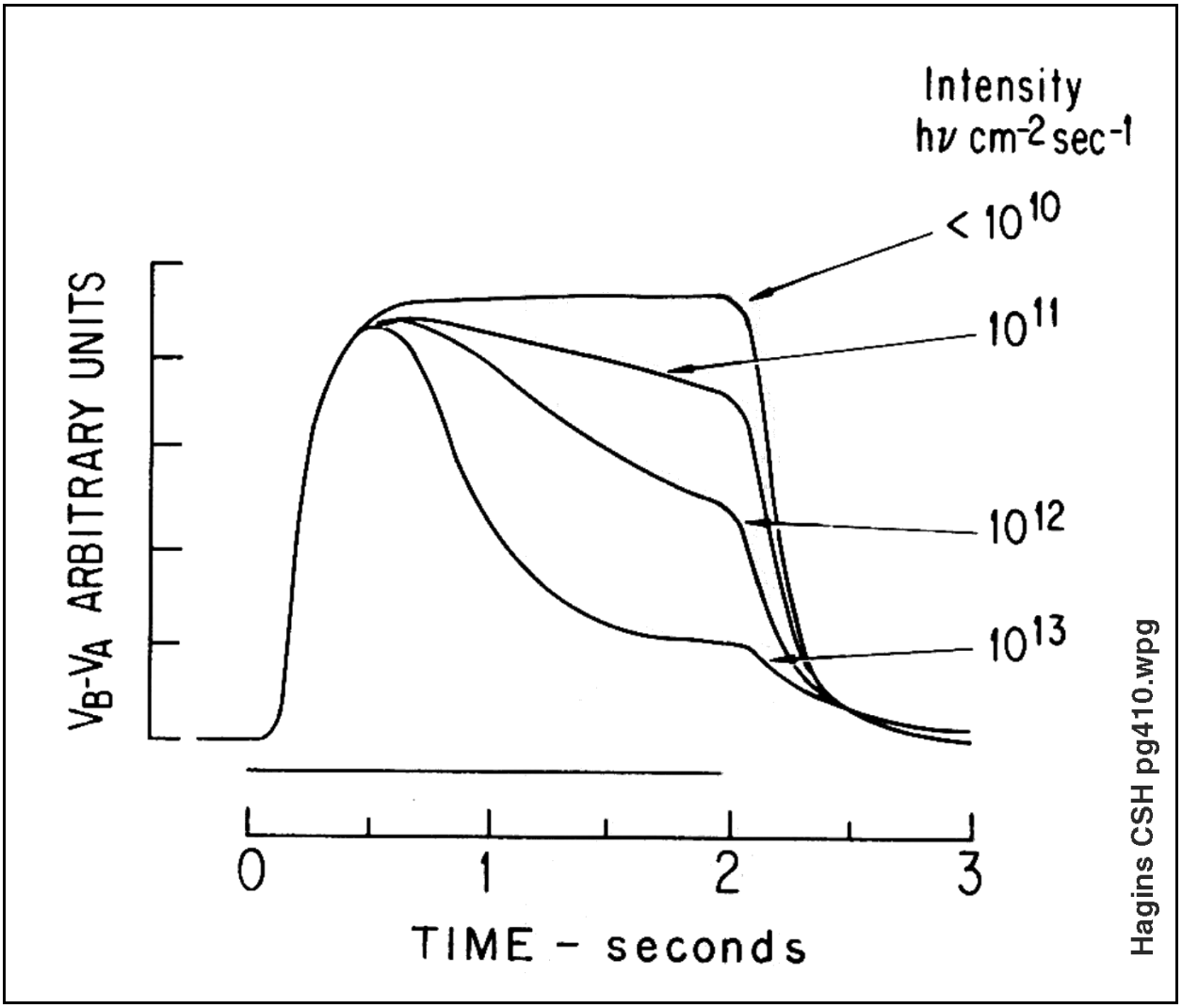


**Figure 12.8.3-1** Transient response of dark adapted squid photoreceptors to 500 nm light. The curves require significant interpretation. The individual responses have been normalized to show the similar rising characteristics when they are significantly different. The curves have also been normalized as to start time when in fact the initial delay after stimulation is an inverse function of the stimulus intensity. See text. From Hagins, 1965.

1. He assumed the rise time of the responses were all the same regardless of stimulus intensity.
2. He assumed the delay of the responses after stimulation were the same regardless of stimulus intensity.

3. He assumed that the rising portion of the response never overshot the mid pulse response.
4. He chose to normalize the waveforms relative to their peak overshoot.

***However, an experienced observer, discerns the features introduced by the P/D Equation in Hagen's plots***.

**12.9 Summary**

The success of the P/D equation and the overall model of the photodetection function of the photoreceptor cell in describing the measured performance of the eye in a variety of animals is remarkable. It's ability to predict completely the details of the test data of Baylor, Torre and Breton demonstrates its correctness. More will be said concerning the data of Breton in the next chapter. Briefly, this model allows one to explain the difference between the a-wave and the b-wave of the ERG. As will be seen later, it does even more than this; it suggests and helps prove that the β-wave consists of more than one signal--quite possibly an early β-wave related to the circuitry in the

Inner Nuclear Layer (INL) and a later β-wave related to subsequent circuitry; which may also be in the INL or may consist of the low passed signals related to the ganglion cells in the Outer Nuclear Layer (ONL).

This success clearly indicates it ranks ahead of other models of the photoreception process. It indicates the "photo-electronic" detection theory is far superior and more accurate than the "photo-isomerization" theory in describing the vision process. Specifically, it is compatible with the excitation/de-excitation process restoring the individual chromophoric molecules to their original state in less than 1 milli-second under most radiance conditions and requires no transport of a molecular species to the RPE for reconstitution. It also eliminates any need for "dark processes" as usually inferred to satisfy the photo-isomerization theory.

The model does not require the physical transport of any ions through a cell wall surrounding the discs; in fact, it does not require any cell wall to surround the discs.

The model does not require any flow of chromophoric molecules in or out of the OS except for normal growth at the end near the IS. For those that do flow into the discs, there is no need to pass through a cell membrane to reach the discs; and it appears there may be physical openings in the collar of the IS to facilitate the flow of chromophoric molecules in that area.

The explanation of the "hyperpolarization" of the photoreceptor cell due to photoexcitation is completely explained by this theory. The output signal consists of a quantity of electrons which is numerically related to the photon flux and there is no inversion in the neural amplifiers of the photoreceptor neuron.

The description of a biological transistor as described above may be a bit difficult for some biologists to accept, and its detailed elucidation may require considerable analysis. However, the structures available in a biological membrane are very comparable with the "back to back diode" description of a semiconductor transistor of a non-biological type.

Employment of an ion transport related mechanism to generate a current in a biological transistor located on the OS side of the OS/IS interface would require transport of ions from the IS to the OS (or the dendritic structure) in large numbers, at high rates and high ion current densities to accommodate a 30 pA current within a very small diameter structure. This appears unlikely at first glance. It is more likely that the walls of the dendritic structure (possibly in conjunction with the membranes of the discs) are acting as a biological transistor based entirely on electron charge transport--the only ionic motion would be that of a standing wave type, as in ocean waves.

It would be extremely interesting to see the results of Baylor's and Lamb's work repeated for light in the vicinity of 0.64 microns. Such data would determine the characteristic of the "exciton" to electron transducer if it is in fact related to the energy of the incident photons. **[See Kraft, et. al. 1990]**

It should be noted that so far, no distinction has been made in this chapter between the different types of photoreceptors. Whether they were sensitive in the long, medium, short or UV spectrum has not been of concern. Up to this point, they all operate alike. Each photoreceptor operates in a quantum-mechanical mode and can detect and report the absorption of a single photon at a signal level that can be processed by the follow-on signaling stages. Their instantaneous dynamic range is logarithmic and controlled by the input characteristic of the dendritic tissue of the photoreceptor neuron.

The adaptation mechanism is virtually instantaneous with rising stimulation but is slow to recover after the cessation of stimulation. The more important property is the ability of the adaptation mechanism to maintain a constant signal output from the OS to the IS by maintaining the product of the stimulus intensity and the absorption coefficient a constant over many orders of magnitude of stimulation intensity.

# TABLE OF CONTENTS 7/4/19


12 Primary Signal Processing--Signal Detection . . . 3
12.1 Introduction . . . 3
12.1.1 Glossary . . . 3
12.1.2 Background . . . 4
12.1.2.1 Relative Physics . . . 4
12.1.2.2 Common wisdom of the past . . . 5
12.1.2.3 Framework of this theory . . . 6
12.1.2.3.1 Architecture & integration of the visual system . . . 7
12.1.3 Definition of the cytological situation . . . 7
12.1.4 Derivation of the Circuit Analog . . . 8
12.1.5 Falsification of “rods & cones” concept . . . 10
12.2 The physiological character of the stage 1 photoreceptors . . . 10
12.2.1 The cytological character of a generic neuron . . . 10
12.2.2 The morphological character of a photoreceptor neuron . . . 11
12.3 Mechanism of the photodetection process . . . 13
12.3.1 Electronic Characteristics of the Chromophores . . . 13
12.3.1.1 The Photo-Electron Excitation Process . . . 13
12.3.1.2 The Electron-Neural De-excitation Process . . . 15
12.4 Earlier conception of the amplification process in neurons . . . 15
12.5 The Complete Stage 1 Photo Detection Process . . . 16
12.5.1 The Transduction Block in vision . . . 20
12.5.1.1 Fundamentals of biological transduction in vision . . . 20
12.5.1.2 Fundamental quantum-mechanics of biological transduction in vision . . . 21
12.5.1.2.1 Quiescent operation . . . 22
12.5.1.2.2 Operation with illumination . . . 22
12.5.1.2.3 Transient operation . . . 23
12.5.1.3 The quasi-static transduction process . . . 23
12.5.2 The Transduction and Translation blocks of the photoreceptor neuron . . . 26
12.5.2.1 Histology and electrical schematic of photoreceptor neuron outer segment . . . 26
12.5.2.1.1 Histology of the outer segment . . . 26
12.5.2.1.2 Schematic of the outer segment . . . 28
12.5.2.2 Polarity, signal amplitude & Impedance of the photoreceptor amplifiers . . . 30
12.5.2.3 The photoreceptor neuron from a different physiological perspective . . . 30
12.5.2.4 The *special* case of the long wavelength visual channel(s)–a 2-exciton process . . . 32
12.5.2.5 The *general* case of multiple spectral channels affected by temperature–a 2-exciton process . . . 35
12.5.2.5.1 The UV & mid-wavelength visual channels in an exotherm–*Limulus* . . . 35
12.5.2.5.2 The proposed band gap of liquid-crystalline water versus temperature . . . 36
12.5.2.5.3 The impact on visual discrimination of the 2-exciton mode of photodetection . . . 36
12.5.2.5.4 The impact on the P/D Equation of the 2-exciton mode of photodetection . . . 36
12.5.2.5.5 Potential impact on the sensory modalities of exothermic animals . . . 37
12.5.3 CRUCIAL MECHANISM: Adaptation of the outer segment–the phenomenon of bleaching . . . 38
12.5.4 Effect of dis-assembly in the laboratory . . . 39
12.5.4.1 Probing . . . 39
12.5.4.2 Dissection . . . 40
12.5.4.3 Extraction of the chromophores of vision–the Rhodonines . . . 40
12.6 (Reserved) . . . 41
12.7 The Transfer Functions of Stage 1–Based on the P/D Equation . . . 41
12.7.1 The Large Signal Model . . . 41
12.7.1.1 Short term large signal model– milliseconds duration . . . 43
12.7.1.2 Longer term large signal model– seconds or longer duration . . . 43
12.7.2 The Small Signal Model . . . 44
12.7.4 The transient state transfer function EMPTY . . . 44
12.8 Comparison with data in the Literature . . . 45

12.8.1 The outer segment and the suction pipette technique . . . . . 45
12.8.1.1 The Class C voltage waveform at the outer segment . . . . . 46
12.8.1.2 The Class C current waveform at the outer segment . . . . . 48
12.8.1.3 The Response of the OS according to Schnapf et al.–Inadequate protocol . . . . . 51
12.8.1.3 The peak Class C waveform at different positions along the outer segment . . . . . 53
12.8.2 ERG compared to inter-neuron-probe data of the photoreceptor output . . . . . 54
12.8.2.1 ERG data–An inverted summation of the P/D response + delayed copies . . . 54
12.8.2.1.1 The ERG based on Ganzfeld illumination of Breton et al.–1994 . . 56
12.8.2.1.2 Double pulse ERG exploring rabbits–Bornschein, 1964 . . . . . 59
12.8.2.2 Comparing probe data from *Chordata* and other *Orders* . . . . . 59
12.8.2.3 Probe data for non-chordates . . . . . 60
12.8.3 Earliest descriptions leading to the P/D Equation of photoreceptors–Hagens, 1965 . . . . 64
12.9 Summary . . . . . 65

2236 **Chapter 12 List of Figures** 7/4/19

2237 **Figure 12.1.4-1** Block Diagram of Outer Segment and the translation function . . . . . 9
2238 **Figure 12.1.4-2** The fundamental *electrolytic* circuit of the photoreceptor cell . . . . . 10
2239 **Figure 12.2.1-1** A more fully elaborated *cytological* schematic of a fundamental neuron . . . . . 11
2240 **Figure 12.2.1-2** An exploded *histological* view of the baseline photoreceptor cell . . . . . 12
2241 **Figure 12.5.1-1** Nomenclature, block diagram and overall circuit for Stage 1 . . . . . 18
2242 **Figure 12.5.1-2** The quantum mechanical interface ADD . . . . . 22
2243 **Figure 12.5.1-3** The quasi-static transduction transfer function . . . . . 25
2244 **Figure 12.5.2-1** Graphic details of the photo-detection mechanism of stage 1 . . . . . 27
2245 **Figure 12.5.2-2** Alternate quantum-electrical schematic of the stage 1 photoreceptor neuron . . . . . 31
2246 **Figure 12.5.2-3** Conceptual probabilities of translation from exciton to free electron . . . . . 33
2247 **Figure 12.5.2-4** Data suggesting a 2-exciton mechanism in the Limulus . . . . . 35
2248 **Figure 12.5.2-5** Estimate: Band gap of liquid crystalline water . . . . . 36
2249 **Figure 12.5.3-1 CRUCIAL CONCEPT:** Adaptation & the constant signal output of discs of photoreceptors . . . 38
2250 **Figure 12.7.1-1** Proposed template for the perceived visual brightness as a function of luminance intensity in
2251 humans ADD . . . . . 42
2252 **Figure 12.8.1-1** Waveforms associated with the photoreceptor cell . . . . . 45
2253 **Figure 12.8.1-2** Comparison of P/D Equation with the potential measured by probing. . . . . 47
2254 **Figure 12.8.1-3** Comparison of P/D Equation with current collected by a Faraday cage . . . . . 48
2255 **Figure 12.8.1-4** The Class C current waveform using suction pipette techniques . . . . . 50
2256 **Figure 12.8.1-5** Comparison of the P/D Equation and a delayed & inverted copy with published measurements . 52
2257 **Figure 12.8.1-6** Current captured by a Faraday Cage surrounding the Outer Segment . . . . . 54
2258 **Figure 12.8.2-1** ERG showing a pure photoexcitation/de-excitation response to a step . . . . . 55
2259 **Figure 12.8.2-2** Human ERG using short pulses and Ganzfeld illumination. . . . . 58
2260 **Figure 12.8.2-3** Photodetection waveforms for Invertebrates & Vertebates. From Laughlin (1981) . . . . . 62
2261 **Figure 12.8.3-1** Transient response of dark adapted squid photoreceptors to 500 nm light . . . . . 65

SUBJECT INDEX (using advanced indexing option)

1010 . . . . . 24
2-exciton . . . . . 1, 32-37
2-photon . . . . . 33
action potential . . . . . 5, 61, 64
Activa . . . . . 1, 8, 9, 11-13, 15, 17-19, 21, 23, 24, 26-33, 35-39, 43-46, 49-51, 57, 63
adaptation . . . . . 1, 3, 6-10, 12, 16, 17, 19, 24-26, 28, 29, 32, 36, 38, 39, 41-47, 51, 53, 55, 59, 66
adaptation amplifier . . . . . 3, 9, 10, 12, 17, 19, 25, 28, 29, 32, 36, 43, 45-47
amplification . . . . . 15-17, 24, 25, 29, 39, 55-57, 63
anisotropic . . . . . 20, 21, 26, 28, 41, 46, 54
attention . . . . . 40, 56
axoplasm . . . . . 19, 46
a-wave . . . . . 53-58, 65
band gap . . . . . 22, 32-37
bipolar . . . . . 39, 51, 57, 60
bleach . . . . . 15, 24
bleaching . . . . . 8, 16, 25, 26, 38
boundary layer . . . . . 32
broadband . . . . . 36
b-wave . . . . . 53-57, 65, 66
calibration . . . . . 59
carboxylic acid system . . . . . 1, 41
cGMP . . . . . 6, 56
class A . . . . . 45, 51
class B . . . . . 45, 46
common-emitter . . . . . 29
compensation . . . . . 64
compound eye . . . . . 55, 60, 61
cross section . . . . . 13, 26, 31, 41-43
cross-section . . . . . 13, 15, 20, 25
cut-in . . . . . 42
dark adaptation . . . . . 7, 17, 24, 38, 42, 46
diode . . . . . 17, 19, 26, 27, 30, 31, 44, 66
dopamine . . . . . 45
double layer . . . . . 32
dynamic range . . . . . 10, 16, 38, 41, 43, 44, 66
E/D . . . . . 38, 41
eccentric cell . . . . . 45, 59, 60, 64
Electrolytic Theory of the Neuron . . . . . 1, 30, 56
electrostenolytics . . . . . 1, 45
endothermic animals . . . . . 35, 36
ERG . . . . . 17, 19, 35, 53-59, 64, 65
exocrine . . . . . 7
exothermic animals . . . . . 36, 37
expanded . . . . . 8, 13, 27, 30, 60
external feedback . . . . . 16
feedback . . . . . 16, 42, 46
GABA . . . . . 45
Gaussian . . . . . 56
glance . . . . . 66
glutamate . . . . . 16, 45, 53
g-protein . . . . . 55, 56
Helmholtz double layer . . . . . 32
Hodgkin Condition . . . . . 1
hole . . . . . 4, 9, 15, 19, 23
hydronium . . . . . 9, 29, 32
ice . . . . . 32, 36
index of refraction . . . . . 14, 27

internal feedback . . . . . 16
in-vitro . . . . . 15, 51, 52
in-vivo . . . . . 5, 19, 53
light adaptation . . . . . 17, 46
Limulus . . . . . 6, 34-36, 45, 55, 59, 64
liquid-crystal . . . . . 1, 20
liquid-crystalline . . . . . 1, 9, 24, 31, 36, 37, 40, 41, 45
LOT . . . . . 55
Medulla . . . . . 60
mesotopic . . . . . 25
microtubule . . . . . 7, 9, 21-23, 27-29, 31, 32, 63
microvilli . . . . . 60, 62
modulation . . . . . 5
monopolar . . . . . 51, 60
morphogenesis . . . . . 7
narrow band . . . . . 47
navigation . . . . . 1
neurites . . . . . 24, 29
night blindness . . . . . 55
noise . . . . . 46, 53, 59, 64
n- . . . . . 6, 9, 13-15, 17, 18, 31, 32, 34, 36, 37, 44
n-type . . . . . 17, 31, 32, 36, 37
orbitals . . . . . 24, 25
P/D equation . . . . . 1, 3, 7, 20, 31, 36, 37, 41, 44-48, 51-54, 56, 57, 59, 60, 63-65
pain . . . . . 26, 43
parametric . . . . . 25
parvocellular . . . . . 60
Pauli exclusion principle . . . . . 1, 4, 29, 41
pnp . . . . . 1, 28-30, 36
podites . . . . . 13
poditic . . . . . 19
probabilistic . . . . . 32, 40
propagation velocity . . . . . 15
protocol . . . . . 51
quantum-mechanical . . . . . 1, 3-5, 7, 24, 26-29, 31, 32, 37, 66
reading . . . . . 8, 49
rectifier . . . . . 51
residue . . . . . 41
resonance . . . . . 20, 21, 40
rhabdom . . . . . 60, 64
rhabdomere . . . . . 60, 63
roadmap . . . . . 3
saccule . . . . . 16
slow wave . . . . . 14, 20, 64
square law . . . . . 33
stage 1 . . . . . 3, 7, 9, 10, 16-18, 27, 30-32, 39, 41, 51, 57
stage 2 . . . . . 29, 30, 32, 40, 51, 56, 57
stage 4 . . . . . 39, 40, 44
stage 5 . . . . . 44
synapse . . . . . 5
threshold . . . . . 15, 31, 32, 34, 57
transduction . . . . . 1, 4, 6-8, 17, 20, 21, 23, 25, 26, 28, 30, 38, 56
transistor action . . . . . 49
translation . . . . . 7-9, 17, 23, 26, 32-34, 36
Verhoeff's . . . . . 45
verification . . . . . 29
waveguide . . . . . 27
xxx . . . . . 1, 6, 44, 53, 64